LITHOGRAPHIC PATTERNING PROCESSES FOR ORGANIC ELECTRONICS AND BIOMATERIALS

A Dissertation

Presented to the Faculty of the Graduate School

of Cornell University

In Partial Fulfillment of the Requirements for the Degree of

Doctor of Philosophy

by

Priscilla Grace Taylor

January 2011

LITHOGRAPHIC PATTERNING PROCESSES FOR ORGANIC ELECTRONICS AND BIOMATERIALS

Priscilla Grace Taylor, Ph. D.

Cornell University 2011

Organic electronics is a newly developed field that promises inexpensive, mechanically-flexible, large-area devices. Through the use of solution-processable organic materials, electronic devices can be fabricated on large-area, lightweight, flexible substrates to produce a new class of electronics.

Patterning methods for organic electronics represents one of the major obstacles to be overcome in organic device fabrication. A high-resolution, high-throughput system with good registration capabilities is required to realize the potential for organic electronics, both in performance and commercialization. The well-established photolithographic patterning method has only been marginally useful in patterning organic electronic materials due to incompatibility issues between the organic materials and conventional lithographic processing solvents and resists. Many alternate patterning methods have thus been developed, however none of which are able to match photolithography in resolution and throughput. This thesis presents research performed toward the goal of developing lithographic patterning methods for organic electronic devices.

Each section of this thesis describes a different resist system, which was developed for patterning organic electronic devices. All of the systems consist of fluorinated resist materials, which were designed and synthesized to be fully processable in

hydrofluoroether solvents. These fluorinated materials and solvents can be used to lithographically pattern organic electronic devices in a high-resolution and high-throughput manner, without the typical incompatibility issues that exist between organic materials and conventional processing solvents and resists.

BIOGRAPHICAL SKETCH

Priscilla Grace Taylor was born in October 1985 in North Carolina. Her family soon after moved to the small town of Searcy, Arkansas, where she grew up. From an early age, she particularly enjoyed reading. She also spent a lot of time playing outside with her two brothers and their neighborhood friends. Priscilla's parents encouraged her to try a lot of different activities, hence she learned to play the piano, flute and harp, took ballet and art classes, and played many sports, including softball, tennis, soccer, golf and basketball. Eventually, her family moved to Texas where Priscilla began high school. She soon transferred to the Texas Academy of Mathematics and Science, where she attended school away from home. She made many lasting friendships and truly enjoyed her time there. After graduating from high school in 2003, Priscilla began as an undergraduate at Rice University where she majored in Chemistry. When she started working in Prof. James Tour's lab, she was strongly encouraged to go to graduate school. After graduating from Rice in 2005, Priscilla spent the next year teaching English at a small college in China. She then began her graduate work at Cornell in the Fall of 2006.

At Cornell, Priscilla served as a committee chair for Expanding Your Horizons (EYH), a program to encourage middle school girls in math and science. She also served as president of Women in Materials Science and Engineering (WIMSE) in 2009. Priscilla has enjoyed both her research and spending time with the good friends she has made at Cornell.

To my Grandmother, Ella Taylor, who has always been a source of inspiration to me through her character, faith and accomplishments

To my parents and role models, David and Grace Taylor, who have always taken care of me and given me so many opportunities

ACKNOWLEDGMENTS

I would like to sincerely thank Prof. Christopher Ober for his support and guidance during my time at Cornell. Thank you for sending me to Australia and Greece and so many conferences. You've given me a rich and enjoyable graduate school experience.

I'm equally grateful to Dr. Jin-Kyun Lee who has been a daily source of direction and wisdom. You are a brilliant chemist and a great mentor. I don't know what I would have done without you!

I'm thankful to the entire Ober Group for always being ready to give help and advice. I've enjoyed working with you all and could not have asked for a better research group.

Thank you to all the MS&E girls for all the baked goodies and fun times, and especially for being my friends. I love you all and I'll miss you so much!

Most of all, I'd like to thank my parents who have always supported me and taken care of me.

TABLE OF CONTENTS

BIOGRPAHICAL SKETCH…….iii

DEDICATION……...iv

ACKNOWLEDGEMENTS……v

TABLE OF CONTENTS……...vi

LIST OF FIGURES……....x

LIST OF TABLES……....xii

LIST OF ABBREVIATIONS……..xiii

CHAPTER 1: PATTERNING METHODS FOR ORGANIC ELECTRONICS

1.1 Background for Organic Electronics……..1

1.1.1 Organic Electronic Devices: Transistors, Light-emitters and Photovoltaics

1.1.2 Device Manufacture and Marketability

1.2 Patterning Methods in Organic Electronics……...5

1.2.1 Inkjet Printing

1.2.2 Microcontact Printing and Related Methods

1.2.3 Imprint Lithography and Related Methods

1.2.4 Shadow Masks

1.2.5 Photolithography and Light-based Patterning Techniques

1.3 Direct Photolithographic Patterning for Organic Electronic Materials……..15

1.3.1 Novel Processing Methods

1.3.2 Processing in Orthogonal Solvents

1.4 Summary……26

References…….29

CHAPTER 2: A NON-CHEMICALLY AMPLIFIED NEGATIVE-TONE PHOTORESIST FOR PATTERNING ORGANIC ELECTRONICS WITH HYDROFLUOROETHER SOLVENTS

Abstract……..……37

2.1 Introduction……38

2.2 Experimental Section……42

2.2.1 Materials

2.2.2 Synthesis of the polymer photoresist **2-3**

2.2.3 Characterization of the polymer photoresist **3-3**

2.2.4 Lithographic Evaluation

2.2.5 Device Fabrication

2.3 Results……44

2.4 Lithographic Evaluation……44

2.5 Discussion……...46

2.6 Conclusion……..54

Acknowledgements……...54

References…….55

CHAPTER 3: A NON-CHEMICALLY AMPLIFIED POSITIVE-TONE PHOTORESIST FOR PATTERNING ORGANIC ELECTRONICS WITH HYDROFLUOROETHER SOLVENTS

Abstract……..……57

3.1 Introduction……58

3.2 Experimental Section…….59

3.2.1 Materials

3.2.2 Synthesis

3.2.3 Characterization

3.2.4 Lithographic Evaluation

3.3 Results…….65

3.4 Lithographic Evaluation……71

3.5 Discussion……...76

3.6 Conclusion……..82

Acknowledgements……...83

References…….84

CHAPTER 4: ORTHOGONAL SELF-PATTERNABLE ELECTROLUMINESCENT MATERIALS FOR ORGANIC ELECTRONIC DEVICES

Abstract……87

4.1 Introduction……88

4.2 Experimental Section…….90

4.2.1 Materials

4.2.2 Synthesis

4.2.3 Characterization

4.2.4 Lithographic Evaluation

4.3 Results……...103

4.4 Discussion……...……...112

4.5 Conclusion……117

Acknowledgements…….118

References……...119

CHAPTER 5: BENIGN PROCESSING METHODS FOR PATTERNING MULTIPLE BIOMOLECULES

***Abstract*……..……..121**

5.1 Introduction: Multicomponent Patterning Methods for Biomolecules…..…...121

5.1.1 Photolithography

5.1.2 Soft Lithography

5.1.3 Dip-pen Lithography

5.1.4 Spot-arraying

5.1.5 Outlook

5.2 Experimental Section……..129

5.2.1 Materials

5.2.2 Synthesis

5.2.3 Characterization

5.2.4 Lithographic Evaluation

5.2.5 BSA Assay

5.2.6 Monoclonal Antibodies Assay

5.2.7 Multiple-Cycles Tests

5.2.8 Fabrication of Protein Arrays

5.2.9 Protein-Assisted Cell Patterning

5.3 Results……...137

5.4 Discussion……..……...147

5.5 Conclusion……154

Acknowledgements…….155

References……...157

OUTLOOK AND FUTURE DIRECTIONS……..161

LIST OF FIGURES

CHAPTER 1

Figure 1.1: Standard photolithographic patterning scheme……..17

Figure 1.2: Photolithographic patterning scheme used by Tian *et al.*……20

Figure 1.3: Photolithographic patterning schemes used by DeFranco *et al*……..22

Figure 1.4: Photolithographic patterning scheme used by Hwang *et al*……...24

Figure 1.5: Photolithographic patterning scheme used by Lee *et al*…….25

CHAPTER 2

Figure 2.1: Synthesis of the UV-sensitive polymer acid stable resist **2-3**……40

Figure 2.2: 3M Novec Hydrofluoroether structures…...……41

Figure 2.3: Patterned photoresist images……..45

Figure 2.4: Contrast curve at 248 nm of polymer **2-3**…….....47

Figure 2.5: Contrast curve at 365 nm of polymer **2-3**…….....48

Figure 2.6: PEDOT:PSS PH500 film conductivity test…….....50

Figure 2.7: Optical microscope images of patterned PEDOT:PSS…….....52

Figure 2.8: PEDOT:PSS/Pentacene bottom-contact OTFT…….....53

CHAPTER 3

Figure 3.1: Synthesis of the non-chemically amplified polymer resist **3-3**……..66

Figure 3.2: Synthesis of the DNQ-based polymer resist **3-11**…...…….68

Figure 3.3: Synthesis of the DNQ-based small molecule resists……..……72

Figure 3.4: Patterned photoresist images…….....74

Figure 3.5: 3M Novec Hydrofluoroether structures…….....75

Figure 3.6: Contrast curve at 365 nm of polymer resist **3-3**…….....77

Figure 3.7: Contrast curve at 248 nm of polymer resist **3-3**…….....78

Figure 3.8: SEM images of resist **3-3** profile patterned at 365 nm …….....81

CHAPTER 4

Figure 4.1: Synthetic scheme for compound **4-10**……..105

Figure 4.2: X-ray diffraction spectrum of compound **4-10**…...……...107

Figure 4.3: Synthetic scheme for compound **4-20**……..……109

Figure 4.4: Optical microscope images of patterned oligomer **4-20**…….....111

Figure 4.5: Synthetic scheme for compound **4-25**…….....113

Figure 4.6: Method of decomposition for compound **4-25**…….....116

CHAPTER 5

Figure 5.1: Synthetic scheme for polymer resist **5-1**……..139

Figure 5.2: Polymer resist **5-1** patterned by imprint lithography…...……..140

Figure 5.3: Results of BSA/resist biocompatibility assay……...141

Figure 5.4: Results of monoclonal antibody/resist biocompatibility assay ……...142

Figure 5.5: Results from multiple-cycle tests…..…….....144

Figure 5.6: Patterning process scheme…….....145

Figure 5.7: Fluorescence microscope images of patterned proteins…….....146

Figure 5.8: Fluorescence microscope images of patterned cells……..…….....148

LIST OF TABLES

CHAPTER 1

Table 1.1: Common patterning methods for organic electronics……4

CHAPTER 3

Table 3.1: Polymer composition tested…….67

Table 3.2: Polymer compositions tested…..……..69

Table 3.3: Solubility properties ……73

LIST OF ABBREVIATIONS

ABTS……...….2,2’-Azino-bis(3-ethylbenzthiazoline-6-sulphonic acid)

AFM…….Atomic force microscopy

AIBN…….……Azobisisobutyronitrile

BSA……..Bovine serum albumin

CAR……..Chemically-amplified resist

DMTS……...…...(N,N’-Dimethylamino)trimethylsilane

DNP…….2,4-Dinitrophenyl

DNQ…….Diazonapthoquinone

DPN…….….Dip-pen lithography

HFE……..….Hydrofluoroether

HMDS……Hexamethyldisilazane

HRP…….Horseradish peroxidase

IgE……..…….Immunoglobulin E

IgG……..Immunoglobulin G

ITO……..…Indium tin oxide

n-BuLi……...……n-Butyllithium

nTP…….Nanotransfer printing

OLED……..Organic light-emitting diode

OPV…….Organic photovoltaic

OTFT…….Organic thin-film transistor

P3HT……...Poly(3-hexylthiophene)

PAG……...Photoacid generator

PBS…….….Phosphate buffer solution

PDMS…….Polydimethylsiloxane

PEDOT:PSS……..Poly(3,4-ethylenedioxythiophene):poly(styrenesulfonate)

PI……...Polyimide

PMMA……..……..Poly(methyl methacrylate)

PSA……..….Prostate-specific antigen

RBL-2H3……Rat basophilic leukemia 2H3

SAM……..Self-assembled monolayer

$ScCO_2$……..…Supercritical carbon dioxide

SiO_2……..……Silicon dioxide

t-BuLi…….*tert*-Butyllithium

THF…….……....Tetrahydrofuran

XRD……...X-ray diffraction

µCP……..…..Microcontact printing

µFN……Mircrofluidic network

CHAPTER 1

PATTERNING METHODS FOR ORGANIC ELECTRONICS

1.1 Background for Organic Electronics

Organic electronics is a newly developed field that promises inexpensive, mechanically-flexible, large-area devices[1]. Through the use of solution-processable organic materials, electronic devices can be fabricated on large-area, lightweight, flexible substrates to produce a new class of electronics.

The first light-emitting diodes based on small molecules were reported in 1982[2]. In 1986, a transistor using polythiophene as a semiconductor was reported[3]. A few years later, in 1990 an organic transistor on a plastic substrate was reported using vacuum-evaporated films of α-sexithiophene as the semiconductor on a flexible polymer film made from poly(parabanic acid) resin (PPA) as a substrate [4]. That same year, polymer-based light-emitting diodes were also reported[5]. Although the field of organic electronics is relatively new, it has received significant attention and has been the subject of extensive research in recent years.

Organic electronics have even begun to see some commercial success, especially in the manufacture of organic light-emitting diodes (OLEDs). Sony, LG and in particular Samsung, lead the market in commercial production of OLED displays. Displays for cellular phones are the most common product; OLED television displays are also now commercially available. OLEDs for lighting applications are currently being developed for commercial manufacture by General Electric, among others. Organic thin-film transistors (OTFTs) are also being developed for commercial production. Plastic Logic has used inkjet printing to produce an OTFT-driven electronic reading device. Sony has also been working to commercially produce

OTFTs for flexible OLED displays. Many companies, including Konarka, are working toward the commercial production of organic photovoltaics (OPVs).

1.1.1 Organic Electronic Devices: Transistors, Light-emitters and Photovoltaics

The representative classes of organic electronic devices are thin-film transistors, light-emitting diodes and photovoltaics. These devices promise to revolutionize the electronics field by complementing and improving upon traditional semiconducting devices, offering lower cost and new possibilities in form and structure[6,7].

Although OTFTs do not offer sufficient performance to replace conventional transistors, due to their ability to be manufactured on flexible plastic substrates, OTFTs offer unique mechanical and structural possibilities to complement the existing inorganic semiconductor field[8,9]. Graz *et al*. have recently reported a flexible pentacene OTFT fabricated directly onto elastomeric polydimethylsiloxane (PDMS) membranes at room temperature. The channel stack was shown to withstand repeated mechanical flexing without cracking or electrical failure[10]. This type of flexibility is not possible with conventional semiconductors.

OLEDs have shown better brightness and higher contrast in comparison to traditional inorganic light-emitting diodes[11]. In addition to better performance, the ability to carry out large-area manufacture on plastic substrates opens the possibility for thin, flexible and large-area lighting and displays. Recently, a full color active matrix OLED display on a flexible polyimide (PI) substrate, driven by amorphous indium gallium zinc oxide thin-film transistors was reported. The electrical properties of the TFTs on the flexible PI substrate were indistinguishable from those fabricated on glass substrates. The TFTs showed no performance degradation after bending under tension and compression[12]. In application to general lighting, an OLED was recently reported that is capable of yielding natural sunlight chromaticities with a

color-temperature range fully covering that of entire daylight at different times and regions. The OLED is capable of simultaneously generating all the emissions required to form a series of daylight chromaticities[13]. These and many other examples demonstrate the potential of OLEDs for creating a new class of electronic devices not possible with conventional semiconductors.

Due to their capability for solution processing and plastic substrates, OPVs have the potential to replace their conventional silicon counterparts on the basis of lower cost[14,15]. Conventional photovoltaics, or solar cells, are traditionally manufactured on silicon, which is expensive as well as rigid. Plastic solar cells offer the potential for flexible, lightweight and inexpensive devices. Large-area organic solar cells have recently been reported, using metal sub-electrodes on an indium tin oxide (ITO) anode[16].

1.1.2 Device Manufacture and Marketability

The fabrication or manufacture of organic electronic devices is directly linked to their marketability and ultimately their survival as a viable technology. One of the dominant claims for the pursuit of this field is that organic electronics may enable lower cost electronics. This lower cost claim originates from the potential that organic electronics have for low-cost processing and fabrication. However, for the majority of devices, efficient fabrication and low-cost processing has remained elusive[17].

Patterning methods for organic electronics represents one of the major obstacles to be overcome in organic device fabrication. Depending on device requirements and architecture, patterning methods should provide both high resolution and good registration and be capable of parallel processing for high throughput fabrication[18]. Equipment cost is another major consideration. A patterning method must be developed that is not only able to produce these devices, but at low cost as well.

Table 1.1: Common patterning methods for organic electronics, listed with the predominant strengths and weaknesses of each method.

Patterning Method	**Advantages**	**Disadvantages**
Inkjet Printing	Suitable for large-area devices and roll-to-roll processing	Resolution is on the order of tens of microns, serial process
Microcontact Printing	Inexpensive, parallel process	Poor registration capabilities
Imprint Lithography	High resolution, parallel process	Only applicable to some materials
Shadow Masks	Parallel process, commercially established	Resolution is on the order of tens of microns, requires high-vacuum environment
Photolithography	High resolution, high throughput, registration, well-established	Expensive equipment, harsh processing materials and solvents

Table 1.1 lists the most common patterning methods for organic electronics along with their predominant strengths and weaknesses.

1.2 Patterning Methods in Organic Electronics

Unfortunately, a single patterning method that provides high-resolution, high-throughput, good registration and is universally applicable to all materials and processes does not currently exist. Consequently, numerous methods have been developed to enable patterning of organic electronics; each method has advantages and disadvantages depending upon the device materials and fabrication requirements.

1.2.1 Inkjet Printing

Inkjet printing is perhaps the most prominent of the myriad patterning methods that exist for organic electronic devices. The popularity of this method lies in its potential to scale to large substrates and adapt to continuous processing (roll-to-roll). Inkjet printing also offers a simple additive patterning process and essentially no materials waste. Inkjet printing techniques are already well established, in part because similar systems have long been in use in graphic arts and have thus become well developed[18].

There is a significant push for continuous, roll-to-roll processing in organic electronics fabrication due to its low-cost potential. Roll-to-roll processing is based on the idea that a large-area flexible substrate in a roll, can be unrolled section-by-section, have electronic circuitry patterned on it, and then rolled-up again for the next process step. This is potentially a very high-throughput and cost-effective process. Because inkjet printing is a directly additive process, it is ideally suited to this type of processing.

Additionally, inkjet printing offers a great advantage in its ability to precisely place patterns onto a substrate. Most lithographic patterning methods involve coating an entire substrate with material and selectively removing parts of it to create patterns. Furthermore, the common method of coating a substrate with material is through spin-coating, where material in solution is deposited onto a substrate which is then spun to evenly cast the material across the substrate in a uniform film. During the spin-coating process, most of the material is lost or wasted. In contrast, inkjet printing offers a method of patterning that escapes the inherent wastefulness of traditional patterning processes; the material is directly placed on the substrate in the desired pattern, without need for completely coating the substrate or selective removal of the material.

Inkjet printing operates through scanned small-diameter nozzles, which deposit materials in the liquid phase onto a substrate. Most inkjet printers are drop-on-demand systems, which require either thermally or piezoelectrically generated pulses to eject solution droplets through the nozzle from a reservoir.

Inkjet printing of many organic materials, including poly(3,4-ethylenedioxythiophene) (PEDOT), polyaniline (PANI) and poly(3-hexylthiophene) (P3HT) has been demonstrated[18]. Inorganic materials, such as silicon can also be patterned through this method. For example, cyclopentasilane, a Si-based liquid precursor, can be inkjet printed and then transformed to large-grain poly-Si through pulsed laser annealing[19]. Through the use of photolithgraphically patterned areas of wettability[20], all-polymer TFTs with 5 μm poly(3,4-ethylenedioxythiophene):poly(styrenesulfonate) (PEDOT:PSS) channel length resolution have been produced[21]. By using electron beam (e-beam) lithography to first define hydrophobic mesa structures on the substrate, 500 nm channel lengths have been demonstrated[22]. OLEDs have been fabricated through inkjet printing of

polyvinylcarbazole (PVK) solutions doped with dyes onto an ITO-coated polyester sheet. The smallest pixels were 150 μm in diameter[18]. Another strategy for OLED fabrication is to inkjet print PEDOT onto ITO followed by a blanket deposition of light-emitting layers[23]. A 40-inch full-color OLED display prototype has been recently fabricated using inkjet printing of light-emitting polymers[18].

Despite the great advances that have been made, inkjet printing offers limited resolution and registration capabilities. Typical inkjet printers give drop placement errors of 10 μm; feature resolution is in the tens of micrometers[24-26]. Recent developments in electrohydrodynamic inkjet printing have shown PEDOT:PSS features with 2 μm resolution[27], although this method has only shown compatibility with certain materials. Lack of thickness uniformity may also prove to be an issue. Because evaporation from the edges of an inkjet droplet printed onto a substrate is faster than that from the center, an uneven thickness occurs in each dried film.

1.2.2 Microcontact Printing and Related Methods

Microcontact printing (μCP) was developed nearly two decades ago as an inexpensive patterning technique[28,29]. Microcontact printing is based on a straightforward stamping method and does not require a clean room or expensive photolithographic equipment. This method is able to achieve good resolution and also can be a high-throughput process due to its parallel operation[18]. Furthermore, because the stamps are made of very flexible elastomeric materials, non-planar substrates can also be patterned using this method.

Generally, patterning occurs by a stamp delivering a material to a substrate through direct physical contact. Stamps are made of elastomeric materials, usually PDMS[30]. Contact with the substrate occurs through generalized adhesion forces, without the need for externally applied force[31,32].

One of the primary methods of microcontact printing involves stamping a self-assembled monolayer (SAM) onto a substrate, to be used as a wet etch mask[33]. PDMS is able to take up small, hydrophobic molecules in solution by diffusion through the stamp[34]. Often, the small molecules used are alkanethiols, which are able to form self-assembled monolayers on noble and coinage metals[35-37]. Alkanephosphonic acids can be used to form SAMs on aluminum[38,39] and organosilanes on silica or silicon oxide[40]. These monolayers serve as a mask against a wet etchant. Also SAMs once formed, are actually dewetting surfaces for their ink solutions and because the formation of the SAM is self-limiting[41,42], the stamped monolayer can be uniform regardless of the uniformity of the stamp inking. PDMS stamps can also be inked with hydrophilic solutions, but first require additional treatments of oxidation or functionalization to ensure good loading[39,43].

This method can be used to pattern metal electrodes on OTFTs with submicrometer resolution[44]. Bottom-gate OTFTs of dihexyl quaterthiophene (DH4T) with close to 100 nm channel lengths have been reported[45]. With the use of alkanethiol SAMs, practical resolution limits are about 100 nm[18]. Device performance for these organic devices, patterned through microcontact printing, is comparable to that of devices fabricated through more traditional approaches[46]. OTFTs patterned through microcontact printing have been used to build sexithiophene/F_{16}CuPc complimentary inverter circuits[47], polymer-dispersed liquid crystal (PDLC)[48] and electrophoretic displays[46]. Microcontact printing has even been applied to roll-to-roll processing in the fabrication of P3HT OTFTs[49]. Large-area microcontact printing has been demonstrated in the fabrication of flexible displays[46].

Microcontact printing can also be used to form dewetting templates for use in patterning[50]. Siloxane oligomers already present in PDMS can be stamped onto a substrate to function as a dewetting template[51,52]. Patterning occurs because organic

materials in solution will wet the unstamped areas but leave the stamped areas dry. Organic conductors and semiconductors have been patterned through this method with 1 μm resolution[51]. Other SAMs that create dewetting templates have also been successfully applied to device fabrication[40,50]. Microcontact printing methods that explore wetting templates, as opposed to dewetting, have also had some success[53,54].

A variation of microcontact printing, called transfer printing, enables functional materials to be directly stamped onto a substrate without the need for resists or other imaging materials. This purely additive process is a great advantage because it simplifies fabrication by reducing the number of steps and also doesn't require solvent processing. Transfer printing of metals, nanotransfer printing (nTP), has been used to pattern electrodes in OTFTs[55], OLEDs[56] and OPVs[57]. Nanotransfer printing allows for ~100 nm resolution metal patterning[57]. Small passive matrix OLED displays[56,58] and simple circuits[59] have been fabricated through nTP. Organic conductors such as PEDOT have been transfer printed in the patterning of OLEDs[60] and high-performance top-gate pentacene TFTs[61]. PEDOT transfer printing has also been utilized in the fabrication of all-organic TFTs with pentacene semiconducting layers. Organic semiconductors, such as P3HT[62] and pentacene[63], have been directly patterned by transfer printing to give functional devices. Red, green and blue (RGB) OLED pixels have been fabricated in nanoscale resolution using this method[64]. Subtractive patterning of functional materials has also been developed[65].

One of the greatest disadvantages of microcontact printing is the lack of multilevel registration capability. Several methods have been proposed to address this problem. One method attempts to reduce distortion by minimizing stamp handling: the substrate is laminated against a stabilized PDMS stamp[46]. This method shows distortions of 50-100 μm. Other methods utilize stamps with high-modulus mechanical backings[66,67]. A

method called wave printing achieves 2 μm registration through the use of a glass-backed stamp and an array of pneumatic valves which drive contact and separation [68].

1.2.3 Imprint Lithography and Related Methods

Imprint lithography is emerging as a promising patterning technique for cost-effective patterning of high-resolution devices. This patterning method has extremely high-resolution capabilities as well as the potential for scalability to large-area substrates. Imprint lithography is a parallel operation, and thus high-throughput. Furthermore, imprint lithography equipment is relatively inexpensive. Accurate multi-layer registration is possible. Commercial imprint lithography tools are now common in academic and industrial cleanrooms[18].

Imprint lithography operates by molding a film on a planar substrate through contact with a rigid stamp. The molded, or embossed, film is left with relief features. The thin areas of the film are aniostropically etched to give isolated features. Early imprint methods used high temperatures and pressures to emboss PMMA films[69]. Step and flash imprint lithography (SFIL) was developed as an imprint lithography technique that operates at low pressures and room temperature[70].

OLEDs have been fabricated with imprint lithography having pixel sizes of 2 μm. Poly(methyl methacrylate) (PMMA) on ITO-coated glass was first patterned by imprint lithography. A hole-transporting layer, PEDOT:PSS, and an emissive layer, polyfluorene were consecutively spin-cast. Aluminum (Al) was then deposited to form the cathode[71]. Mechanically flexible OLEDs have also been demonstrated through imprint lithography. ITO on polyethylene terephthalate (PET) was patterned by imprinting and subsequent etching of PMMA. Copper phthalocyanine (CuPc), a hole-injection layer, N,N'-di(napthalen-1-yl)-N,N'-diphenylbenzidine (NPB), a hole-transport layer, tris(8-hydroxyquinolinato)aluminum (Alq_3), an electron transport and

emissive layer, and a cathode layer of lithium fluoride (LiF)/Al were subsequently deposited. Device performance was comparable to similar devices patterned through conventional techniques[69].

Imprint lithography is also used in OTFT electrode patterning. Seventy nanometer channel lengths have been reported for all-polymer TFTs patterned by imprint lithography[72]. In this example, a heavily doped n-type silicon (Si) substrate with a thermally grown oxide and polymeric resist layer was imprinted to pattern gold source and drain electrodes by lift-off. P3HT was then deposited over the electrodes.

Although OTFT patterning has been demonstrated, it may be difficult practically to fabricate more complicated structures such as integrated circuits or probing structures because features with a wide range of sizes are difficult to form with imprint lithography[73]. The challenge is due to the difficulty in filling the relief features of the mold during imprint patterning and in achieving uniformity in the thin areas to be etched. A hybrid system has been developed to address this issue[74]. PMMA is first deposited onto a substrate of highly doped n-type silicon with a thermally grown oxide, followed by a layer of thermally evaporated germanium (Ge), and finally a spin-coated layer of SU-8 resist. The SU-8 is imprinted and then UV-irradiated to cross-link it. The resist is developed and the sample etched through the Ge and PMMA layers and gold (Au) was deposited on top. Lift-off of the resist left source and drain finger electrodes separated by 50 nm and large metal pads (150 μm) for probing.

A fundamental challenge associated with imprint lithography concerns the difficulty in constructing a system of materials and processing conditions that result in good pattern formation. The interaction between the imprint stamp and the organic films they mold is critical. The stamp surface should provide enough wettability to the organic film in order to direct material flow into the recessed structure of the stamp.

At the same time, the surface of the stamp should avoid adhesion with the organic film, which would make clean separation between the stamp and film difficult. Additionally, there are several parameters that must be optimized for each material set including imprint temperature, pressure and time[18].

Embossing is a related patterning method that has found use mostly in photonic and optoelectronic systems. Embossing forms a relief structure in a thin film on a substrate by contact with a rigid stamp. Some degree of external pressure is generally required to form relief features. Polymeric waveguides, distributed feedback (DFB) and distributed Bragg reflector lasers (DBR), 2D photonic crystal structures and lasers, and nonlinear optical (NLO) polymer-based electro-optic devices have all been fabricated by embossing[18]. OLEDs have also been demonstrated with sub-micrometer feature resolution[75].

Capillary molding is another variant of imprint lithography where a flexible mold is laminated against a substrate and the relief spaces are filled with liquid and either used directly or solidified to form a resist or functional device components. OTFT electrodes have been patterned through capillary molding with micrometer resolution[76].

1.2.4 Shadow Masks

Shadow masks have found extensive applications in device patterning. It is typically small molecule organics and metals that are patterned by this method. Shadow masks are physical masks through which vaporized materials are directed onto a substrate. This process occurs at high vacuum. One advantage of shadow mask patterning is that the process is purely additive; sequential layers may be directly deposited.

This patterning process is well established and is already in commercial use. Many commercialized organic devices, including full-color OLED displays, have been fabricated by this patterning method[6,77].

Despite its commercial use, shadow mask patterning leaves much to be desired. Shadow mask resolution is generally on the order of tens of microns[78]. Registration accuracy is of the same order[79]. It is an inherently wasteful process; most of the vaporized material is lost in patterning. Shadow mask patterning also requires a high vacuum chamber. The process is also not easily scalable to large-area substrates.

Shadow masks are typically constructed from thin metal foils. More recently, masks constructed from polymers, such as PDMS, have been developed. These polymer masks are easily fabricated and give higher resolution (5 μm)[80]. Being flexible, they can also be used to pattern non-planar substrates.

Screen printing is a related patterning method which uses a physical mask to pattern liquid materials on a substrate. This is a simple, low-cost patterning process. Many commercially available devices, such as printed circuit boards (PCBs) and solar cells are fabricated through screen printing. Even large-area devices can be patterned very quickly. Screen printing has been used to pattern components of OTFTs and OLEDs[18]. However resolution is limited; feature sizes are ~75 μm, although features as small as 20 μm may be possible[81].

1.2.5 Photolithography and Light-based Patterning Techniques

Photolithography is the most developed and widespread patterning method in many science and technology areas, being the standard patterning method for the semiconductor industry for the past five decades. Countless time and resources have been invested in developing this technique. Photolithography offers many advantages, including very high resolution, excellent registration capabilities and high-throughput.

Direct implementation of this patterning method to organic electronics has been hindered due to the incompatibility of organic electronic materials, with standard photolithographic resists, solvents and developers[82]. Delicate organic materials are often degraded or otherwise damaged by contact with harsh lithographic solvents and resists. For this reason, many methods have been proposed to circumvent this incompatibility issue. However, some materials, which are used in organic devices, such as metals, are not so susceptible to damage by photoresists and solvents as electronic polymers for example, and may be patterned straightforwardly by photolithography.

One approach to addressing the incompatibility issue is to use photoactive precursors, which form functional organic materials upon UV exposure. In this way, the materials are self-patternable, without the need for traditional photoresists or developers. Several precursors for the organic semiconductor pentacene have been reported[83,84]. Mobilities for these materials are slightly lower than with conventionally patterned pentacene[83]. Similar precursor methods for self-patterning of organic conductors, such as polyaniline[85] and polythiophenes[86] have been developed. Organic light-emitting materials have also been self-patterned by photolithography without photoresists or developers[87]. Precursor methods have been demonstrated as well as photobleaching methods[88,89].

Another approach to patterning organic devices by photolithography is a technique called optical soft lithography. This technique has been demonstrated primarily in patterning metals for application in organic devices. In place of a standard photomask, an elastomeric PDMS relief mask is placed directly in contact with the substrate and photoactive film. Upon UV exposure, the light is modulated according to the relief patterns of the mask. Upon development, patterns as small as 100 nm are formed

(with 365 nm light)[90]. A metal layer may be deposited on the resist and patterned by subsequent lift-off.

Focused laser beam scanning is a light-based method that has been demonstrated for organic electronic materials patterning. Patterning occurs through either direct laser ablation or selective laser polymerization of organic electronic materials. A neodymium-doped yttrium aluminium garnet (Nd:YAG) laser was used to pattern a pentacene OTFT by laser ablation[91]. In another example, a 248 nm excimer laser was used to pattern PEDOT in 1 μm resolution by laser ablation in an organic field-effect transistor (OFET[92]). A 442 nm helium cadmium (He-Cd) laser has been shown to pattern P3HT films by selective cross-linking[93]. Resolutions of 1 μm were achieved in poly(3-methylthiophene) (P3MT) and poly(3-butylthiophene) (P3BT) films by crosslinking with a 325 nm He-Cd laser[94].

1.3 Direct Photolithographic Patterning for Organic Electronic Materials

Despite the chemical incompatibility issues that have prevented the direct patterning of organic electronic materials and devices[95], photolithography remains the most mature and developed patterning technique, with sophisticated equipment and a highly successful manufacturing infrastructure already in place. Photolithography is the only patterning method available which simultaneously delivers very high resolution and high throughput capabilities as well as excellent registration and is also generically applicable to nearly all materials and processes.

Photolithographic patterning proceeds by UV exposure of a film of photoactive material on a substrate, through a patterned mask. The mask defines the pattern to be formed on the photoactive film. The photoactive film is called a photoresist. The photoresist has a property such that it chemically differentiates upon UV exposure, so that the areas of the film that were exposed are chemically different from the areas that

were protected from exposure by the mask. Usually this chemical difference is designed to be a solubility change. In this way, with a proper developing solvent, the exposed areas are dissolved and washed away (positive-tone system) to leave the desired patterns in the photoresist. Alternatively, in a negative-tone system, the exposed areas are left behind as patterns and the unexposed areas are dissolved and washed away. Generally, a functional material has been first deposited in a layer below the photoresist; this functional material can then be etched, with the photoactive film serving as an etch mask or resist, protecting the underlying functional material in the desired pattern. Upon removal of the photoresist, the patterned functional material is left on the substrate. The photolithographic process is illustrated in Figure 1.1.

The first photoresists were based on a diazonapthoquinone (DNQ)-Novolac system[96]. The photoactive DNQ molecule, distributed in a matrix of Novolac resin, forms a positive-tone resist system. The hydrophobic DNQ molecule acts as a dissolution inhibitor for the mildly acidic Novolac polymer in aqueous base solutions. Upon UV exposure, the DNQ undergoes a Wolff rearrangement to a hydrophilic indenecarboxylic acid. This carboxylic acid no longer prevents dissolution and UV-exposed regions can be washed away, or developed, by an aqueous base solution, typically a tetramethylammonium hydroxide solution, to leave positive-tone patterns. UV exposure is carried out using 365 or 436 nm light, produced by a mercury arc lamp.

In an effort to increase efficiency and decrease feature sizes, the semiconductor industry turned to chemically amplified resists. In this patterning system, a photoacid generator (PAG) is mixed with an acid-sensitive resist material to form a photoresist layer. Upon UV exposure, the PAG generates a strong acid. With subsequent heating, the generated acid reacts with the acid-sensitive resist material, changing it into a soluble form, while simultaneously regenerating the acid catalyst. This acid catalyst

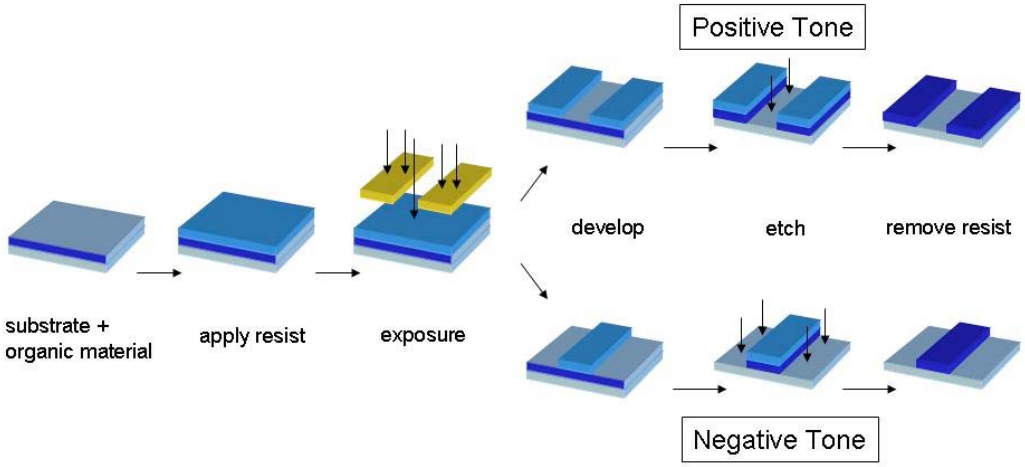

Figure 1.1: Standard photolithographic patterning scheme.

has a turnover rate on the order of 1000, depending on the resist/PAG system. On development, the exposed areas are solubilized and washed away to leave positive-tone patterns. A representative positive-tone chemically amplified resist system is poly(*tert*-butoxycarbonyloxystyrene) (PT-BOCST) and an onium salt PAG. Negative-tone chemically amplified systems have also been developed[96].

It is the incompatibility of organic materials with these photoresists and their processing solvents and developers that is the obstacle to organic electronic materials patterning by photolithography. The ability to directly extend this highly successful patterning technique to organic electronics could revolutionize the field in terms of device possibilities and performance, cost and marketability.

1.3.1 Novel Processing Methods

Several reports have shown that by careful selection of materials and methods, it is possible to pattern some organic electronic materials and devices by photolithography. One of the first approaches, a photolithographically patterned OLED with 300 μm features, was described by Tian *et al*.[97]. ITO on a glass substrate was first coated with polyimide, which was then patterned by standard photolithographic procedures. A layer of silicon dioxide (SiO_2) was then deposited followed by deposition of photoresist. The photoresist layer was patterned by standard photolithographic procedures and the SiO_2 layer was etched to give an undercut profile, by wet etching. Small molecule OLED layers were deposited through vacuum evaporation with a normal, direct incidence angle. After all functional layers had been deposited, a 0.5 μm thick Ag layer was obliquely deposited by vacuum evaporation to cover one side of the organic material. Another oblique deposition at a 180° rotation covered the other side of the organic material to result in a full, protective metal cap. With the organic material fully encapsulated by the metal layer, the photoresist was lifted off to

give the finished, patterned device. The patterning process is shown in Figure 1.2. The protective metal cap has the additional advantage that it also protects the device from environmental contaminants.

Another approach fabricates P3HT OTFTs with 2 μm features patterned by subtractive photolithography[98]. This approach uses a standard photolithographic patterning process, albeit with carefully chosen resists, solvents and organic materials. Gold source and drain electrodes were evaporated and photolithographically patterned onto highly-doped silicon wafers with a thermally grown oxide. A tosylate (OTS) monolayer was deposited to improve the interface between P3HT and the oxide layer. P3HT was deposited onto the substrate, followed by photoresist deposition. A common, commercially available positive-tone resist was used. The photoresist was patterned by standard photolithographic techniques. The P3HT underlayer was then etched and the photoresist was lifted-off to give a patterned P3HT OTFT. Device performance was better for patterned P3HT devices than for the unpatterned P3HT control devices.

DeFranco *et al*. report a direct photolithographic patterning method for organic electronic materials that utilizes poly(*para*-xylene) (Parylene-C) as a protective layer[99]. A pentacene transistor with 2 μm resolution is demonstrated by this patterning method. Parylene is a chemical vapor deposited (CVD) polymer that can be coated at room temperature, gives pinhole-free coatings, and is nearly inert. These properties make it an ideal protective layer for organic electronic materials. Parylene exhibits adhesion properties toward organic films such that it is strong enough to stay in place through processing steps, but is weak enough to allow the parylene to be peeled off the organic layer. Both additive and subtractive patterning methods are enabled by this method. In the subtractive patterning approach, an organic material is first deposited on a substrate. Onto this, a layer of parylene is deposited, followed by photoresist

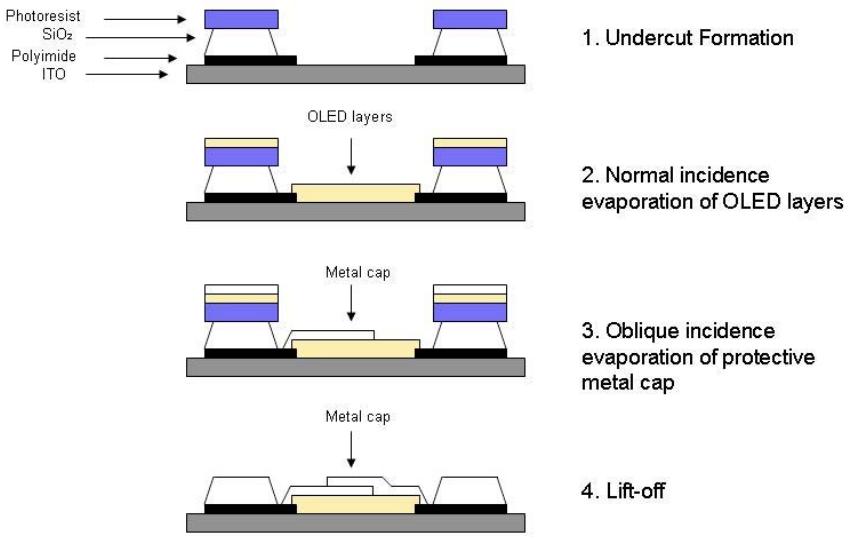

Figure 1.2: Photolithographic patterning scheme used by Tian *et al*.[97]

deposition. The resist is patterned by standard photolithographic procedures and the pattern is transferred through the parylene and organic layers by etching. The parylene layer is then peeled off the organic layer, removing the overlying photoresist layer as well. This approach produces patterned organic materials while avoiding contact between the organic materials, and photoresists and solvents. Subtractive patterning methods are also possible. Both additive and subtractive methods are illustrated in Figure 1.3.

Another approach uses a layer of SU-8 underneath the organic layer[95]. SU-8 is a commercially available negative-tone photoresist. In this approach, a substrate is coated with photoresist and the organic layer is subsequently deposited. This assembly is photolithographically patterned and the resist is developed to leave the patterned organic layer on top of the remaining patterned layer of resist. This approach has been used to fabricate flexible OLEDs and photodiodes.

All of these approaches, though innovative, enable photolithographic patterning of only particular materials and very limited device geometries.

1.3.2 Processing in Orthogonal Solvents

Another approach to the incompatibility issue between organic electronic materials and photolithographic resists and solvents has been to develop benign photolithographic resists and solvents.

One of the first examples of a benign photolithographic resist and solvent system was reported by Hwang *et al*[100]. This approach uses supercritical carbon dioxide ($scCO_2$) as a developing solvent. $ScCO_2$ is non-toxic and environmentally friendly as well as a nondestructive medium for organic electronic materials. By using a gentle processing solvent and compatible photoresist, organic electronic materials may be

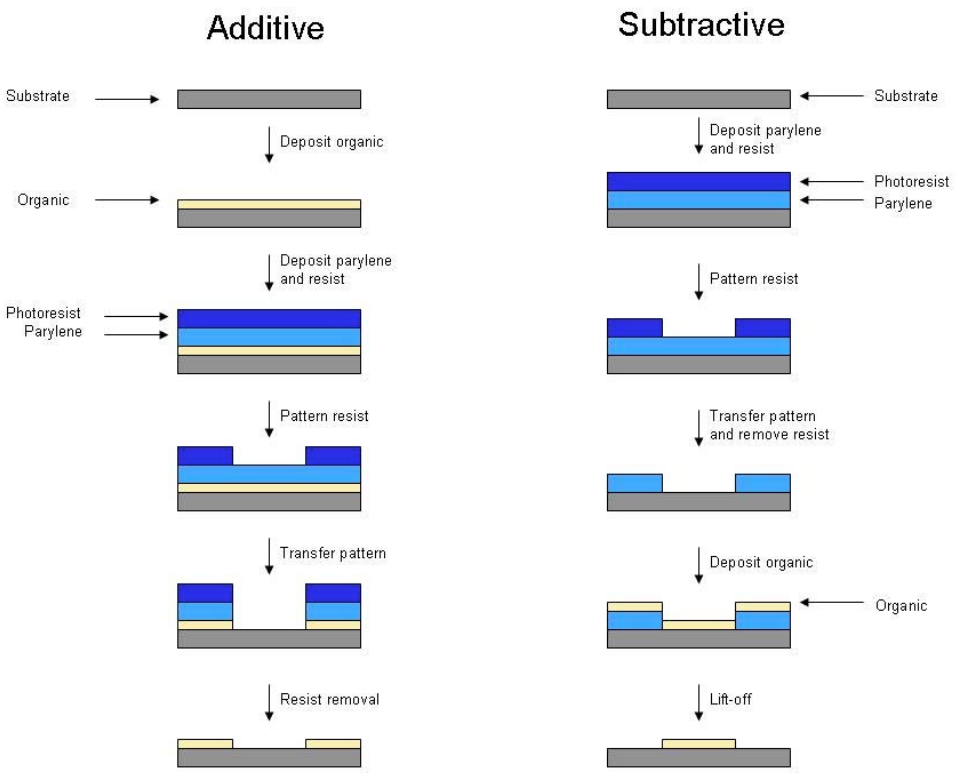

Figure 1.3: Photolithographic patterning schemes used by DeFranco *et al*.[99]

patterned without the swelling, cracking and delamination that is typical of photolithographically patterned organic materials. The photoresist used was highly fluorinated and was synthesized as a copolymer of 1*H*,1*H*,2*H*,2*H*-perfluorodecyl methacrylate (FDMA) and *tert*-butyl methacrylate (TBMA). The patterning process follows the standard photolithographic scheme, but with non-damaging photoresists and processing solvents in place of traditional patterning materials. The active organic material is deposited on a substrate, followed by photoresist deposition. The photoresist is exposed and patterned, using $scCO_2$ as a developing solvent. The pattern is transferred through the active organic layer by etching and the photoresist is removed to give undamaged patterned functional materials. The patterning process is illustrated in Figure 1.4. A patterned OLED with micrometer resolution was also demonstrated.

Another example of this approach uses hydrofluoroether solvents as a benign processing solvent, instead of $scCO_2$. It has been shown recently that hydrofluoroethers are chemically benign materials to organic electronics[101]. In a recent study, representative OLEDs and OTFTs were shown to operate while immersed in boiling hydrofluoroether solvents without any degradation of device performance or other adverse effects. Organic electronic materials are unaffected by these solvents. Furthermore, these solvents have been shown to be non-toxic and environmentally friendly. By developing a photoresist, processable in these solvents and which is also benign to organic electronic materials, a novel imaging system for photolithographic patterning of organic electronics is demonstrated[102]. The photoresist used was a heavily fluorinated small molecule molecular glass structure. With addition of a PAG, it is solubilized in and deposited from hydrofluoroether solvents onto a substrate. Standard photolithographic patterning and subsequent development in hydrofluoroethers yields patterned photoresist. The functional organic material is

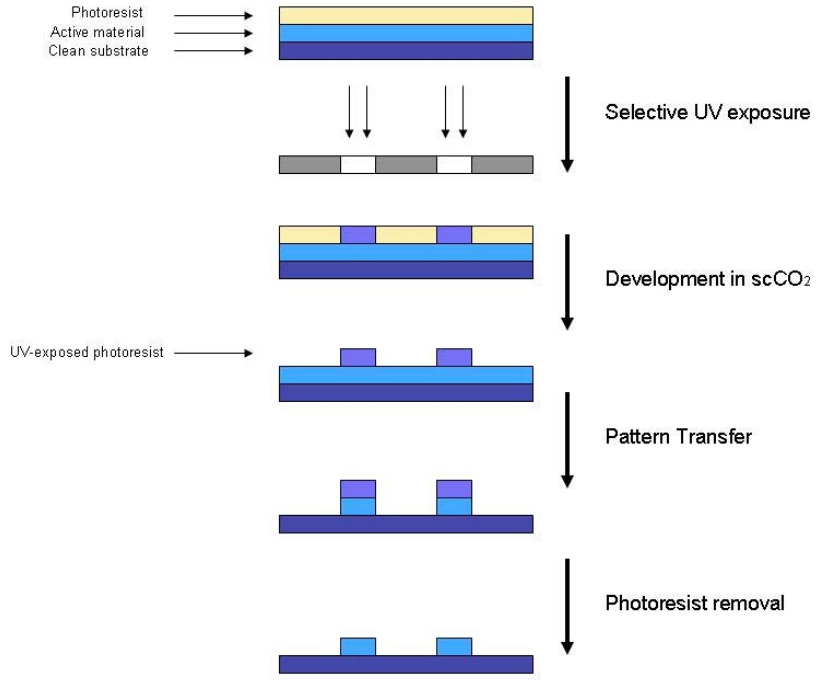

Figure 1.4: Photolithographic patterning scheme used by Hwang *et al*.[100]

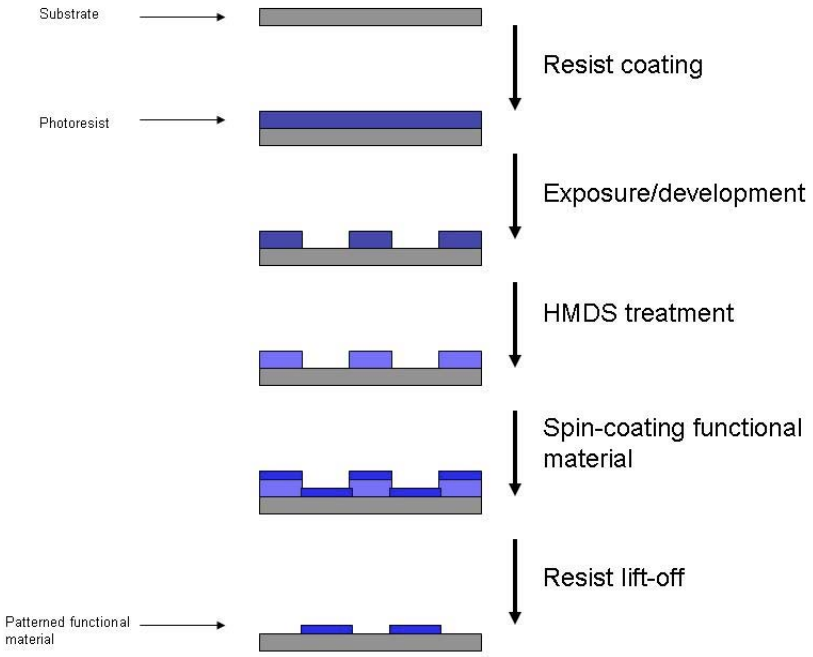

Figure 1.5: Photolithographic patterning scheme used by Lee *et al*.[102]

deposited and the patterned resist is lifted-off by dissolution in hydrofluoroethers, leaving the patterned functional organic material behind. The general patterning scheme is illustrated in Figure 1.5.

These methods employing benign photoresists and processing solvents are promising in that they enable the straightforward photolithographic patterning of organic electronic materials. However, the materials are expensive and uncommon.

1.4 Summary

Based upon these findings, a significant need still exists to identify an ideal patterning method for organic electronic devices. A high-resolution, high-throughput system with good registration capabilities is required to realize the potential for organic electronics, both in performance and commercialization. Despite the extensive research that has been accomplished in this field thus far, such a system has not yet been developed. This thesis presents research performed toward the goal of developing patterning methods for organic electronic devices.

This thesis is organized into sections, each describing a different resist system, which was developed for patterning organic electronic devices. All of the systems consist of fluorinated resist materials, which were designed and synthesized to be fully processable in hydrofluoroether solvents. These fluorinated materials and solvents can be used to lithographically pattern organic electronic devices in a high-resolution and high-throughput manner, without the typical incompatibility issues that exist between organic materials and conventional processing solvents and resists.

In Chapter 2, a negative-tone non-chemically amplified photoresist is described. This photoresist is particularly useful for patterning acidic materials, namely the widely used conducting polymer PEDOT:PSS. By nature, chemically-amplified resists are acid-sensitive, relying on a photoacid generator to activate them. This

property causes premature and nonspecific activation of the resist when patterning an acidic material with an acid-sensitive resist. By using a non-acid sensitive system, even acidic materials can be easily patterned. However, negative-tone patterns do not necessarily enable all device geometries. Positive-tone patterning is also a valuable capability. Chapter 3 presents a non-chemically amplified positive-tone resist system. With both negative-tone and positive-tone photoresist systems, essentially all device geometries are attainable.

These photoresists are passive materials in organic electronics fabrication, meaning that they are used to facilitate fabrication, but are not present in the finished device. Alternatively, functional materials are those that are present in the actual device, performing some function. Chapter 4 presents a novel system based on the idea of a self-patternable functional material. An electroluminescent organic material was designed and synthesized with patternable end-groups. Typically, a functional material is coated on a substrate, followed by photoresist deposition and patterning. The pattern is then transferred through to the functional material. Alternatively, the photoresist layer can be patterned first and then the functional material deposited onto this and patterned by lift-off. Following either route, two separate layers are required: a functional layer and a passive layer (photoresist), which serves to pattern the functional layer. By creating a functional electroluminescent material, which is also photopatternable, the need for a separate photoresist layer is circumvented; the functional material is self-patternable.

Chapter 5 describes the design and synthesis of another fluorinated resist system, patternable by imprint lithography. To further demonstrate the benign properties of these fluorinated materials and solvents, this patterning system was applied to biomolecule patterning. Biomolecule patterning is not only useful for organic electronic biosensor applications, but also for the fabrication of biomolecule arrays for

fundamental biological studies and tissue engineering, among many other applications. By demonstrating both patterning capabilities of the resist system and the benign properties of these materials toward biomolecules, a lithographic method for straightforwardly patterning biomolecules is enabled. Chapter 6 discusses future directions for this work and the research as a whole, presented in this thesis.

REFERENCES

(1) Malliaras, G.; Friend, R. *Phys. Today* **2005**, *58*, 53-58.

(2) Vincett, P. S.; Barlow, W. A.; Hann, R. A.; Roberts, G. G. *Thin Solid Films* **1982**, *94*, 171-183.

(3) Tsumura, A.; Koezuka, H.; Ando, T. *Appl. Phys. Lett.* **1986**, *49*, 1210-1212.

(4) Garnier, F.; Horowitz, G.; Peng, X. H.; Fichou, D. *Adv. Mater.* **1990**, *2*, 592-594.

(5) Burroughes, J. H.; Bradley, D. D. C.; Brown, A. R.; Marks, R. N.; Mackay, K.; Friend, R. H.; Burns, P. L.; Holmes, A. B. *Nature* **1990**, *347*, 539-541.

(6) Forrest, S. R. *Nature* **2004**, *428*, 911-918.

(7) Kelley, T. W.; Baude, P. F.; Gerlach, C.; Ender, D. E.; Muyres, D.; Haase, M. A.; Vogel, D. E.; Theiss, S. D. *Chem. Mat.* **2004**, *16*, 4413-4422.

(8) Horowitz, G. *J. Mater. Res.* **2004**, *19*, 1946-1962.

(9) de Leeuw, D. M.; Cantatore, E. *Materials Science in Semiconductor Processing* **2008**, *11*, 199-204.

(10) Graz, I. M.; Lacour, S. P. *Appl. Phys. Lett.* **2009**, *95*, 3.

(11) Forrest, S. R.; Thompson, M. E. *Chem. Rev.* **2007**, *107*, 923-925.

(12) Park, J. S.; Kim, T. W.; Stryakhilev, D.; Lee, J. S.; An, S. G.; Pyo, Y. S.; Lee, D. B.; Mo, Y. G.; Jin, D. U.; Chung, H. K. *Appl. Phys. Lett.* **2009**, *95*, 3.

(13) Jou, J. H.; Wu, M. H.; Shen, S. M.; Wang, H. C.; Chen, S. Z.; Chen, S. H.; Lin, C. R.; Hsieh, Y. L. *Appl. Phys. Lett.* **2009**, *95*, 3.

(14) Hoppe, H.; Sariciftci, N. S. *J. Mater. Res.* **2004**, *19*, 1924-1945.

(15) Brunetti, F. G.; Kumar, R.; Wudl, F. *J. Mater. Chem.*, *20*, 2934-2948.

(16) Park, S. Y.; Jeong, W. I.; Kim, D. G.; Kim, J. K.; Lim, D. C.; Kim, J. H.; Kim, J. J.; Kang, J. W. *Appl. Phys. Lett.*, *96*, 3.

(17) Sheats, J. R. *J. Mater. Res.* **2004**, *19*, 1974-1989.

(18) Menard, E.; Meitl, M. A.; Sun, Y. G.; Park, J. U.; Shir, D. J. L.; Nam, Y. S.; Jeon, S.; Rogers, J. A. *Chem. Rev.* **2007**, *107*, 1117-1160.

(19) Shimoda, T.; Matsuki, Y.; Furusawa, M.; Aoki, T.; Yudasaka, I.; Tanaka, H.; Iwasawa, H.; Wang, D. H.; Miyasaka, M.; Takeuchi, Y. *Nature* **2006**, *440*, 783-786.

(20) Sirringhaus, H.; Kawase, T.; Friend, R. H.; Shimoda, T.; Inbasekaran, M.; Wu, W.; Woo, E. P. *Science* **2000**, *290*, 2123-2126.

(21) Khatavkar, V. V.; Anderson, P. D.; Duineveld, P. C.; Meijer, H. H. E. *Macromol. Rapid Commun.* **2005**, *26*, 298-303.

(22) Wang, J. Z.; Zheng, Z. H.; Li, H. W.; Huck, W. T. S.; Sirringhaus, H. *Nat. Mater.* **2004**, *3*, 171-176.

(23) Bharathan, J.; Yang, Y. *Appl. Phys. Lett.* **1998**, *72*, 2660-2662.

(24) Cheng, K.; Yang, M. H.; Chiu, W. W. W.; Huang, C. Y.; Chang, J.; Ying, T. F.; Yang, Y. *Macromol. Rapid Commun.* **2005**, *26*, 247-264.

(25) Creagh, L. T.; McDonald, M. *MRS Bull.* **2003**, *28*, 807-811.

(26) de Gans, B. J.; Duineveld, P. C.; Schubert, U. S. *Adv. Mater.* **2004**, *16*, 203-213.

(27) Li, D.; Xia, Y. N. *Adv. Mater.* **2004**, *16*, 1151-1170.

(28) Kumar, A.; Whitesides, G. M. *Appl. Phys. Lett.* **1993**, *63*, 2002-2004.

(29) Wilbur, J. L.; Kumar, A.; Kim, E.; Whitesides, G. M. *Adv. Mater.* **1994**, *6*, 600-604.

(30) Truong, T. T.; Lin, R. S.; Jeon, S.; Lee, H. H.; Maria, J.; Gaur, A.; Hua, F.; Meinel, I.; Rogers, J. A. *Langmuir* **2007**, *23*, 2898-2905.

(31) Huang, Y. G. Y.; Zhou, W. X.; Hsia, K. J.; Menard, E.; Park, J. U.; Rogers, J. A.; Alleyne, A. G. *Langmuir* **2005**, *21*, 8058-8068.

(32) Zhou, W.; Huang, Y.; Menard, E.; Aluru, N. R.; Rogers, J. A.; Alleyne, A. G. *Appl. Phys. Lett.* **2005**, *87*, 3.

(33) Xia, Y. N.; Zhao, X. M.; Whitesides, G. M. *Microelectron. Eng.* **1996**, *32*, 255-268.

(34) Balmer, T. E.; Schmid, H.; Stutz, R.; Delamarche, E.; Michel, B.; Spencer, N. D.; Wolf, H. *Langmuir* **2005**, *21*, 622-632.

(35) Geissler, M.; Schmid, H.; Michel, B.; Delamarche, E. *Microelectron. Eng.* **2003**, *67-8*, 326-332.

(36) Kumar, A.; Biebuyck, H. A.; Whitesides, G. M. *Langmuir* **1994**, *10*, 1498-1511.

(37) Tate, J.; Rogers, J. A.; Jones, C. D. W.; Vyas, B.; Murphy, D. W.; Li, W. J.; Bao, Z. A.; Slusher, R. E.; Dodabalapur, A.; Katz, H. E. *Langmuir* **2000**, *16*, 6054-6060.

(38) Geissler, M.; Wolf, H.; Stutz, R.; Delamarche, E.; Grummt, U. W.; Michel, B.; Bietsch, A. *Langmuir* **2003**, *19*, 6301-6311.

(39) Goetting, L. B.; Deng, T.; Whitesides, G. M. *Langmuir* **1999**, *15*, 1182-1191.

(40) Kagan, C. R.; Breen, T. L.; Kosbar, L. L. *Appl. Phys. Lett.* **2001**, *79*, 3536-3538.

(41) Biebuyck, H. A.; Whitesides, G. M. *Langmuir* **1994**, *10*, 4581-4587.

(42) Biebuyck, H. A.; Whitesides, G. M. *Langmuir* **1994**, *10*, 2790-2793.

(43) Delamarche, E.; Geissler, M.; Bernard, A.; Wolf, H.; Michel, B.; Hilborn, J.; Donzel, C. *Adv. Mater.* **2001**, *13*, 1164-+.

(44) Delamarche, E.; Schmid, H.; Bietsch, A.; Larsen, N. B.; Rothuizen, H.; Michel, B.; Biebuyck, H. *J. Phys. Chem. B* **1998**, *102*, 3324-3334.

(45) Leufgen, M.; Lebib, A.; Muck, T.; Bass, U.; Wagner, V.; Borzenko, T.; Schmidt, G.; Geurts, J.; Molenkamp, L. W. *Appl. Phys. Lett.* **2004**, *84*, 1582-1584.

(46) Rogers, J. A.; Bao, Z.; Baldwin, K.; Dodabalapur, A.; Crone, B.; Raju, V. R.; Kuck, V.; Katz, H.; Amundson, K.; Ewing, J.; Drzaic, P. *Proc. Natl. Acad. Sci. U. S. A.* **2001**, *98*, 4835-4840.

(47) Rogers, J. A.; Bao, Z. N.; Dodabalapur, A.; Makhija, A. *IEEE Electron Device Lett.* **2000**, *21*, 100-103.

(48) Mach, P.; Rodriguez, S. J.; Nortrup, R.; Wiltzius, P.; Rogers, J. A. *Appl. Phys. Lett.* **2001**, *78*, 3592-3594.

(49) Rogers, J. A.; Bao, Z. N.; Makhija, A.; Braun, P. *Adv. Mater.* **1999**, *11*, 741-745.

(50) Lee, K. S.; Blanchet, G. B.; Gao, F.; Loo, Y. L. *Appl. Phys. Lett.* **2005**, *86*, 3.

(51) Briseno, A. L.; Roberts, M.; Ling, M. M.; Moon, H.; Nemanick, E. J.; Bao, Z. N. *J. Am. Chem. Soc.* **2006**, *128*, 3880-3881.

(52) Glasmastar, K.; Gold, J.; Andersson, A. S.; Sutherland, D. S.; Kasemo, B. *Langmuir* **2003**, *19*, 5475-5483.

(53) Huang, Z. Y.; Wang, P. C.; MacDiarmid, A. G.; Xia, Y. N.; Whitesides, G. *Langmuir* **1997**, *13*, 6480-6484.

(54) Hidber, P. C.; Helbig, W.; Kim, E.; Whitesides, G. M. *Langmuir* **1996**, *12*, 1375-1380.

(55) Cosseddu, P.; Bonfiglio, A. *Appl. Phys. Lett.* **2006**, *88*, 3.

(56) Kim, C.; Burrows, P. E.; Forrest, S. R. *Science* **2000**, *288*, 831-833.

(57) Kim, C.; Shtein, M.; Forrest, S. R. *Appl. Phys. Lett.* **2002**, *80*, 4051-4053.

(58) Rhee, J.; Lee, H. H. *Appl. Phys. Lett.* **2002**, *81*, 4165-4167.

(59) Loo, Y. L.; Willett, R. L.; Baldwin, K. W.; Rogers, J. A. *Appl. Phys. Lett.* **2002**, *81*, 562-564.

(60) Granlund, T.; Nyberg, T.; Roman, L. S.; Svensson, M.; Inganas, O. *Adv. Mater.* **2000**, *12*, 269-273.

(61) Li, D. W.; Guo, L. J. *Appl. Phys. Lett.* **2006**, *88*, 3.

(62) Park, S. K.; Kim, Y. H.; Han, J. I.; Moon, D. G.; Kim, W. K. *IEEE Trans. Electron Devices* **2002**, *49*, 2008-2015.

(63) Hines, D. R.; Mezhenny, S.; Breban, M.; Williams, E. D.; Ballarotto, V. W.; Esen, G.; Southard, A.; Fuhrer, M. S. *Appl. Phys. Lett.* **2005**, *86*, 3.

(64) Choi, J. H.; Kim, K. H.; Choi, S. J.; Lee, H. H. *Nanotechnology* **2006**, *17*, 2246-2249.

(65) Wang, Z.; Zhang, J.; Xing, R.; Yuan, J. F.; Yan, D. H.; Han, Y. C. *J. Am. Chem. Soc.* **2003**, *125*, 15278-15279.

(66) Burgin, T.; Choong, V. E.; Maracas, G. *Langmuir* **2000**, *16*, 5371-5375.

(67) Menard, E.; Bilhaut, L.; Zaumseil, J.; Rogers, J. A. *Langmuir* **2004**, *20*, 6871-6878.

(68) Burdinski, D.; Brans, H. J. A.; Decre, M. M. J. *J. Am. Chem. Soc.* **2005**, *127*, 10786-10787.

(69) Kao, P. C.; Chu, S. Y.; Chen, T. Y.; Zhan, C. Y.; Hong, F. C.; Chang, C. Y.; Hsu, L. C.; Liao, W. C.; Hon, M. H. *IEEE Trans. Electron Devices* **2005**, *52*, 1722-1726.

(70) Bailey, T. C.; Johnson, S. C.; Sreenivasan, S. V.; Ekerdt, J. G.; Willson, C. G.; Resnick, D. J. *J. Photopolym Sci. Technol.* **2002**, *15*, 481-486.

(71) Cheng, X.; Hong, Y. T.; Kanicki, J.; Guo, L. J. *J. Vac. Sci. Technol. B* **2002**, *20*, 2877-2880.

(72) Austin, M. D.; Chou, S. Y. *Appl. Phys. Lett.* **2002**, *81*, 4431-4433.

(73) Gottschalch, F.; Hoffmann, T.; Torres, C. M. S.; Schulz, H.; Scheer, H. C. *Solid-State Electron*. **1999**, *43*, 1079-1083.

(74) Cheng, X.; Li, D. W.; Guo, L. J. *Nanotechnology* **2006**, *17*, 927-932.

(75) Rogers, J. A.; Bao, Z. N.; Dhar, L. *Appl. Phys. Lett.* **1998**, *73*, 294-296.

(76) Rogers, J. A.; Bao, Z. N.; Raju, V. R. *Appl. Phys. Lett.* **1998**, *72*, 2716-2718.

(77) Bartic, C.; Jansen, H.; Campitelli, A.; Borghs, S. *Org. Electron.* **2002**, *3*, 65-72.

(78) Ling, M. M.; Bao, Z. N. *Chem. Mat.* **2004**, *16*, 4824-4840.

(79) Tian, P. F.; Bulovic, V.; Burrows, P. E.; Gu, G.; Forrest, S. R.; Zhou, T. X. *J. Vac. Sci. Technol. A-Vac. Surf. Films* **1999**, *17*, 2975-2981.

(80) Duffy, D. C.; Jackman, R. J.; Vaeth, K. M.; Jensen, K. F.; Whitesides, G. M. *Adv. Mater.* **1999**, *11*, 546-+.

(81) Bao, Z. N.; Feng, Y.; Dodabalapur, A.; Raju, V. R.; Lovinger, A. J. *Chem. Mat.* **1997**, *9*, 1299-&.

(82) Logothetidis, S. *Mater. Sci. Eng. B-Adv. Funct. Solid-State Mater.* **2008**, *152*, 96-104.

(83) Afzali, A.; Dimitrakopoulos, C. D.; Graham, T. O. *Adv. Mater.* **2003**, *15*, 2066-+.

(84) Weidkamp, K. P.; Afzali, A.; Tromp, R. M.; Hamers, R. J. *J. Am. Chem. Soc.* **2004**, *126*, 12740-12741.

(85) Drury, C. J.; Mutsaers, C. M. J.; Hart, C. M.; Matters, M.; de Leeuw, D. M. *Appl. Phys. Lett.* **1998**, *73*, 108-110.

(86) Yu, J. F.; Abley, M.; Yang, C.; Holdcroft, S. *Chem. Commun.* **1998**, 1503-1504.

(87) Muller, C. D.; Falcou, A.; Reckefuss, N.; Rojahn, M.; Wiederhirn, V.; Rudati, P.; Frohne, H.; Nuyken, O.; Becker, H.; Meerholz, K. *Nature* **2003**, *421*, 829-833.

(88) Pogantsch, A.; Rentenberger, S.; Langer, G.; Keplinger, J.; Kern, W.; Zojer, E. *Adv. Funct. Mater.* **2005**, *15*, 403-409.

(89) Kocher, C.; Montali, A.; Smith, P.; Weder, C. *Adv. Funct. Mater.* **2001**, *11*, 31-35.

(90) Rogers, J. A.; Dodabalapur, A.; Bao, Z. N.; Katz, H. E. *Appl. Phys. Lett.* **1999**, *75*, 1010-1012.

(91) Yagi, I.; Tsukagoshi, K.; Aoyagi, Y. *Appl. Phys. Lett.* **2004**, *84*, 813-815.

(92) Schrodner, M.; Stohn, R. I.; Schultheis, K.; Sensfuss, S.; Roth, H. K. *Org. Electron.* **2005**, *6*, 161-167.

(93) Abdou, M. S. A.; Zi, W. X.; Leung, A. M.; Holdcroft, S. *Synth. Met.* **1992**, *52*, 159-170.

(94) Wong, T. K. S.; Gao, S.; Hu, X.; Liu, H.; Chan, Y. C.; Lam, Y. L. *Mater. Sci. Eng. B-Solid State Mater. Adv. Technol.* **1998**, *55*, 71-78.

(95) Huang, J.; Xia, R.; Kim, Y.; Wang, X.; Dane, J.; Hofmann, O.; Mosley, A.; de Mello, A. J.; de Mello, J. C.; Bradley, D. D. C. *J. Mater. Chem.* **2007**, *17*, 1043-1049.

(96) Wallraff, G. M.; Hinsberg, W. D. *Chem. Rev.* **1999**, *99*, 1801-1821.

(97) Tian, P. F.; Burrows, P. E.; Forrest, S. R. *Appl. Phys. Lett.* **1997**, *71*, 3197-3199.

(98) Balocco, C.; Majewski, L. A.; Song, A. M. *Org. Electron.* **2006**, *7*, 500-507.

(99) DeFranco, J. A.; Schmidt, B. S.; Lipson, M.; Malliaras, G. G. *Org. Electron.* **2006**, *7*, 22-28.

(100) Hwang, H. S.; Zakhidov, A. A.; Lee, J. K.; Andre, X.; DeFranco, J. A.; Fong, H. H.; Holmes, A. B.; Malliaras, G. G.; Ober, C. K. *J. Mater. Chem.* **2008**, *18*, 3087-3090.

(101) Zakhidov, A. A.; Lee, J. K.; Fong, H. H.; DeFranco, J. A.; Chatzichristidi, M.; Taylor, P. G.; Ober, C. K.; Malliaras, G. G. *Adv. Mater.* **2008**, *20*, 3481-+.

(102) Lee, J. K.; Chatzichristidi, M.; Zakhidov, A. A.; Taylor, P. G.; DeFranco, J. A.; Hwang, H. S.; Fong, H. H.; Holmes, A. B.; Malliaras, G. G.; Ober, C. K. *J. Am. Chem. Soc.* **2008**, *130*, 11564-+.

CHAPTER 2

A NON-CHEMICALLY AMPLIFIED NEGATIVE-TONE PHOTORESIST FOR PATTERNING ORGANIC ELECTRONICS WITH HYDROFLUORETHER SOLVENTS

Portions of this chapter are adapted from *Advanced Materials,* **2009**, *21,* 2314-2317, with permission from the publisher.

Abstract

Organic electronics is a new field promising flexible, large-scale devices with better performance and at lower cost than traditional electronics. However, one of the major obstacles that this field has experienced is the difficulty in patterning organic electronic materials. Conventional electronic devices are patterned by photolithography. Unfortunately, this high-resolution, high-throughput and well-established patterning method has not yet been successfully extended to organic electronics patterning due to incompatibility issues between delicate organic materials and the harsh solvents and resists typical of photolithographic processing. A new patterning system based on a specially tailored fluorinated polymer photoresist is presented. This fluorinated photoresist is processable in hydrofluoroether solvents, which have previously been shown to be benign solvents to organic electronic materials. By replacing the traditional photolithographic resists and processing solvents with organic materials-compatible fluorinated photoresists and solvents, photolithography can be directly applied to organic electronic materials patterning. Submicron resolution at 365 nm exposure and 100 nm resolution with electron-beam lithography is demonstrated with this system. Thin-film transistors with PEDOT:PSS

electrodes and a pentacene channel were fabricated and device performance was shown to be comparable to the reported values of similar devices which were fabricated through more traditional routes. These results show that this fluorinated photolithographic patterning system is not damaging to organic electronic materials.

2.1 Introduction

Organic electronics is an emerging technology opening new opportunities in the field of large area electronics.[1] It has received enormous attention as a technology platform enabling flexible, large-scale devices, by exploiting the unique properties of organic materials.[2] In addition, organic electronics offers the possibility of affordable manufacture of devices through solution processing of active materials.[3,4]

Before this vision is realized, several challenges must be overcome, particularly issues of patterning. Patterning of electronic materials enables microscale device structures to be defined for organic light-emitting diode (OLED) displays and organic thin-film transistors (OTFT). Additionally, patterning enhances device performance by preventing cross-talk, increasing transconductance and preventing high off-currents in transistor arrays or drivers.[5]

In spite of the proven technical advantages, conventional photolithography has not been recognized as a suitable technique for patterning organic electronic materials. It is presently hindered by concerns of chemical deterioration of active organic materials upon exposure to process solvents for lithography.[6] By introducing a new set of benign processes involving new specially tailored photopolymers, this problem can be circumvented.[7]

Recently, hydrofluoroethers (HFEs), a family of non-toxic and environmentally-friendly solvents,[8] have been identified as chemically benign to non-fluorinated organic electronic materials. Not only are they benign, but HFEs are orthogonal

solvents to many organic compounds, that is, the organic compounds are insoluble and are not swollen in HFEs.[9,10] This is a particularly useful property in the fabrication of multi-level devices since new layers can be added without damage to existing ones.[11]

The challenge was therefore to develop compatible lithographic materials for these new process solvents. By employing a fluorinated photoresist, compatible with HFEs, sub-micron photolithographic patterning of organic electronic materials can be demonstrated.

Poly(3,4-ethylenedioxythiophene):poly(styrenesulfonate) (PEDOT:PSS) is a mechanically flexible, transparent and highly conductive polymer blend, which has found various applications in organic electronics including serving as the electrode material for plastic substrates due to its low-temperature processing requirements, and as charge injection/extraction layers in OLEDs and photovoltaic devices.[12-14] However, photolithographic patterning of PEDOT:PSS for device components is not straightforward because i) PEDOT:PSS films are damaged by aqueous solutions, which are standard developers in conventional photolithography and ii) acid sensitive photoresists are adversely affected by the acidic PEDOT:PSS.

Here, a unique acid stable imaging material for PEDOT:PSS and organic electronic materials in general is presented. The sub-micron patterning of PEDOT:PSS films is reported and their subsequent application to the fabrication of a field-effect transistor, in which an organic semiconductor material, pentacene, is patterned by the same protocol.

In designing an HFE-compatible photoresist, it was most important that the photoresist be soluble in the fluorous solvents. In general, fluorous solvents dissolve highly fluorinated materials.[15] The copolymer **2-3** derived from the highly fluorinated monomer **2-1** and photo-labile monomer **2-2** was expected to yield a material which

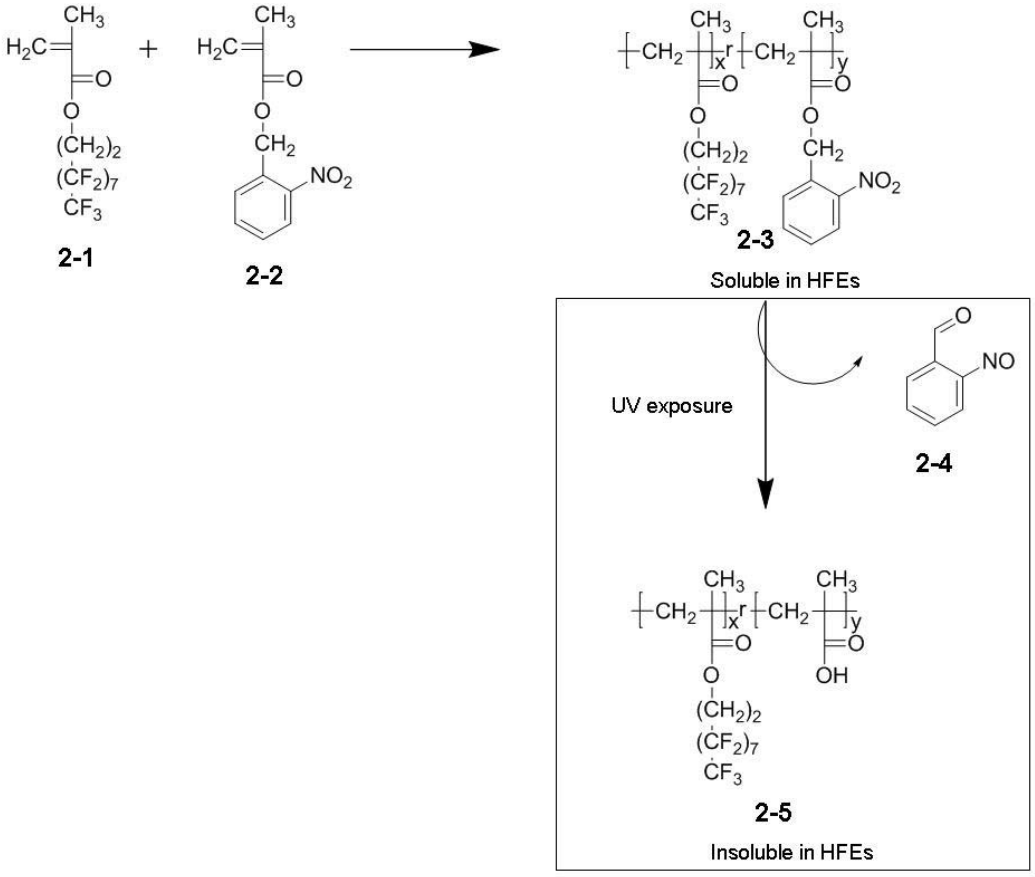

Figure 2.1: Synthesis of the UV-sensitive polymer acid stable resist **2-3** and photo-induced deprotection reaction to polymeric carboxylic acid **2-5**.

a)

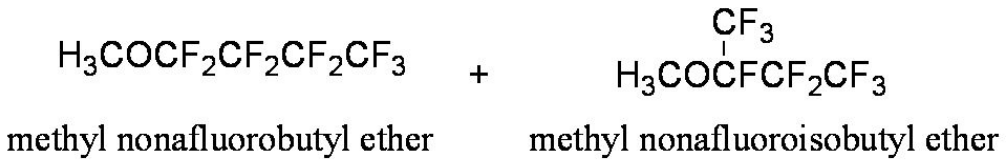

methyl nonafluorobutyl ether methyl nonafluoroisobutyl ether

b)

ethyl nonafluorobutyl ether ethyl nonafluoroisobutyl ether

c)

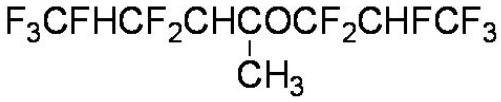

1,1,1,2,3,3,-hexafluoro-4-(1,1,2,3,3,3-hexafluoropropoxy)-pentane

Figure 2.2: 3M Novec Hydrofluoroether structures. (a) HFE-7100 (isomeric mixture of methyl nonafluorobutyl ether and methyl nonafluoroisobutyl ether), (b) HFE-7200 (isomeric mixture of ethyl nonafluorobutyl ether and ethyl nonafluoroisobutyl ether), (c) HFE-7600 (1,1,1,2,3,3-hexafluoro-4-(1,1,2,3,3,3-hexafluoropropoxy-pentane).

exhibits a solubility switch following UV irradiation (Figure 2.1).[7,16] The photo-labile component, the ester of 2-nitrobenzyl alcohol and methacrylic acid, decomposes under UV exposure to yield a carboxylic acid and nitrosobenzaldehyde **2-4**.[17] The resulting polymer **2-5** is no longer soluble in HFEs. Following development in HFEs, the still-soluble unexposed regions are washed away to leave the insoluble exposed area as a negative-tone image.

2.2 Experimental Section

2.2.1 Materials

3,3,4,4,5,5,6,6,7,7,8,8,9,9,10,10,10-Heptadecafluorodecyl methacrylate **2-1** and benzotrifluoride were purchased from Sigma-Aldrich and used as received. AIBN was recrystallized from $CHCl_3$. 3M™ Novec™ Engineered Fluid HFE-7100, 7200, and 7600 were donated from 3M USA (Structures shown in Figure 2.2). PEDOT:PSS was purchased from H. C. Starck and used as received. Pentacene was purchased from Kintec and used as received.

2.2.2 Synthesis of the polymer photoresist **2-3**

2-Nitrobenzyl methacrylate **2-2** (prepared according to the literature procedure[16], further purified by recrystallization from CH_2Cl_2-hexanes mixed solvent after column chromatography) (1.05 g, 4.75 mmol) and 3,3,4,4,5,5,6,6,7,7,8,8,9,9,10,10,10-heptadecafluorodecyl methacrylate (5.95 g, 11.2 mmol) were added to a 25 cm^3 schlenk tube. Benzotrifluoride (7 cm^3) and AIBN (0.07 g, 0.43 mmol) were then added to the mixture. The tube was sealed then degassed by three freeze-thaw cycles in liquid N_2 under reduced pressure. The solution was

magnetically stirred at 72 °C for 12 h under a N_2 atmosphere. The solution was precipitated in hexanes then dried under reduced pressure to give a colorless solid **2-3** (5.5 g).

2.2.3 Characterization of the polymer photoresist **2-3**

IR (KBr): ν = 3002, 1737, 1537, 1480, 1348, 1211, 1151, 971, 788, 734, 705, 654 cm^{-1}; ^1H NMR (400 MHz, $CDCl_3$ (1 part by volume) + $CFCl_3$ (1 part by volume), δ): = 8.05 (br s, 1H, Ar-*H*), 7.67 (br s, 2H, Ar-*H*), 7.52 (br s, 1H, Ar-*H*), 5.39 (br s, 2H, ArCH_2O), 4.26 (br s, 6H, CH_2CF_2), 2.50 (br s, 6H, $CH_2CH_2CF_2$), 2.21-0.66 ppm (m, 20H); M_n = 17,000, M_w/M_n = 2.4.

2.2.4 Lithographic Evaluation

The lithographic properties of the polymer **2-3** using two different substrates (Si and glass wafer) were investigated using a GCA Autostep 200 DSW i-line Wafer Stepper. The resist films were spin-coated from a resist (0.15 g) solution in HFE-7600 (1.5 g) at 2000 rpm followed by post-apply bake at 110 °C. The resulting film had a thickness of *ca.* 460 nm. After UV exposure, the film was baked at 110 °C for 60 s, developed in HFE-7200 for 40 s.

2.2.5 Device Fabrication

Bottom-contact transistors were prepared as follows: A thin film of PEDOT:PSS (Clevios PH500, H.C. Stark) was spin-coated onto a Si wafer with 360 nm of thermally grown oxide and baked at 180 °C for 10 min. A layer of the polymer **2-3** was spin-coated onto the PEDOT:PSS film. The resist film was patterned in HFE-

7200 and the remaining image was then transferred onto the PEDOT:PSS film via O_2-plasma etch. The resist film was then washed away in a 2-propanol (10% by volume) HFE-7100 mixture. Onto this patterned PEDOT:PSS film was spin-coated another layer of the resist **2-3** which was also photo-patterned. A thin film (*ca.* 20 nm) of pentacene was thermally evaporated (substrate temperature - 50 °C, residue gas pressure $<5x10^{-7}$ Torr, at a rate of 0.05 Å/s) onto the substrate. Then the resist film was lifted off in a 2-propanol (10% by volume) HFE-7100 mixture to leave patterned pentacene on top of patterned PEDOT:PSS film.

2.3 Results

The two monomers (**2-1** and **2-2)** were randomly copolymerized by radical initiation using 2,2'-azobis(2-methylpropionitrile) (AIBN). Multiple polymers were synthesized with varying compositions; polymers which lacked sufficient incorporation of the fluorinated monomer proved insoluble in HFEs. Conversely, polymers without sufficient incorporation of the photosensitive monomer proved unpatternable. Percent compositions of the two monomers were varied to obtain optimum photosensitivity while still retaining enough fluorination to be processable in HFEs.

2.4 Lithographic Evaluation

To demonstrate patterning properties, polymer **2-3** was lithographically evaluated on both silicon (Si) and glass substrates. Photoresist was spin-coated from HFE-7600 and then patterned under 248 and 365 nm exposure conditions. Pattern development was carried out in HFE-7200. Figure 2.3 shows well-resolved sub-micron lines on Si and glass. It is notable that this photoresist is soluble in HFEs, without co-solvents, and that all processing steps are achieved through HFEs.

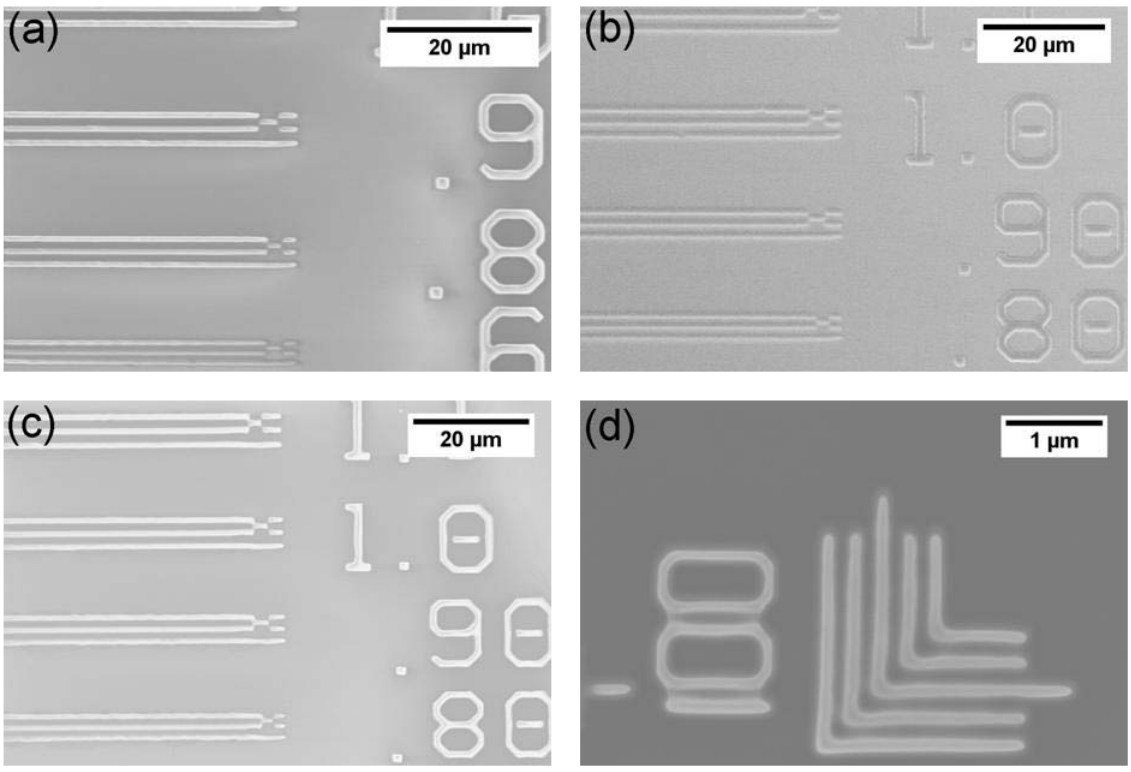

Figure 2.3: Patterned photoresist images (a) at 365nm on Si, (b) at 365 nm on glass, (c) at 365nm on PEDOT:PSS film, and (d) e-beam exposure on Si.

Sensitivity profiles were obtained for polymer **2-3** at both 248 and 365 nm (Figures 2.4 and 2.5). The polymer exhibits very different sensitivities at different wavelengths. At 248 nm, the dose is 84 mJ cm^{-2} whereas at 365 nm, the dose is 2700 mJ cm^{-2}. However, this behavior is expected as the nitrobenzyl group is likely to undergo faster decomposition by the irradiation of high energy photons.[17]

To further explore the patterning properties, the photoresist was also patterned under electron-beam (e-beam) exposure conditions. Well-resolved lines down to 100 nm were obtained, shown in Figure 2.3 (d).

2.5 Discussion

It should be emphasized that the photosensitive monomer **2-2** was carefully selected to enable non-chemically amplified patterning; an imaging mechanism which does not rely on acid-catalyzed deprotection reactions.[18] The advantages of this pathway are substantial, in particular, for the patterning of PEDOT:PSS films. PEDOT:PSS is a difficult material to pattern with acid-sensitive photoresists (i.e. photoresists requiring a photoacid generator) in that PEDOT:PSS itself, being highly acidic, can decompose the resist. Typically, following patterning with a chemically amplified resist, a thin layer (*ca*. 10-20 nm) of decomposed photoresist is left on the PEDOT:PSS interface.[7,19]

Preliminary studies in PEDOT:PSS patterning were first carried out with our acid-stable photoresist. PEDOT:PSS was spin-coated onto an Si wafer in a thin film. The polymer **2-3** was then applied and subsequently removed. Before and after

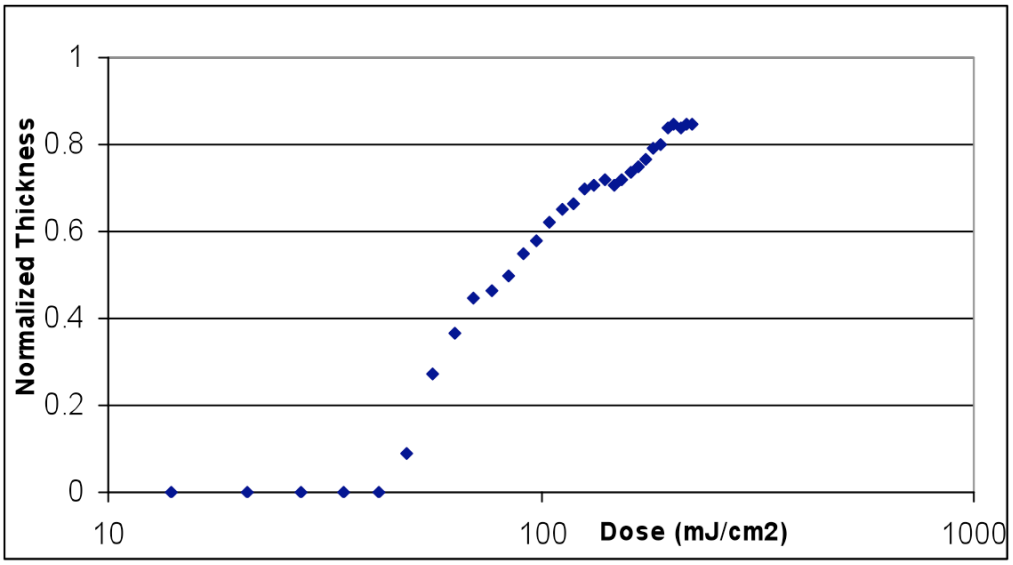

Figure 2.4: Contrast curve at 248 nm of polymer **2-3**.

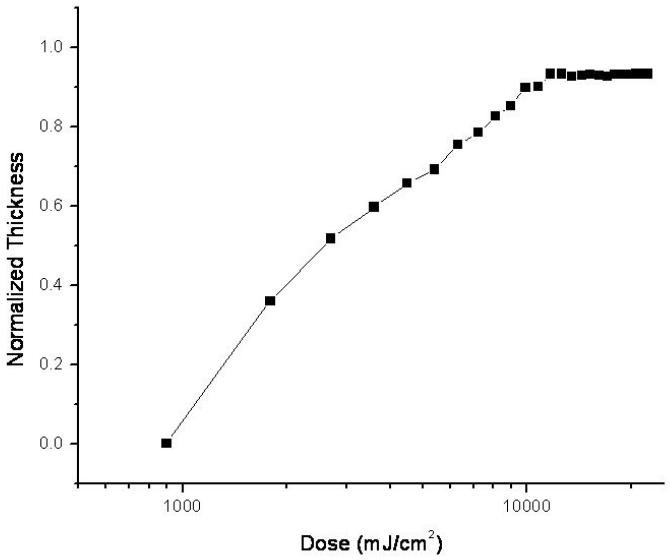

Figure 2.5: Contrast curve at 365 nm of polymer **2-3**.

measurements showed the thickness of the PEDOT:PSS film to remain exactly the same (51 nm), indicating no resist decomposition. Similarly, PEDOT:PSS was spun-cast, followed by photoresist application. The photoresist was then flood-exposed with 248 nm UV light and subsequently removed. Before and after thickness measurements again show the PEDOT:PSS film unchanged (51 nm). Therefore, no residual layers of decomposed resist were found, as with chemically-amplified resists. The PEDOT:PSS interface is left clean and unaffected following resist removal.

As an ultimate proof-of-concept study we fabricated and tested two sets of indium tin oxide (ITO)/PEDOT:PSS/Metal devices, one with PH500 and one with AI4083 (PH500 and AI4083 commercially-available from H. C. Starck). A layer of photoresist was deposited onto the PEDOT:PSS films, flood-exposed with UV light and then removed. Reference devices were fabricated with pristine PEDOT:PSS films. Both sets of test devices showed essentially the same resistance and current-voltage (I-V) curves as the reference devices (Figure 2.6), indicating that our photoresist has no detrimental effects on device performance. These results collectively suggest our non-chemically amplified photoresist as an ideal candidate for PEDOT:PSS patterning.

The actual patterning of PEDOT:PSS film was then demonstrated. Photoresist films were spun-cast onto films of PEDOT:PSS and then patterned at 365 nm, shown in Figure 2.3. Pattern resolution was consistent with that of the photoresist patterned on Si alone. Patterns were transferred to PEDOT:PSS via oxygen-plasma etching and the photoresist was subsequently removed. PEDOT:PSS patterns with sub-micron resolution were obtained (Figure 2.7).

To demonstrate the potential of this resist, we fabricated simple bottom-contact OTFTs with patterned pentacene film on top of patterned PEDOT:PSS source and drain electrodes. The optical image and atomic force microscopy (AFM) images of a

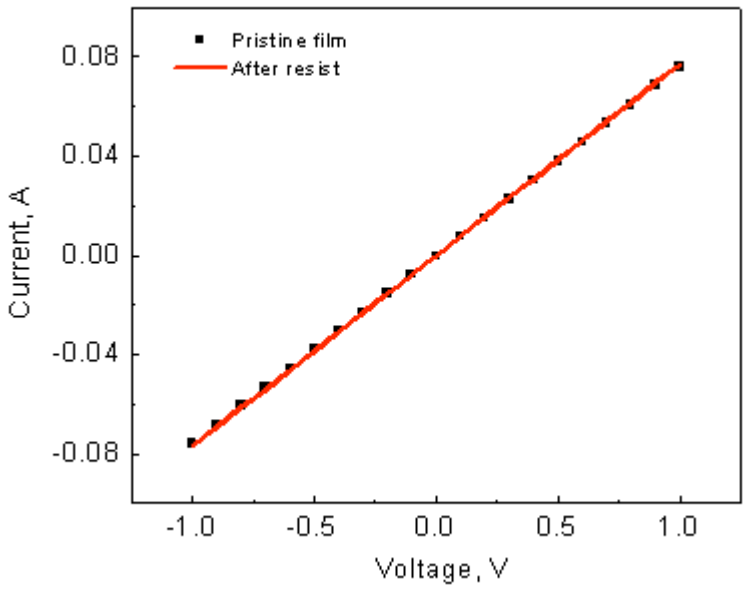

Figure 2.6: PEDOT:PSS PH500 film conductivity test.

typical 5 μm channel length OTFT device are shown in Figure 2.8. Figure 2.8(b) shows that the pentacene fully covers both the transistor channel and the PEDOT:PSS contacts, without any observable delamination occurring after lift-off in HFE. Figure 2.8(c) shows that larger grains (~ 0.5 μm) are formed inside the channel, with a mean roughness of 40 nm. Pentacene attempts to grow into islands (~ 80 nm height) on the PEDOT:PSS contacts.

Transistor performance was evaluated in a high vacuum probe station. OTFTs with channel lengths of 5, 10, 20, and 50 microns were fabricated and tested. The typical electrical characteristics of a fabricated 5 μm channel length OTFT are shown in Figure 2.8(e, f). The field effect mobility in the saturation regime was extracted from the transfer characteristics using the following equation:

$$I_{DS,saturation} = \frac{W}{2L} \cdot \mu_{sat} \cdot C_r \cdot (V_G - V_{TH})^2,$$

where I_{DS} is the drain current, C_r is the capacitance per unit area of the gate dielectric layer, V_G is the gate voltage, V_{TH} is the threshold voltage. V_{TH} was determined from the intercept in the plot of $(I_{DS})^{1/2}$ vs. V_G. For the presented device, the value of 0.03 $cm^2\ V^{-1}s^{-1}$ was obtained for the charge carrier mobility in the saturation regime. The on-off current ratio was found to be more than 10^4. For all fabricated devices, the channel length to channel width ratio was kept the same—therefore all other devices show similar performance. The obtained values for carrier mobility are higher or comparable to previously reported values for pentacene channel, PEDOT:PSS electrode OTFTs obtained by other patterning techniques.[20-22]

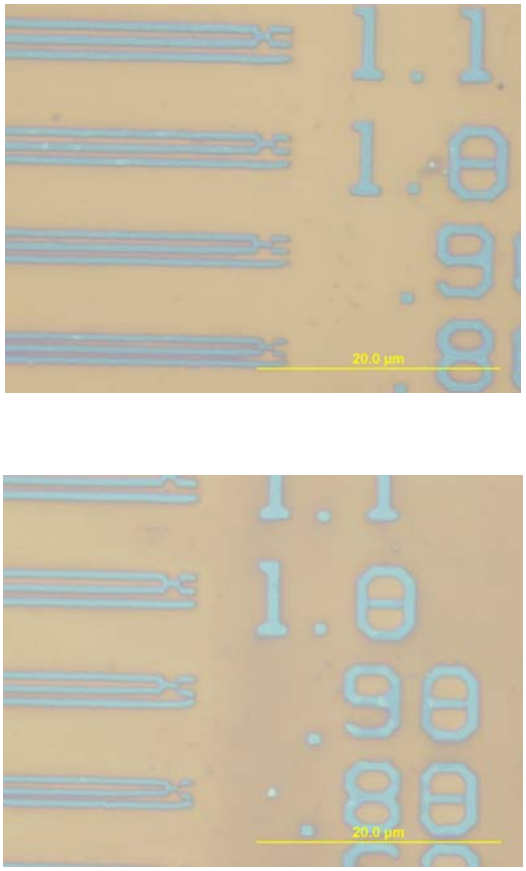

Figure 2.7: Optical microscope images of patterned PEDOT:PSS on Si wafer.

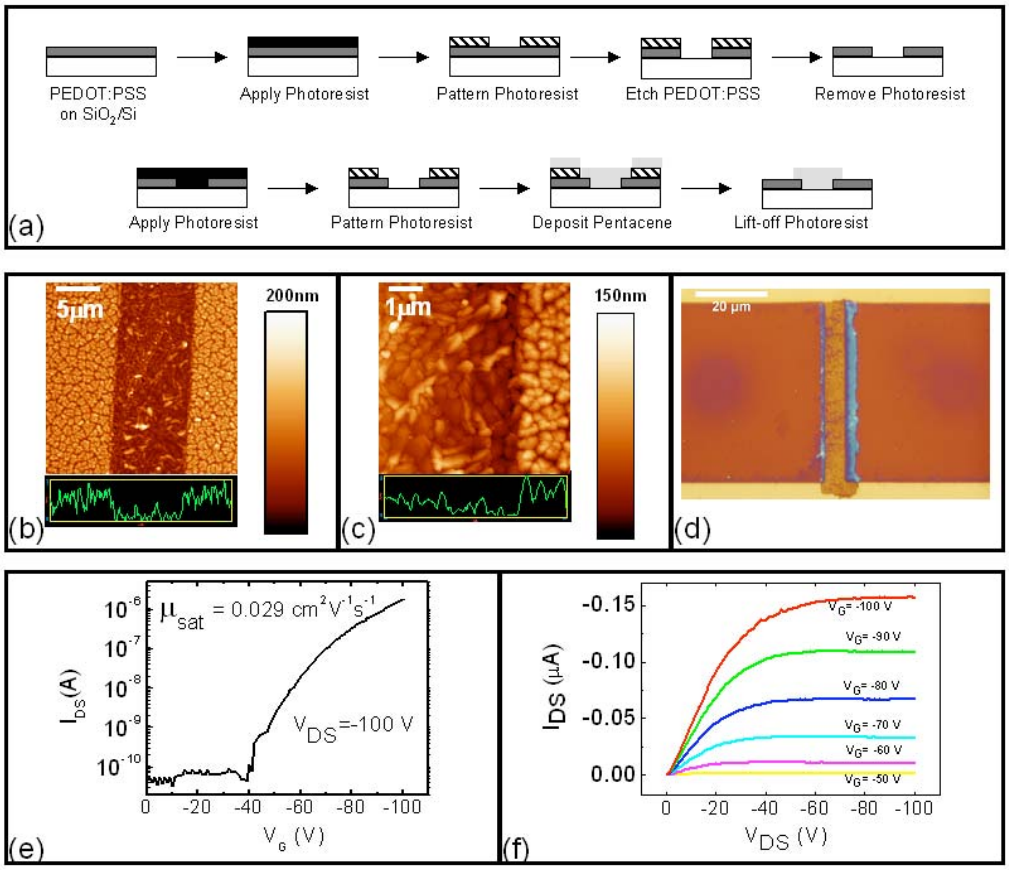

Figure 2.8: PEDOT:PSS/Pentacene bottom-contact OTFT (a) Schematic illustration of device fabrication, (b) and (c) AFM images of a 5μm (width) x 50μm (length) pentacene channel between PEDOT:PSS electrodes (d) optical image of OTFT, (e) and (f) device performance plots.

2.6 Conclusion

In conclusion, the design of a novel, non-chemically amplified acid stable resist for patterning organic electronic materials has been described. Sub-micron patterning capabilities at 248 nm and 365 nm conditions and 100 nm resolution under e-beam exposure have been demonstrated. Sub-micron patterning of PEDOT:PSS, a material for which our photoresist is particularly suitable, has also been shown. Finally, it has been demonstrated that a bottom-contact transistor patterned with this photoresist shows comparable or better performance than previously reported bottom-contact transistors of the same type obtained by other patterning techniques.

Acknowledgements

I gratefully acknowledge support from the National Science Foundation (Materials World Network DMR-0602821) and the IGERT Fellowship. The work was performed in part at the Cornell NanoScale Facility, a member of the National Nanotechnology Infrastructure Network, which is supported by the National Science Foundation (Grant ECS-0335765). Special thanks to Dr. Jin-Kyun Lee for his guidance and insight throughout this project, to Dr. Alexander Zakhidov for his assistance with device fabrication and to Dr. Margarita Chatzichristidi for her lithographic advice (Cornell University). Also thank you to Mr. Eisuke Murotani (Asahi Glass, Japan) for the fluorinated GPC measurements.

REFERENCES

(1) Malliaras, G.; Friend, R. Phys. Today 2005, 58, 53-58.

(2) Forrest, S. R. Nature 2004, 428, 911-918.

(3) Menard, E.; Meitl, M. A.; Sun, Y. G.; Park, J. U.; Shir, D. J. L.; Nam, Y. S.; Jeon, S.; Rogers, J. A. Chem. Rev. 2007, 107, 1117-1160.

(4) Loo, Y. L. Aiche Journal 2007, 53, 1066-1074.

(5) Balocco, C.; Majewski, L. A.; Song, A. M. Org. Electron. 2006, 7, 500-507.

(6) Huang, J.; Xia, R.; Kim, Y.; Wang, X.; Dane, J.; Hofmann, O.; Mosley, A.; de Mello, A. J.; de Mello, J. C.; Bradley, D. D. C. Journal of Materials Chemistry 2007, 17, 1043-1049.

(7) Hwang, H. S.; Zakhidov, A. A.; Lee, J. K.; Andre, X.; DeFranco, J. A.; Fong, H. H.; Holmes, A. B.; Malliaras, G. G.; Ober, C. K. Journal of Materials Chemistry 2008, 18, 3087-3090.

(8) Tsai, W. T. Journal of Hazardous Materials 2005, 119, 69-78.

(9) Meerholz, K. Nature 2005, 437, 327-328.

(10) Zakhidov, A. A.; Lee, J.-K.; Fong, H. H.; DeFranco, J. A.; Chatzichristidi, M.; Taylor, P. G.; Ober, C. K.; Malliaras, G. G. Adv. Mater. 2008, 20, 3481-3484.

(11) Lee, J.-K.; Chatzichristidi, M.; Zakhidov, A. A.; Taylor, P. G.; DeFranco, J. A.; Hwang, H. S.; Fong, H. H.; Holmes, A. B.; Malliaras, G. G.; Ober, C. K. Journal of the American Chemical Society 2008, 130, 11564-11565.

(12) Jonas, F.; Schrader, L. Synth. Met. 1991, 41, 831-836.

(13) Groenendaal, B. L.; Jonas, F.; Freitag, D.; Pielartzik, H.; Reynolds, J. R. Adv. Mater. 2000, 12, 481-494.

(14) Kirchmeyer, S.; Reuter, K. Journal of Materials Chemistry 2005, 15, 2077-2088.

(15) Horvath, I. T.; Rabai, J. Science 1994, 266, 72-75.

(16) Doh, J.; Irvine, D. J. Journal of the American Chemical Society 2004, 126, 9170-9171.

(17) Bochet, C. G. J. Chem. Soc., Perkin Trans. 1 2002, 125-142.

(18) Ito, H. Adv. Polym. Sci. 2005, 172, 37-245.

(19) Stewart, M. D.; Tran, H. V.; Schmid, G. M.; Stachowiak, T. B.; Becker, D. J.; Willson, C. G. Journal of Vacuum Science & Technology B 2002, 20, 2946-2952.

(20) DeFranco, J. A.; Schmidt, B. S.; Lipson, M.; Malliaras, G. G. Org. Electron. 2006, 7, 22-28.

(21) Parashkov, R.; Becker, E.; Ginev, G.; Riedl, T.; Johannes, H. H.; Kowalsky, W. Jpn. J. Appl. Phys., Part 2 2004, 43, L130-L132.

(22) Kang, H. S.; Lee, J. W.; Kim, M. K.; Joo, J.; Ko, J. M.; Lee, J. Y. Journal of Applied Physics 2006, 100.

CHAPTER 3

A NON-CHEMICALLY AMPLIFIED POSITIVE-TONE PHOTORESIST FOR PATTERNING ORGANIC ELECTRONICS WITH HYDROFLUOROETHER SOLVENTS

Abstract

Orthogonal lithography has been presented recently as a new approach to patterning organic electronics with photolithography, through the use of benign photoresists and solvents. Although the well-established photolithographic method has, until now, been only marginally applicable to organic electronics patterning due to incompatibility between organic materials and traditional processing solvents and resists, this technique enables straightforward photolithographic patterning of organic electronic materials in a high-resolution and high-throughput manner. Thus far, only negative-tone photoresist systems of this kind have been reported. Though negative-tone resists are very useful, certain device architectures can only be achieved with a positive-tone resist. An orthogonal positive-tone polymeric photoresist, fully processable in orthogonal solvents is reported here for the first time. The polymer is composed of a nitrobenzyl-based photoactive component and a fluorinated component. The polymer is processable in hydrofluoroether solvents, which have been previously reported as benign to organic electronic materials. Positive-tone development is achieved through the use of a silylating reagent in hydrofluoroether solvent. Submicron resolution at 365 nm is demonstrated.

3.1 Introduction

The field of organic electronics is motivated by the promise of lightweight, large-area devices that can be flexed and rolled, as well as cost significantly less than conventional electronics[1-3]. One of the major barriers that lies between this vision and its reality is the current inability to pattern organic electronic materials efficiently[4].

The traditional route to electronics patterning is photolithography. Despite the fact that photolithography is a well-established, high-resolution and high-throughput patterning method, its potential drawback is that the resists and processing solvents used are damaging to organic electronic materials[5]. To circumvent this problem, myriad methods have emerged for organic electronics patterning[4,6-10]. However, no method has yet been proposed that can match photolithography in resolution and efficiency.

Ober and coworkers have recently published studies of novel fluorinated resists and processing solvents and their application to photolithography, called *orthogonal* lithography[11]. They have shown that these fluorinated materials are non-damaging to organic electronic materials[12] and are also very capable of serving as substitute photoresists and processing solvents for photolithographic patterning[13-16]. Through the use of fluorinated photoresists and hydrofluoroether (HFE) solvents, they show that organic electronic materials can be patterned straightforwardly through conventional photolithographic methods. Due to its benign properties, this system also enables the facile processing of multiple-layer device architectures.

Thus far, chemically amplified polymeric[15] and molecular glass photoresists[13], and a non-chemically amplified polymeric photoresist[14], all negative-tone, have been reported which are based on the orthogonal lithography concept. Though negative-tone resists are very useful, certain device architectures can only be achieved with a positive-tone resist.

Hence, a hydrofluoroether-processable positive-tone resist was designed to address this shortcoming. Three fluorinated resists were designed and tested, both polymer and small molecule-based structures. The design and results of these resists are discussed. Of these, a functional positive-tone resist system is presented. This orthogonal photoresist is highly fluorinated and fully processable in hydrofluoroethers. Submicron resolution is easily achieved at 365 nm exposure.

3.2 Experimental Section

3.2.1 Materials

3,3,4,4,5,5,6,6,7,7,8,8,9,9,10,10,10-Heptadecafluorodecyl methacrylate (**3-2)** and benzotrifluoride (TFT) were purchased from Sigma-Aldrich and used as received. 2,2'-Azobis(2-methylpropionitrile) (AIBN) was purchased from Sigma-Aldrich and was recrystallized from chloroform ($CHCl_3$). (N,N-Dimethylamino)trimethyl-silane (DMTS) (**3-6)** was purchased from Gelest and used as received. 2-(Trimethylsilyloxy)-ethylmethacrylate **(3-8)**, tetrabutylammonium fluoride (1.0 M solution in tetrahydrofuran (THF)) and THF were purchased from Sigma-Aldrich and used as received. 2-Diazo-1,2-napthoquinone-5-sulfonyl chloride (DNQ-Cl) (**3-10)** was purchased from Wako and used as received. Triethylamine and acetone were purchased from Sigma-Aldrich and used as received. α,α,α'-Tri(4-hydroxyphenyl)-1-ethyl-4-isopropylbenzene (**3-13)** was purchased from TCI America and used as received. Potassium carbonate and dimethylformamide (DMF) were purchased from Sigma-Aldrich and used as received. 3M^{TM} Novec^{TM} Engineered Fluid HFE-7200 and 7600 were purchased from 3M USA.

3.2.2 Synthesis

Polymer Photoresist **3-3**

2-Nitrobenzyl methacrylate **3-1** (prepared according to the literature procedure [17], further purified by recrystallization from methylene chloride (CH_2Cl_2)-hexanes mixed solvent after column chromatography) (2.09 g, 9.45 mmol) and 3,3,4,4,5,5,6,6,7,7,8,8,9,9,10,10,10-heptadecafluorodecyl methacrylate (4.88 g, 9.17 mmol) **3-2** were added to a 25 cm^3 Schlenk tube. Benzotrifluoride (7 cm^3) and AIBN (0.07 g, 0.43 mmol) were then added to the mixture. The tube was sealed then degassed by three freeze-thaw cycles in liquid N_2 under reduced pressure. The solution was magnetically stirred at 70 °C for 12 h under a N_2 atmosphere. The solution was precipitated in hexanes then dried under reduced pressure to give a colorless solid **3-3** (5.09 g) in approximately 73 % yield.

Polymer Photoresist **3-11**

2-(Trimethylsilyloxy)-ethylmethacrylate (TMS-HEMA) **3-8** (0.92 g, 4.55 mmol) and 3,3,4,4,5,5,6,6,7,7,8,8,9,9,10,10,10-heptadecafluorodecyl methacrylate **3-2** (6.05 g, 11.37 mmol) were added to a 25 cm^3 Schlenk tube. Benzotrifluoride (7 cm^3) and AIBN (0.07 g, 0.43 mmol) were then added to the mixture. The tube was sealed then degassed by three freeze-thaw cycles in liquid N_2 under reduced pressure. The solution was magnetically stirred at 72 °C for 12 h under a N_2 atmosphere. The solution was precipitated in hexanes then dried under reduced pressure to give a colorless solid (6.73 g) in approximately 97 % yield. This random copolymer was then immediately deprotected, without characterization: the copolymer (4.00 g, 2.28 mmol TMS groups), tetrabutylammonium fluoride (1 M in THF) (2.28 cm^3, 2.28 mmol), HFE-7200 (10 cm^3) and tetrahydrofuran (10 cm^3) were added to a

roundbottom flask and magnetically stirred at ambient temperature for 12 h under a N_2 atmosphere. The solution was concentrated under reduced pressure and redissolved in benzotrifluoride. This benzotrifluoride solution was precipitated into stirring methanol and then dried under reduced pressure to give a colorless solid **3-9** (3.36 g) in approximately 88 % yield. Random copolymer **3-9** (1.50 g, 1.26 mmol hydroxyl groups), DNQ-Cl (0.68 g, 2.51 mmol), triethylamine (0.32 g, 3.14 mmol), acetone (15 cm^3) and benzotrifluoride (20 cm^3) were added to a roundbottom flask and magnetically stirred at ambient temperature for 12 h under a N_2 atmosphere. The reaction was quenched with water (1 cm^3) and stirred for an additional hour. This mixture was precipitated in aqueous hydrochloric acid (HCl) solution and then dried under reduced pressure to give a bright yellow solid **3-11** (1.03 g) in approximately 57 % yield.

T-Shape Resist **3-16, 3-18a** and **3-18b**, **3-19a** and **3-19b**

α,α,α'-Tri(4-hydroxyphenyl)-1-ethyl-4-isopropylbenzene **3-13 (**2.00 g, 4.71 mmol), 1,1,1,2,2,3,3,4,4,5,5,6,6,7,7,8,8-heptadecafluoro-12-iododododecane **3-14** (prepared according to the literature procedure[13]) (5.67 g, 9.42 mmol), potassium carbonate (1.30 g, 9.42 mmol) and dimethylformamide (20 cm^3) were added to a roundbottom flask and magnetically stirred for 2 h at 75 ºC under a N_2 atmosphere. The mixture was precipitated in aqueous hydrochloric acid solution. The precipitate was redissolved in ethyl acetate. **3-16** was recrystallized from this solution to give a colorless solid (0.25 g, 0.14 mmol). The remaining solution was separated by column chromatography with ethyl acetate-hexanes mixed solvent to give **3-15a and 3-15 b** as a colorless solid (1.01 g, 0.74 mmol) in 16 % yield.

α,α,α'-Tri(4-hydroxyphenyl)-1-ethyl-4-isopropylbenzene **3-13 (**5.00 g, 11.80 mmol), 1,1,1,2,2,3,3,4,4,5,5,6,6,7,7,8,8-heptadecafluoro-12-iododododecane **3-14**

(prepared according to the literature procedure[13]) (7.09 g, 11.80 mmol), potassium carbonate (3.26 g, 23.60 mmol) and dimethylformamide (30 cm^3) were added to a roundbottom flask and magnetically stirred for 2 h at 70 ºC under a N_2 atmosphere. The mixture was precipitated in aqueous hydrochloric acid solution. The precipitate was redissolved in ethyl acetate, washed with water and brine, then dried over magnesium sulfate and concentrated under reduced pressure. The product was separated by column chromatography with ethyl acetate-hexanes mixed solvent to give **3-17a and 3-17b** as a colorless solid (3.66 g, 4.07 mmol) in 35 % yield.

3-15a and 3-15b (1.23 g. 0.90 mmol), DNQ-Cl (0.24 g, 0.90 mmol), triethylamine (0.11 g, 1.12 mmol) and acetone (25 cm^3) were added to a roundbottom flask and magnetically stirred 2 h at ambient temperature under a N_2 atmosphere. The reaction was quenched with water (2 cm^3) and stirred for an additional hour. The mixture was precipitated in aqueous hydrochloric acid (HCl) solution. The precipitate was redissolved in chloroform and then precipitated again in methanol. This precipitate was dried under reduced pressure to give a bright yellow solid **3-18a and 3-18b** (0.89 g, 0.56 mmol) in 62 % yield.

3-17a and 3-17b (1.00 g. 1.11 mmol), DNQ-Cl (0.60 g, 2.23 mmol), triethylamine (0.28 g, 2.78 mmol) and acetone (20 cm^3) were added to a roundbottom flask and magnetically stirred 2 h at ambient temperature under a N_2 atmosphere. The reaction was quenched with water (2 cm^3) and stirred for an additional hour. The mixture was precipitated in aqueous hydrochloric acid (HCl) solution and then dried under reduced pressure to give a bright yellow solid **3-19a and 3-19b** (1.15 g, 0.86 mmol) in 38 % yield.

3.2.3 Characterization

3-3

IR (neat): ν = 2955, 2116, 1733, 1529, 1372, 1193, 1144, 861, 703, 656, 550 cm^{-1}; ^1H NMR (400 MHz, $CDCl_3$ (1 part by volume) + $CFCl_3$ (1 part by volume), δ): = 8.03 (br s, 1H, Ar-*H*), 7.60 (br s, 2H, Ar-*H*), 7.48 (br s, 1H, Ar-*H*), 5.35 (br s, 2H, ArCH_2O), 4.23 (br s, 4H, CH_2CF_2), 2.47 (br s, 4H, $CH_2CH_2CF_2$), 2.21-0.66 ppm (m, 25H); T_g(DSC) = 72.80 °C, T_d (TGA) = 186.44 °C; M_n=53,529, M_w/M_n= 1.826.

3-9

IR (neat): ν = 1723, 1147, 701, 653, 561 cm^{-1}; ^1H NMR (400 MHz, $CDCl_3$ (1 part by volume) + $CFCl_3$ (1 part by volume), δ): = 4.26 (br s, 2H, CH_2CF_2), 2.47 (m, 2H, $CH_2CH_2CF_2$), 2.41-0.72 ppm (m, 5H); T_g(DSC) = 90.70 °C, T_d (TGA) = 172.29 °C.

3-11

IR (neat): ν = 2159, 2114, 1736, 1192, 1145, 700, 657 cm^{-1}; ^1H NMR (400 MHz, $CDCl_3$ (1 part by volume) + $CFCl_3$ (1 part by volume), δ): = 8.45-6.92 (m, Ar-*H*), 4.24 (br s, CH_2CF_2), 2.50-0.67 ppm (m); T_d (TGA) = 138.59 °C.

3-15a and 3-15b

IR (neat): ν = 2922, 1609, 1510, 1199, 1145, 1014, 831, 704, 655 cm^{-1}; ^1H NMR (400 MHz, $CDCl_3$ (1 part by volume) + $CFCl_3$ (1 part by volume), δ): = 7.17-6.62 (m, 16H, Ar-*H*), 4.44 (m, 1H, ArO*H*), 3.96 (m, 4H, CH_2), 2.07 (s, 3H, CH_3), 1.84 (m, 8H, CH_2CH_2), 1.63 (s, 6H, CH_3) 1.25 ppm (m, 2H, CH_2CH_2); elemental analysis: C (46.22 %), H (2.94 %), N: (<0.05 %), MS calcd for (M+H): 1372.3, found: 1372.3.

3-16

IR (neat): ν = 2965, 2872, 1605, 1509, 1200, 1145, 1014, 953, 829, 704, 655 cm^{-1}; ^1H NMR (400 MHz, $CDCl_3$ (1 part by volume) + $CFCl_3$ (1 part by volume), δ): = 7.20-6.69 (m, 16H, Ar-*H*), 3.97 (m, 6H, C*H*$_2$), 2.20 (m, 6H, C*H*$_2$), 2.10 (s, 3H, C*H*$_3$), 1.84 (m, 12H, C*H*$_2$CH$_2$), 1.43 ppm (s, 6H, C*H*$_3$); elemental analysis: C (42.50 %), H (2.59 %), N (<0.05 %).

3-17a and 3-17b

IR (neat): ν = 3349, 2972, 1613, 1509, 1201, 1144, 1014, 829, 703, 656 cm^{-1}; ^1H NMR (400 MHz, $CDCl_3$ (1 part by volume) + $CFCl_3$ (1 part by volume), δ): = 7.20-6.65 (m, 16H, Ar-*H*), 4.51 (m, 2H, ArO*H*), 3.98 (m, 2H, C*H*$_2$), 2.12 (s, 3H, C*H*$_3$), 1.88 (m, 4H, C*H*$_2$CH$_2$), 1.66 (s, 3H, C*H*$_3$) 1.31 (m, 2H, C*H*$_2$), 0.98 ppm (m, 2H); elemental analysis: C (54.04 %), H (3.64 %), N (<0.05 %), MS calcd for (M+H): 898.2, found: 898.2.

3-18a and 3-18b

IR (neat): ν = 2972, 2868, 2167, 2105, 1601, 1510, 1406, 1197, 1144, 1014, 831, 782, 701, 654, 599 cm^{-1}; ^1H NMR (400 MHz, $CDCl_3$ (1 part by volume) + $CFCl_3$ (1 part by volume), δ): = 7.57-6.67 (m, 21H, Ar-*H*), 4.21 (s, 1H, O*H*), 3.95 (m, 4H, C*H*$_2$), 2.02 (s, 3H, C*H*$_3$), 1.86 (m, 8H, C*H*$_2$CH$_2$), 1.37 (s, 6H, C*H*$_3$) 1.25 ppm (m, 2H, C*H*$_2$CH$_2$); elemental analysis: C (47.04 %), H (2.84 %), N (1.72 %).

3-19a and 3-19b

IR (neat): ν = 2963, 2108, 1597, 1500, 1404, 1364, 1199, 1145, 1016, 849, 777, 655, 601, 558 cm^{-1}; ^1H NMR (400 MHz, $CDCl_3$ (1 part by volume) + $CFCl_3$ (1 part by volume), δ): = 7.72-6.70 (m, 21H, Ar-*H*), 4.28 (m, 1H, O*H*), 3.99 (m, 2H,

CH_2), 2.09 (s, 3H, CH_3), 1.89 (m, 4H, CH_2CH_2), 1.53 (s, 3H, CH_3) 1.31 (m, 2H, CH_2), 0.96 ppm (m, 2H); elemental analysis: C (53.28 %), H (3.18 %), N (4.00 %).

3.2.4 Lithographic Evaluation

The lithographic properties of the polymer **3-3** using two different substrates (silicon and glass wafer) were investigated using a GCA Autostep 200 DSW i-line wafer stepper (365 nm), a JEOL JBX-6300FS 100 kV electron beam (e-beam) lithography system and an ABM contact aligner (248 nm). Resist films were spin-coated from a resist (0.15 g) solution in HFE-7600 (1.5 g) at 2000 rpm followed by post-apply bake at 110 °C. The resulting film had a thickness of *ca.* 460 nm. After UV exposure, the film was developed in a 2 wt.% solution of DMTS in HFE-7200 for one minute.

3.3 Results

2-Nitrobenzyl methacrylate, **3-1,** and 3,4,4,5,5,6,6,7,7,8,8,9,9,10,10,10-heptadecafluorodecyl methacrylate, **3-2,** were randomly copolymerized by radical initiation using AIBN. The synthetic scheme is given in Figure 3.1**.** Multiple polymers were synthesized with varying compositions; the fluorine content of the polymer was modulated such that the final resist would be soluble in HFE-7600 for photoresist deposition and insoluble in HFE-7200 during photoresist development. Polymers which lacked sufficient incorporation of the fluorinated monomer, proved insoluble in HFEs altogether. Conversely, polymers with an excess of fluorination were soluble in all HFEs. Compositions of the two monomers were varied to obtain a polymer photoresist, which could be fully processed in HFEs alone.

Two other photoresist systems were also investigated. Polymer resist **3-11** was synthesized by random copolymerization of 3,4,4,5,5,6,6,7,7,8,8,9,9,10,10,10-

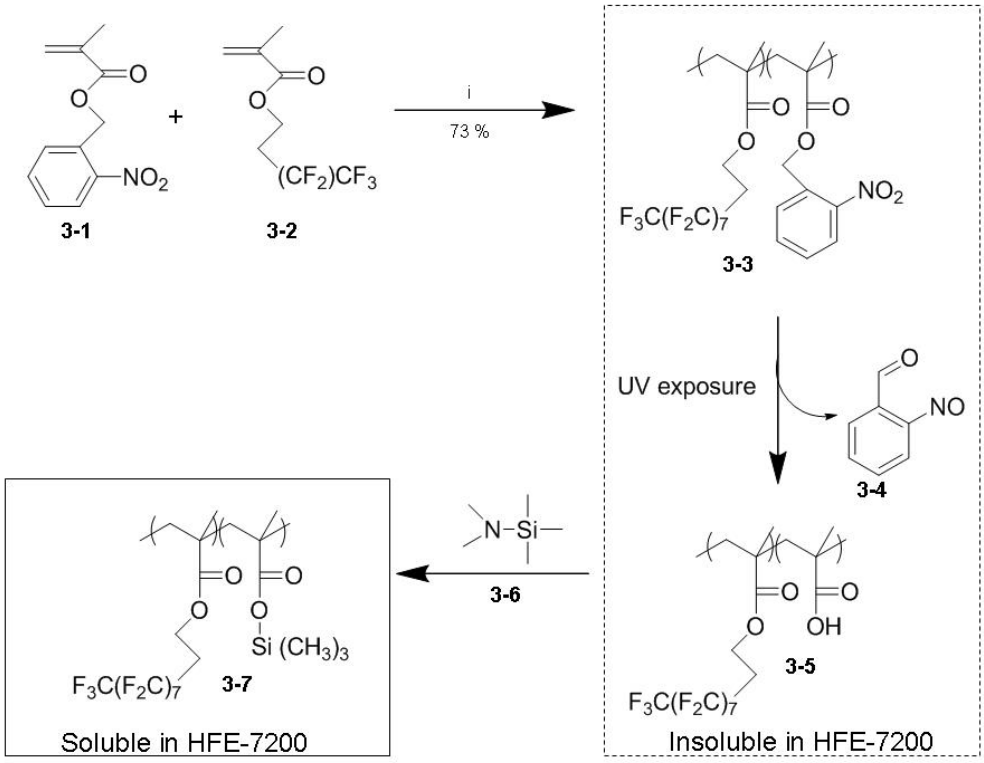

Figure 3.1: Synthesis of the non-chemically amplified polymer resist **3-3,** photo-induced deprotection reaction to polymeric carboxylic acid **3-5** and positive-tone development with **3-6.** Reagents and conditions: (i) TFT, AIBN, 70 °C, 12 h.

Table 3.1: Polymer compositions tested for solubility properties. Compositions reported correspond to the actual monomer incorporation. Polymer C exhibited the target solubility properties.

	Monomer 3-1	**Monomer 3-2**
Polymer A	24%	76%
Polymer B	36%	64%
Polymer C	45%	55%

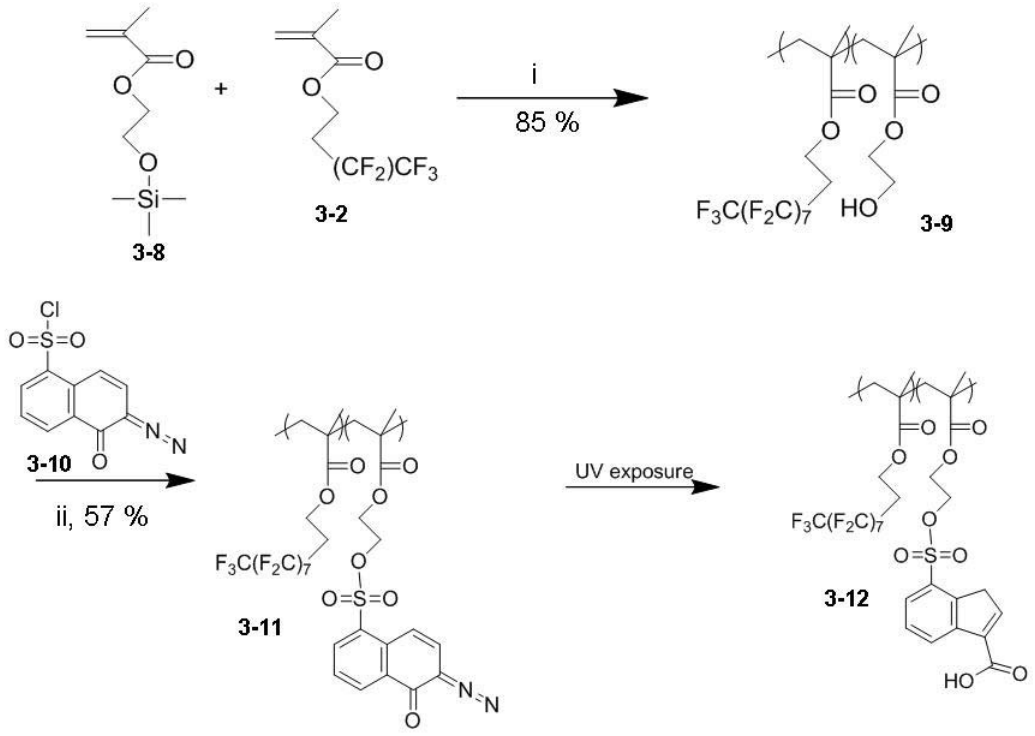

Figure 3.2: Synthesis of the DNQ-based polymer resist **3-11** and photo-induced Wolff rearrangement to **3-12.** Reagents and conditions: (i) TFT, AIBN, 72 °C, 12 h, followed by tetrabutylammonium fluoride, HFE-7200, THF, 12 h; (ii) triethylamine, acetone, TFT, 12 h.

Table 3.2: Polymer compositions tested for solubility properties. Compositions reported correspond to actual compositions polymerized. Polymer A showed HFE solubility; polymer B and C did not show HFE solubility.

	Monomer 3-8	**Monomer 3-2**
Polymer A	10%	90%
Polymer B	20%	80%
Polymer C	30%	70%

heptadecafluorodecyl methacrylate, **3-2,** and 2-((trimethylsilyl)oxy)ethyl methacrylate, **3-8,** followed by deprotection of the polymer to give **3-9** and finally addition of DNQ-Cl to give the polymer resist **3-11.** The synthetic scheme is given in Figure 3.2**.** The relative quantities of the monomers were varied in an attempt to identify a composition, which would have enough fluorination to be processable in HFEs, as well as have enough incorporation of the photosensitive monomer to be patternable. However, all compositions, which were synthesized, proved either insoluble in HFEs or unpatternable.

Another photoresist system, which was investigated, was based on a small molecule structure. 4,4'-(1-(4-(2-(4-((5,5,6,6,7,7,8,8,9,9,10,10,11,11,12,12,12-heptadecafluorododecyl)oxy)phenyl)propan-2-yl)phenyl)ethane-1,1-diyl)bis(((5,5,6,6,7,7,8,8,9,9,10,10,11,11,12,12,12-heptadecafluorododecyl)oxy)benzene), **3-16,** regioisomers 7-((4-(1-(4((5,5,6,6,7,7,8,8,9,9,10,10,11,11,12,12,12-heptadecafluorododecyl)oxy)phenyl)-1-(4-(2-(4-((5,5,6,6,7,7,8,8,9,9,10,10,11,11,12,12,12-heptadecafluorododecyl)oxy)phenyl)propan-2-yl)phenyl)ethyl)phenoxy)sulfonyl)-1*H*-indene-3-carboxylic acid and 7-((4-(2-(4-(1,1-bis(4-((5,5,6,6,7,7,8,8,9,9,10,10,11,11,12,12,12-heptadecafluorododecyl)oxy)phenyl)ethyl)phenyl)propan-2-yl)phenoxy)sulfonyl)-1*H*-indene-3-carboxylic acid, **3-18a and 3-18b,** and regioisomers 7-((4-(2-(4-(1-(4-(((3-carboxy-1*H*-inden-7-yl)sulfonyl)oxy)phenyl)-1-(4-((5,5,6,6,7,7,8,8,9,9,10,10,11,11,12,12,12-heptadecafluorododecyl)oxy)phenyl)ethyl)pheyl)propan-2-yl)phenoxy)sulfonyl)-1*H*-indene-3-carboxylic acid and 7,7'-((4-(1-(4-(2-(4-((5,5,6,6,7,7,8,8,9,9,10,10,11,11,12,12,12-heptadecafluorododecyl)oxy)phenyl)propan-2-yl)phenyl)-1-(4-

(hydrosulfonyloxy)phenyl)ethyl)phenoxy)sulfonyl)bis(1*H*-indene-3-carboxylic acid), **3-19a and 3-19b,** were synthesized by first fluorinating **3-13** with **3-14** at varying degrees to give **3-15a and 3-15b, 3-16, 3-17a and 3-17b.** DNQ-Cl was added to **3-15a and 3-15b, 3-17a and 3-17b** to give the final compounds **3-18a and 3-18b, 3-19a and 3-19b.** The synthetic scheme is given in Figure 3.3**.** Solutions made of various compounds, **3-16, 3-18a and 3-18b, 3-19a and 3-19b**, were tested in an attempt to identify a composition which would have enough fluorination to be processable in HFEs, as well as have enough incorporation of the photoactive group to be patternable. Numerous permutations and ratios of the photoresist compounds were tested. However, no composition was identified which would allow for patternability in HFEs. Photoresist compositions proved to be either insoluble in HFEs or else too soluble, such that they could not be patterned; the entire film dissolved during development

3.4 Lithographic Evaluation

To demonstrate patterning properties, polymer resist **3-3** was lithographically evaluated on both silicon (Si) and glass substrates. Photoresist was spin-coated from HFE-7600 and then patterned under 248 and 365 nm exposure conditions. Pattern development was carried out in a 2 wt.% solution of (N,N-dimethylamino)trimethyl-silane (DMTS) in HFE-7200. Various compositions of DMTS in HFE-7200 were tested. Figure 3.4 shows well-resolved sub-micron lines on Si and glass. It is notable that this photoresist is soluble in HFEs, without co-solvents, and that all processing steps are achieved through HFEs. Structures for HFE-7200 and HFE-7600 are shown in Figure 3.5**.**

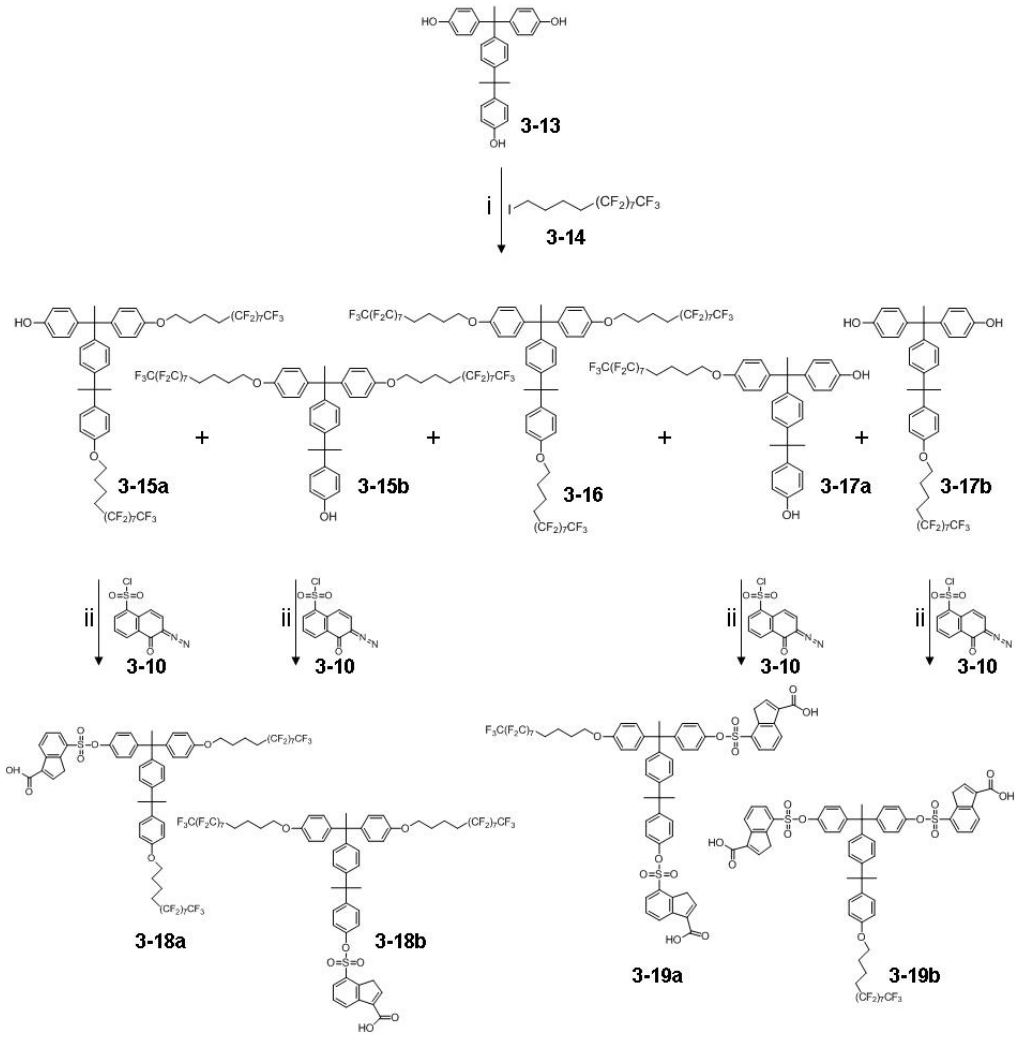

Figure 3.3: Synthesis of the DNQ-based small molecule resists **3-18a and 3-18b, 3-19a and 3-19b.** Reagents and conditions: (i) potassium carbonate, DMF, 2 h, 75 °C, **3-15** (16 % yield); (ii) triethylamine, acetone, 2 h, **3-18** (62 % yield), **3-19** (38 % yield).

Table 3.3: Table showing solubility properties for different compositions of compounds: **3-16, 3-18,** and **3-19.**

	3-16	**3-19**	**3-18**
3-16	3-16 Soluble	1:1 and 3:1 (3-16 : 3-19) Insoluble	1:1 (3-16 : 3:18) Soluble
3-19	1:1 and 3:1 (3-19 : 3-16) Insoluble	3-19 Insoluble	1:1 and 3:1 (3-19 : 3-18) Insoluble
3-18	1:1 (3-18 : 3-16) Soluble	1:1 and 3:1 (3-18 : 3-19) Insoluble	3-18 Soluble

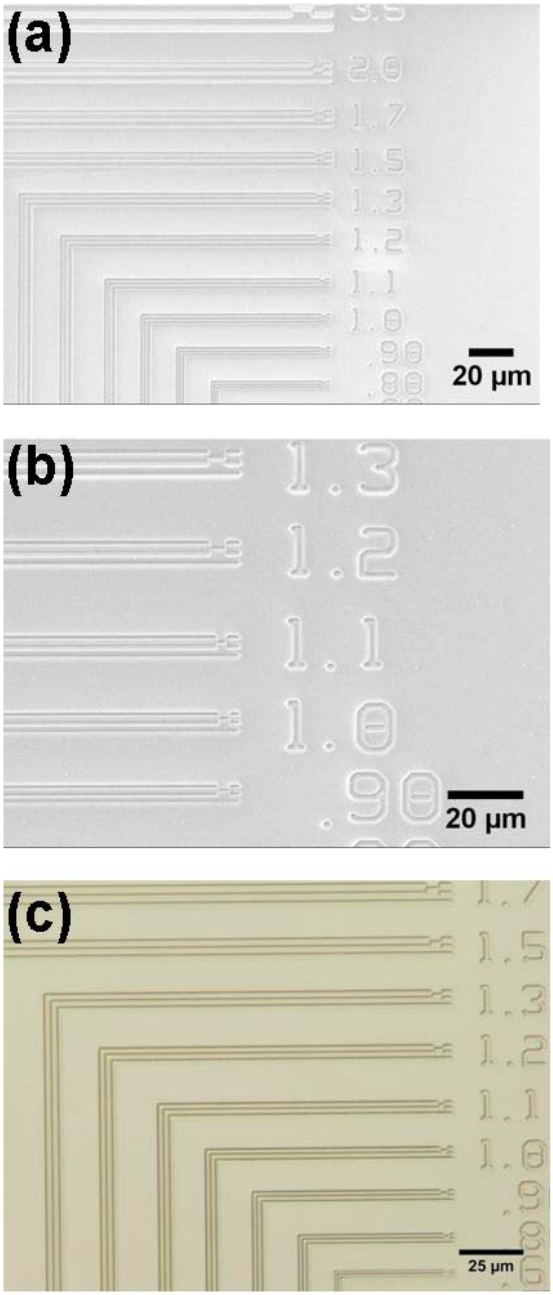

Figure 3.4: Patterned photoresist images (a) and (b) at 365 nm on Si, (c) 365 nm on glass.

a)

ethyl nonafluorobutyl ether ethyl nonafluoroisobutyl ether

b)

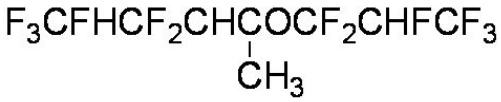

1,1,1,2,3,3,-hexafluoro-4-(1,1,2,3,3,3-hexafluoropropoxy)-pentane

Figure 3.5: 3M Novec Hydrofluoroether structures. (a) HFE-7200 (isomeric mixture of ethyl nonafluorobutyl ether and ethyl nonafluoroisobutyl ether) and (b) HFE-7600 (1,1,1,2,3,3-hexafluoro-4-(1,1,2,3,3,3-hexafluoropropoxy-pentane).

Sensitivity profiles were obtained for polymer resist **3-3** at both 248 and 365 nm (Figures 3.6 and 3.7). The polymer exhibits very different sensitivities at different wavelengths. However, this behavior is expected as the nitrobenzyl group is likely to undergo faster decomposition by the irradiation of higher energy photons.[18] At 248 nm, the required dose to achieve fully-developed patterns is 120 mJ cm^{-2} whereas at 365 nm, the dose is 9800 mJ cm^{-2}. Below these dose thresholds, incomplete development was observed. The photoresist was also shown to be patternable under electron beam (e-beam) exposure conditions.

3.5 Discussion

The structure for polymer resist **3-3** has been previously reported in application to a negative-tone photoresist system, processable in HFEs[14]. In this system, the photoresist, on UV exposure, decomposes to release nitrosobenzaldehyde and leaves a carboxylic acid group behind[17,19]. These carboxylic acid groups, generated in the UV exposed areas, are chemically differentiated enough that they enable a solubility switch of the photoresist in HFEs; the exposed areas are not soluble in HFE-7200. The photoresist is deposited from solution in HFE-7600. After irradiation, the UV-exposed areas are rendered insoluble in the developing solvent HFE-7200, thus leaving behind a negative-tone image.

By using the same basic polymer structure, but varying the ratio of the two monomers, a composition was identified which allows for positive-tone development of the photoresist. Polymer resist **3-3** is fluorinated enough to obtain a 10 wt. % solution of the photoresist in HFE-7600. The 10 wt. % solution is sufficiently concentrated such that it may be into a functional photoresist film. Photoresist **3-3** is also not fluorinated enough to exhibit solubility in HFE-7200; the photoresist film is not visibly damaged

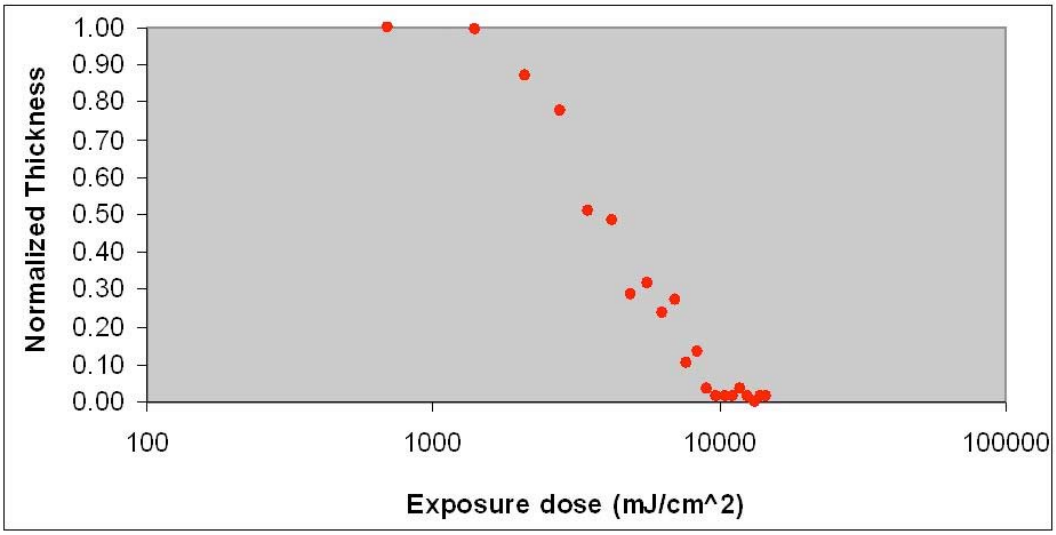

Figure 3.6: Contrast curve at 365 nm of polymer resist **3-3**.

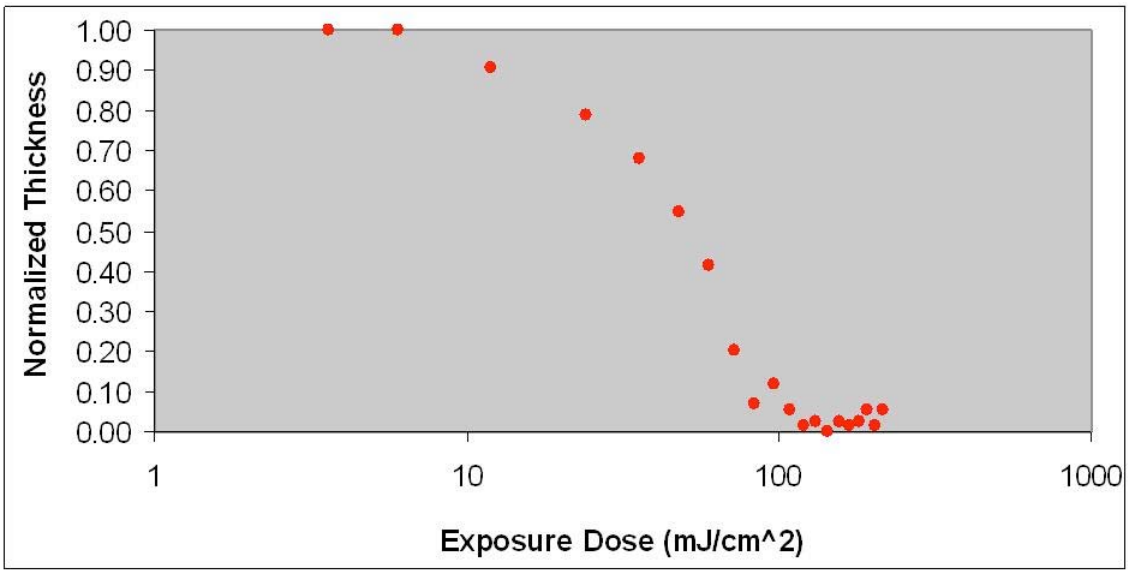

Figure 3.7: Contrast curve at 248 nm of polymer resist **3-3**.

or dissolved in the HFE-7200. Therefore, the resist can be deposited from solution in HFE-7600 and the unexposed film is not damaged by HFE-7200 during development.

It has previously been reported that addition of a silylating reagent, in particular DMTS, can significantly change the solubility characteristics of hydroxyl-terminated polymers[20-22]. Based on these previous findings, DMTS was chosen as a candidate for a developing reagent. In developing polymer resist **3-3,** addition of DMTS to HFE-7200 results in silylation of the carboxylic acid groups in the exposed regions of the film; the silylation of the exposed regions results in solubility in HFEs. Therefore, UV-exposed areas (**3-5)** of polymer resist **3-3** become soluble in HFE-7200, with the addition of DMTS, to leave behind positive-tone patterns.

The idea of silylation as a means to modulate the solubility characteristics of photoresists is not new. The DESIRE (diffusion-enhanced silylating resist) process was introduced in 1987 by Roland *et al*. as an imaging technique which relied on vapor-phase silylation using hexamethyldisilazane (HMDS) on a UV-patterned novolac and napthoquinone diazide resist to form an oxygen plasma etch mask for dry development of the resist[23]. Several other techniques also based on silylation and dry development, which were subsequently reported include the SUPER process developed by Philips and the PRIME process by LETI[24]. Many reports of surface silylation of photoresists[25-29], including liquid phase silylation[24,30] have since been reported. More recently, Ober *et al*. have reported a positive-tone developable photoresist in supercritical carbon dioxide ($scCO_2$) by using vapor phase silylation with HMDS to render UV-exposed methacrylic acid soluble in $scCO_2$ to produce positive-tone patterns[31].

In the search for a fluorinated positive-tone resist system, a DNQ-based polymer structure **3-11** was originally pursued. DNQ is a photoactive group, typical of non-chemically amplified positive-tone resist systems for 365 nm exposure[32]. A simple

structure was chosen, made of two components: a fluorinated monomer and a photoactive monomer. By varying the ratios of the two monomers, it could be possible to find a composition, which included enough fluorination to be soluble in HFEs as well as include enough of the photoactive group to be patternable.

Polymers with many different ratios of these two monomers were synthesized. However, it proved difficult to solubilize the polymers in HFEs alone. Polymers required nearly 90 % incorporation of the fluorinated monomer for even minimal HFE-solubility. With such modest incorporation of the photoactive group (10 %), the polymer proved unpatternable by 365 nm light.

The polymeric system was abandoned in favor of a small molecule-based design in the hopes that small molecules would show better solubility in HFEs. DNQ-based compounds **3-16, 3-18a and 3-18b, 3-19a and 3-19b** were synthesized. **3-19a and 3-19b** in HFE-7600 showed minimal solubility. **3-18a and 3-18b**, with comparably more fluorination, in HFE-7600 showed still poor solubility. Mixtures of **3-19a and 3-19b** with **3-16** and mixtures of **3-18a and 3-18b** with **3-16** and **3-19a and 3-19b** were tested for HFE solubility. Mixtures of **3-18a and 3-18b** with **3-16** exhibited sufficient solubility in HFEs, however the mixture was soluble in both HFE-7600 and HFE-7200. This mixture would not exhibit positive-tone patternability in HFEs alone because any unexposed resist would be removed in HFEs, along with the patterns. Unfortunately, any less fluorine incorporation into the mixture resulted in minimal HFE solubility, such that the resist was not processable.

Due to the solubility problems seen with both sets of DNQ-based resists, a new structure was designed which incorporated a smaller photoactive group as compared to DNQ, with the expectation that the smaller size of the non-fluorinated photoactive group would increase the resist solubility in HFEs. Photoresist structure

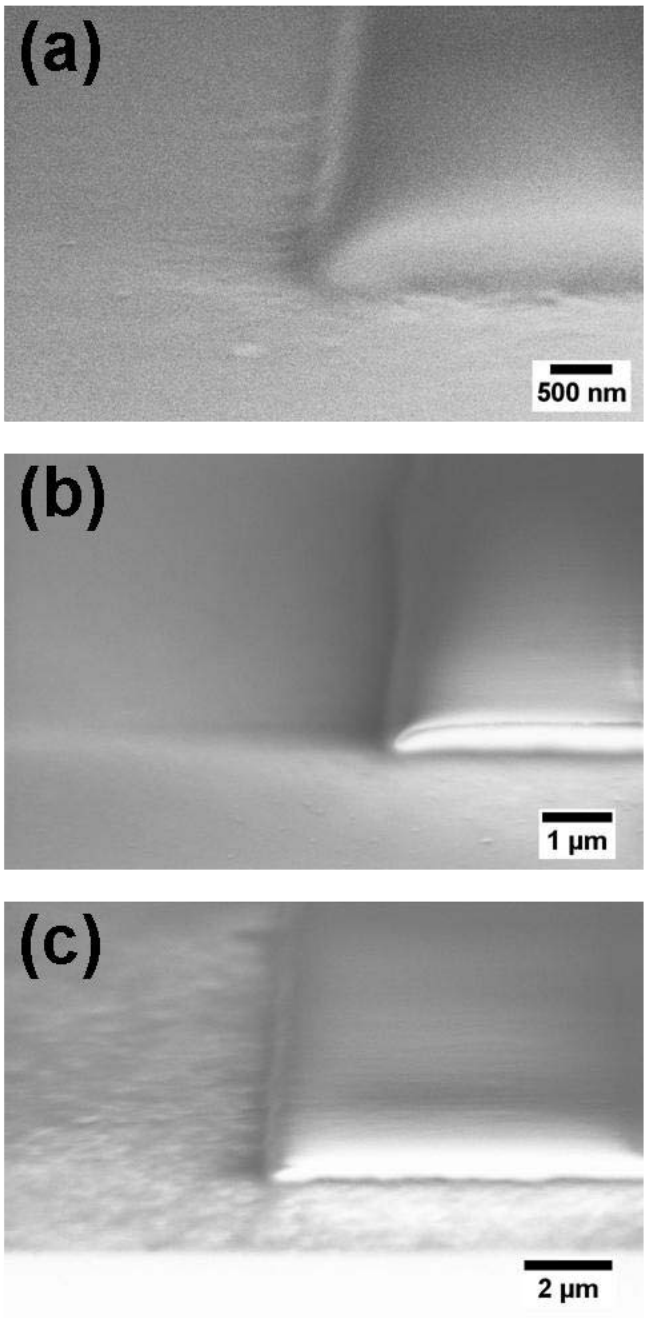

Figure 3.8: SEM images of resist **3-3** profile patterned at 365 nm on Si, with (a) focus offset of 0 µm, (b) focus offset of +3 µm and (c) focus offset of +6 µm.

3-3 was chosen and the relative quantities of the monomers varied until the desired solubility characteristics were achieved.

Positive-tone resists are frequently used in a subtractive patterning scheme in which the photoresist is first deposited and patterned on the substrate. The organic material is subsequently deposited and patterned by lift-off of the underlying photoresist. In order to achieve lift-off of the underlying photoresist, forming an undercut profile in the photoresist is often necessary. In an undercut profile, the top of the resist is wider than the base of the resist, such that the top of the resist creates an overhang. During deposition of active material, the area just below the overhang is protected from deposition and remains clean. This clean space creates a discontinuity in the active material film such that the photoresist below is easily lifted-off. Commonly, an undercut profile is created by offsetting the focus during UV exposure. However, by employing focus offsets of -6 μm to +6 μm during UV exposure, an undercut profile for photoresist **3-3** was still not achieved. Therefore, lift-off patterning with this resist may prove difficult. Figure 3.8 shows profile images of the photoresist at different focus offsets.

3.6 Conclusion

The design and synthesis of a novel, non-chemically amplified positive-tone resist for orthogonal photolithographic patterning of organic electronic materials has been described. The fluorinated photoresist is fully processable in hydrofluoroether solvents, which have been shown to be benign to organic electronic materials. Positive-tone development was achieved through silylation of the UV-exposed regions with DMTS in hydrofluoroether solvents; silylation renders the exposed areas soluble in hydrofluoroethers. Sub-micron patterning capabilities at 248 nm and 365 nm conditions have been demonstrated. This positive-tone resist, in conjunction with

previously reported negative-tone orthogonal resists, effectively enables patterning of any device architecture.

Acknowledgements

I gratefully acknowledge support from the National Science Foundation (Materials World Network DMR-0908994) and the IGERT Fellowship. The work was performed in part at the Cornell NanoScale Facility, a member of the National Nanotechnology Infrastructure Network, which is supported by the National Science Foundation (Grant ECS-0335765). Also, special thanks to Charles Wright and John DeFranco (Orthogonal, Inc.) for providing photoresist materials and for help with the SEM images of the photoresist profile, to Martin Scherer (University of Mainz, Germany) for his help in synthesis of photoresist materials, to Carol Newby for her assistance with lithographic evaluation and to Dr. Jin-Kyun Lee (Cornell University) for his continued advice and guidance.

REFERENCES

(1) Malliaras, G.; Friend, R. *Phys. Today* **2005**, *58*, 53-58.

(2) Forrest, S. R. *Nature* **2004**, *428*, 911-918.

(3) Loo, Y. L. *Aiche J.* **2007**, *53*, 1066-1074.

(4) Menard, E.; Meitl, M. A.; Sun, Y. G.; Park, J. U.; Shir, D. J. L.; Nam, Y. S.; Jeon, S.; Rogers, J. A. *Chem. Rev.* **2007**, *107*, 1117-1160.

(5) Huang, J.; Xia, R.; Kim, Y.; Wang, X.; Dane, J.; Hofmann, O.; Mosley, A.; de Mello, A. J.; de Mello, J. C.; Bradley, D. D. C. *J. Mater. Chem.* **2007**, *17*, 1043-1049.

(6) Sheats, J. R. *J. Mater. Res.* **2004**, *19*, 1974-1989.

(7) de Gans, B. J.; Duineveld, P. C.; Schubert, U. S. *Adv. Mater.* **2004**, *16*, 203-213.

(8) Ling, M. M.; Bao, Z. N. *Chem. Mat.* **2004**, *16*, 4824-4840.

(9) Duffy, D. C.; Jackman, R. J.; Vaeth, K. M.; Jensen, K. F.; Whitesides, G. M. *Adv. Mater.* **1999**, *11*, 546-+.

(10) Khang, D. Y.; Kang, H.; Kim, T.; Lee, H. H. *Nano Lett.* **2004**, *4*, 633-637.

(11) Lee, J. K.; Taylor, P. G.; Zakhidov, A. A.; Fong, H. H.; Hwang, H. S.; Chatzichristidi, M.; Malliaras, G. G.; Ober, C. K. *J. Photopolym Sci. Technol.* **2009**, *22*, 565-569.

(12) Zakhidov, A. A.; Lee, J. K.; Fong, H. H.; DeFranco, J. A.; Chatzichristidi, M.; Taylor, P. G.; Ober, C. K.; Malliaras, G. G. *Adv. Mater.* **2008**, *20*, 3481-+.

(13) Lee, J. K.; Chatzichristidi, M.; Zakhidov, A. A.; Taylor, P. G.; DeFranco, J. A.; Hwang, H. S.; Fong, H. H.; Holmes, A. B.; Malliaras, G. G.; Ober, C. K. *J. Am. Chem. Soc.* **2008**, *130*, 11564-+.

(14) Taylor, P. C.; Lee, J. K.; Zakhidov, A. A.; Chatzichristidi, M.; Fong, H. H.; DeFranco, J. A.; Malliaras, G. C.; Ober, C. K. *Adv. Mater.* **2009**, *21*, 2314-+.

(15) Hwang, H. S.; Zakhidov, A. A.; Lee, J. K.; Andre, X.; DeFranco, J. A.; Fong, H. H.; Holmes, A. B.; Malliaras, G. G.; Ober, C. K. *J. Mater. Chem.* **2008**, *18*, 3087-3090.

(16) Lee, J. K.; Fong, H. H.; Zakhidov, A. A.; McCluskey, G. E.; Taylor, P. G.; Santiago-Berrios, M.; Abruna, H. D.; Holmes, A. B.; Malliaras, G. G.; Ober, C. K. *Macromolecules*, *43*, 1195-1198.

(17) Doh, J.; Irvine, D. J. *J. Am. Chem. Soc.* **2004**, *126*, 9170-9171.

(18) Bochet, C. G. *J. Chem. Soc., Perkin Trans. 1* **2002**, 125-142.

(19) Bochet, C. G. *J. Chem. Soc.-Perkin Trans. 1* **2002**, 125-142.

(20) Macdonald, S. A.; Schlosser, H.; Ito, H.; Clecak, N. J.; Willson, C. G. *Chem. Mat.* **1991**, *3*, 435-442.

(21) Frechet, J. M. J.; Matuszczak, S.; Lee, S. M.; Fahey, J.; Willson, C. G. *Polym. Eng. Sci.* **1992**, *32*, 1471-1475.

(22) Frechet, J. M. J.; Leung, M. K.; Urankar, E. J.; Willson, C. G.; Cameron, J. F.; MacDonald, S. A.; Niesert, C. P. *Chem. Mat.* **1997**, *9*, 2887-2893.

(23) Coopmans, F.; Roland, B. *Solid State Technol.* **1987**, *30*, 93-99.

(24) Roland, B. *Advanced Materials for Optics and Electronics* **1994**, *4*, 129-138.

(25) Baik, K. H.; Vandenhove, L.; Goethals, A. M.; Debeeck, M. O.; Roland, B. *J. Vac. Sci. Technol. B* **1990**, *8*, 1481-1487.

(26) Sviridov, S. M.; Timerov, M. R.; Valiev, K. A.; Velikov, L. V.; Zaroslov, D. Y. *J. Vac. Sci. Technol. B* **1990**, *8*, 1488-1492.

(27) Calabrese, G. S.; Bohland, J. F.; Pavelchek, E. K.; Sinta, R.; Dudley, B. W.; Jones, S. K.; Freeman, P. W. *Microelectron. Eng.* **1993**, *21*, 231-234.

(28) Gogolides, E.; Tzevelekis, D.; Grigoropoulos, S.; Tegou, E.; Hatzakis, M. *J. Vac. Sci. Technol. B* **1996**, *14*, 3332-3338.

(29) Hiraoka, H.; Patlach, A.; Wade, C. *J. Vac. Sci. Technol. B* **1989**, *7*, 1760-1765.

(30) Shaw, J. M.; Hatzakis, M.; Babich, E. D.; Paraszczak, J. R.; Witman, D. F.; Stewart, K. J. *J. Vac. Sci. Technol. B* **1989**, *7*, 1709-1716.

(31) Pham, V. Q.; Ferris, R. J.; Hamad, A.; Ober, C. K. *Chem. Mat.* **2003**, *15*, 4893-4895.

(32) Ito, H. In *Microlithography - Molecular Imprinting*; Springer-Verlag Berlin: Berlin, 2005; Vol. 172, p 37-245.

CHAPTER 4

ORTHOGONAL SELF-PATTERNABLE ELECTROLUMINESCENT MATERIALS FOR ORGANIC ELECTRONIC DEVICES

Abstract

Organic electronics have long attracted attention as a new technology platform able to deliver low-cost, flexible and large-area devices. As organic light-emitting diodes (OLEDs) are, until now, arguably the most promising of the organic electronic technologies, extensive research is being carried out to optimize and further develop these materials and devices. One of the issues which has been the subject of significant research is patterning of OLEDs, and of organic electronic materials in general. The well-established photolithographic patterning method has only been marginally useful in patterning organic electronic materials due to incompatibility issues between the organic materials and conventional lithographic processing solvents and resists. Many alternate patterning methods have thus been developed, however none of which are able to match photolithography in resolution and throughput. To address this issue, the design and synthesis of a novel light-emitting material is presented, based on a fluorene oligomer structure with lithographically patternable end-groups. The structure is fluorinated so as to be soluble in hydrofluoroether solvents, which have previously been shown to be benign and compatible with organic electronic materials. This material is designed to be self-patternable by photolithography in benign processing solvents, thereby circumventing the need for the typically harsh photolithographic processing solvents and even the need for resists. Due to the orthogonal nature of this material, the multiple layer device architectures required by OLEDs are also easily enabled.

4.1 Introduction

Since the report of an efficient and low-voltage organic light-emitting diode (OLED) in 1987 from Kodak[1] and the discovery of electroluminescence in conjugated polymers by Holmes *et al*. in 1990[2], OLEDs have attracted significant attention with their potential to achieve low-cost, flexible and large-area devices[3,4]. Furthermore, OLEDs exhibit high luminous efficiency, a wide-viewing angle, higher contrast, lower power consumption and lower weight as compared to their inorganic counterparts[5]. Although most organic devices, including transistors and photovoltaics, are still largely in developmental stages, organic light-emitting diodes (OLEDs) have already begun to see commercial success: OLED cell phone displays have become common and OLEDs for television displays and general lighting applications are also on the verge of mass production.

Myriad organic light-emitting materials have been reported since their initial discovery[6]. Both small molecule and polymer materials have been extensively developed. One of the main differences between the two types of materials is that small molecule light-emitting materials are vapor-deposited in a high-vacuum environment whereas polymers are solution-processable. Solution processability is one of the primary advantages of polymer-based light-emitting diodes. Particularly, solution processability can enable low-temperature and lower cost processing[7,8].

Polyfluorenes are a promising class of conjugated electroluminescent polymers. They are easily substituted at the 9,9-position in the fluorene unit, thus enabling a high degree of synthetic control in the final structure[9-11]. Modifications in the main chain and in side chains allow elaborate tuning of emission wavelengths to cover the entire visible range, as well as enhancement of device performance and improvement in long-term stability[12]. Polyfluorenes also exhibit excellent solubility and film-forming capabilities[12]. In addition, they have been identified as particularly good candidates

for blue-emitting materials due to their high photoluminescence quantum efficiencies as solid films[13].

As organic light-emitting diodes (OLEDs) are, up to now, arguably the most promising of the organic electronic technologies, extensive research is being carried out to optimize and further develop these materials and devices. Besides material development, one of the issues which has been the subject of significant research is patterning of OLEDs, and of organic electronic materials in general. The well-established photolithographic patterning method has only been marginally useful in patterning organic electronic materials due to incompatibility issues between the organic materials and conventional lithographic processing solvents and resists[14]. Many alternate patterning methods have thus been developed[7], however none of which are able to match photolithography in resolution and throughput.

Recently, Ober *et al*. have reported studies describing the development of highly-fluorinated photoresists, which are processable in hydrofluoroether solvents[15]. The photoresists and hydrofluoroether solvents together make up an *orthogonal* system. The hydrofluoroethers have been demonstrated to be benign and inert to organic electronic materials[16]. The fluorinated photoresists are similarly benign materials. These orthogonal systems enable direct photolithographic patterning of organic electronic materials through the use of benign photoresists and processing solvents. Furthermore, because the fluorinated imaging materials are inert and non-damaging to organic electronic materials, subsequent organic layers can be deposited in a device such that they do not damage previously deposited layers. In this way, multi-layered architectures are readily achievable. Thus far, negative-tone photoresists including chemically-amplified polymeric[17] and molecular glass-based[18] systems as well as a non-chemically amplified polymeric photoresist[19] have been reported.

Based on this orthogonal concept, a novel self-patternable light-emitting material was designed and synthesized as a model compound. The material was also heavily fluorinated to enable processability in hydrofluoroether solvents. Three sets of fluorinated fluorene oligomers with patternable end-groups are described. This model compound was developed to demonstrate the concept of an orthogonal self-patternable functional material.

4.2 Experimental Section

4.2.1 Materials

2,7-Dibromofluorene, 1-iodopropane, *mono-tert*-butyl malonate, N, N'-dicylohexylcarbodiimide (DCC), bis(pinacolato)diboron, [1,1'-bis(diphenylphosphino)-ferrocene]dichloropalladium (II) (complex with dichloromethane (1:1)) ($Pd(dppf)Cl_2$), potassium acetate (KOAc), 2-isopropoxy-4,4,5,5,tetramethyl-1,3,2-dioxaboralane, *tert*-butyllithium (1.7 M solution in pentane) (t-BuLi), chlorotrimethylsilane (TMS-Cl), tetraethylammoniumhydroxide (20 wt. % solution in water) (Et_4NOH), iodine monochloride (1.0 M solution in methylene chloride) (ICl), 1-iodohexane, Aliquat® 336 and bis(4-*tert*-butylphenyl)iodonium perfluoro-1-butanesulfonate (IOD-Nf) were purchased from Sigma-Aldrich and used as received. Solvents: anhydrous toluene, anhydrous diethyl ether, anhydrous dimethylformamide (DMF), anhydrous dimethylsulfoxide (DMSO), anhydrous tetrahydrofuran (THF) and o-xylene were all purchased from Sigma-Aldrich and used as received. Tetrabuytlammonium bromide (TBAB) and propionaldehyde were purchased from Fluka and used as received. *n*-Butyllithium (1.6 M) solution in hexanes (n-BuLi) and 4-dimethylaminopyridine (DMAP) were purchased from Acros and used as received. Tetrakis(triphenylphosphino) palladium (0) $Pd(PPh_3)_4$ was

purchased from Strem Chemicals and used as received. Potassium carbonate (anhydrous) (K_2CO_3) was purchased from Mallinckrodt and used as received.

4.2.2 Synthesis

Electroluminescent compound **4-10**

2,7-Dibromofluorene (10.00 g, 30.90 mmol) (**4-1**), iodopropane (15.7 g, 92.6 mmol), tetrabutylammonium bromide (0.99 g, 3.09 mmol), sodium hydroxide pellets (30.00 g, mmol), water (30 cm^3), and toluene (30 cm^3) were added to a roundbottom flask and magnetically stirred for 12 h at 80 °C under a N_2 atmosphere. The product was extracted with hexanes, washed with water and dried over magnesium sulfate. The solution was purified by passing through a short plug of silica gel with hexanes. The product was recrystallized from hexanes to give a colorless solid **4-2** (9.47 g) in 75 % yield.

Compound **4-2** (3.00 g, 6.09 mmol) and anhydrous diethyl ether (30 cm^3) were added to a roundbottom flask and magnetically stirred under a N_2 atmosphere. The solution was cooled to -78 °C and n-BuLi (5.71 cm^3, 9.14 mmol) was added dropwise. The solution was warmed to ambient temperature and again cooled to -78 °C and propionaldehyde was added to the reaction mixture. The reaction was warmed to ambient temperature and magnetically stirred for 15 minutes at ambient temperature under a N_2 atmosphere. The product was extracted with diethyl ether, washed with water and brine, dried over magnesium sulfate and purified by column chromatography with ethyl acetate-hexanes mixed solvent to give a colorless viscous liquid **4-3** (2.21 g, 5.71 mmol) in 94 % yield.

Compound **4-3** (2.64 g, 6.82 mmol), tert-butyl malonate (1.64 g, 10.22 mmol), dicyclocarbodiimide (2.11 g, 10.22 mmol), dimethylaminopyridine (0.08 g, 0.68 mmol) and methylene chloride (20 cm^3) were added to a roundbottom flask and

magnetically stirred for 2 h at ambient temperature under a N_2 atmosphere. The product was filtered through a short plug of silica gel with methylene chloride, then further purified by column chromatography with methylene chloride-hexanes mixed solvent to give a colorless viscous liquid **4-4** (2.54 g) in 70 % yield.

Compound **4-4** (2.54 g, 4.80 mmol), bis(pinacolato)diboron (1.52 g, 6.00 mmol), Pd(dppf)Cl_2 DCM (0.20 g, 0.24 mmol), potassium acetate (1.41 g, 14.39 mmol) and dimethylformamide (20 cm^3) were added to a Schlenk tube and magnetically stirred for 2 h at 80 °C under a N_2 atmosphere. The product was extracted with ether, washed with water and brine, dried over magnesium sulfate and purified by column chromatography with methylene chloride to give a colorless viscous liquid **4-5** (1.25 g) in 45 % yield.

Compound **4-2** (2.80 g, 6.86 mmol) and anhydrous THF (30 cm^3) were added to a roundbottom flask and magnetically stirred under a N_2 atmosphere. The reaction mixture was cooled to -78 °C and t-BuLi (20.18 cm^3, 34.30 mmol) was added dropwise and magnetically stirred for 10 minutes at -78 °C. The solution was warmed to ambient temperature and cooled again to -78 °C. 2-Isopropoxy-4,4,5,5,tetramethyl-1,3,2-dioxaboralane (3.19 g, 17.15 mmol) was added dropwise and the reaction was magnetically stirred for 5 minutes at -78 °C. The reaction was warmed to ambient temperature and magnetically stirred for 90 minutes at ambient temperature under a N_2 atmosphere. The product was extracted with methylene chloride, washed with water, dried over magnesium sulfate and recrystallized from methylene chloride to give a colorless solid **4-6** (1.75 g) in 51 % yield.

Compound **4-2** (4.00 g, 9.80 mmol) and anhydrous diethyl ether (30 cm^3) were added to a roundbottom flask and magnetically stirred under a N_2 atmosphere. The reaction mixture was cooled to -78 °C and n-BuLi (7.35 cm^3, 11.8 mmol) was added dropwise. The reaction mixture was warmed to ambient temperature and then cooled

again to -78 °C. Trimethylsilyl chloride (1.38g, 12.7 mmol) was added and the reaction mixture was magnetically stirred for 10 minutes at -78 °C. The reaction was warmed to ambient temperature and magnetically stirred for 30 minutes at ambient temperature under a N_2 atmosphere. The product was extracted with hexanes, washed with a sodium bicarbonate solution, washed with brine, dried over magnesium sulfate, and purified by column chromatography with hexanes to give a colorless solid **4-7** (3.04 g) in 77 % yield.

Compound **4-6** (1.10 g, 2.18 mmol), compound **4-7** (2.01 g, 5.01 mmol), tetrakis(triphenylphosphine) palladium (0.08 g, 0.67 mmol), tetraethylammonium hydroxide (10 cm^3) and anhydrous toluene (10 cm^3) were added to a Schlenk tube and magnetically stirred 1 h at 90 °C under a N_2 atmosphere. The product was extracted with toluene, washed with water, dried over magnesium sulfate and passed through a plug of silica gel with methylene chloride-hexanes mixed solvent. The product was recrystallized from methylene chloride-hexanes mixed solvent to give a colorless solid **4-8** (0.86 g) in 44 % yield.

Compound **4-8** (0.86 g, 0.97 mmol) and anhydrous methylene chloride (10 cm^3) were added to a roundbottom flask and magnetically stirred under a N_2 atmosphere. The reaction mixture was cooled to 0 °C and iodochloride (2.41 cm^3, 2.41 mmol) was added to the reaction. The solution was magnetically stirred at 0 °C for 30 minutes. The solution was warmed to ambient temperature and stirred for 90 minutes at ambient temperature under a N_2 atmosphere. The product was extracted with methylene chloride, washed with an aqueous sodium bicarbonate solution, dried over magnesium sulfate and passed through a plug of silica gel with methylene chloride. The product was recrystallized from toluene to give a colorless solid **4-9** (0.52 g) in 54 % yield.

Compound **4-5** (0.65 g, 1.12 mmol) and compound **4-9** (0.49 g, 0.49 mmol), tetrakis(triphenylphosphine) palladium (0.02 g, 0.01 mmol), tetraethylammonium hydroxide (10 cm^3) and anhydrous toluene (10 cm^3) were added to a Schlenk tube and magnetically stirred for 1 h at 90 °C under a N_2 atmosphere. The product was extracted with toluene, washed with water, dried over magnesium sulfate and purified by column chromatography with methylene chloride to give a colorless solid **4-10** (0.08 g, 0.05 mmol) in 10 % yield.

Electroluminescent compound **4-20**

2,7-Dibromofluorene (10.00 g, 30.90 mmol) (**4-1**), iodohexane (19.63 g, 92.6 mmol), tetrabutylammonium bromide (0.99 g, 3.09 mmol), sodium hydroxide pellets (30.00 g, mmol), water (30 cm^3), and toluene (30 cm^3) were added to a roundbottom flask and magnetically stirred for 12 h at 80 °C under a N_2 atmosphere. The product was extracted with hexanes, washed with water and dried over magnesium sulfate. The solution was purified by passing through a short plug of silica gel with hexanes. The product was recrystallized from hexanes to give a colorless solid **4-11** (9.05 g, 18.38 mmol) in 60 % yield.

Compound **4-11** (4.00 g, 8.12 mmol) and anhydrous diethyl ether (40 cm^3) were added to a roundbottom flask and magnetically stirred under a N_2 atmosphere. The solution was cooled to -78 °C and n-BuLi (6.09 cm^3, 9.75 mmol) was added dropwise. The solution was warmed to ambient temperature and again cooled to -78 °C and propionaldehyde (0.94 g, 16.25 mmol) was added to the reaction mixture. The reaction was warmed to ambient temperature and magnetically stirred for 15 minutes at ambient temperature under a N_2 atmosphere. The product was extracted with diethyl ether, washed with water and brine, dried over magnesium sulfate and purified

by column chromatography with methylene chloride-hexanes mixed solvent to give a colorless viscous liquid **4-12** (2.69 g, 5.71 mmol) in 70 % yield.

Compound **4-12** (2.65 g, 5.61 mmol), tert-butyl malonate (1.42 g, 8.42 mmol), dicyclocarbodiimide (1.74 g, 8.42 mmol), dimethylaminopyridine (0.07 g, 0.56 mmol) and methylene chloride (25 cm^3) were added to a roundbottom flask and magnetically stirred for 5 h at ambient temperature under a N_2 atmosphere. The product was filtered through a short plug of silica gel with methylene chloride, then further purified by column chromatography with methylene chloride-hexanes mixed solvent to give a colorless viscous liquid **4-13** (2.67 g, 4.35 mmol) in 77 % yield.

Compound **4-13** (2.60 g, 4.23 mmol), bis(pinacolato)diboron (1.34 g, 5.29 mmol), Pd(dppf)Cl_2 DCM (0.16 g, 0.21 mmol), potassium acetate (1.25 g, 12.70 mmol) and dimethylsulfoxide (20 cm^3) were added to a Schlenk tube and magnetically stirred for 12 h at 80 °C under a N_2 atmosphere. The product was extracted with ether, washed with water and brine, dried over magnesium sulfate and purified by column chromatography with methylene chloride to give a colorless viscous liquid **4-14** (0.97 g, 1.47 mmol) in 35 % yield.

Compound **4-11** (3.55 g, 7.28 mmol) and anhydrous diethyl ether (30 cm^3) were added to a roundbottom flask and magnetically stirred under a N_2 atmosphere. The reaction mixture was cooled to -78 °C and n-BuLi (19.7 cm^3, 11.8 mmol) was added dropwise. The reaction mixture was warmed to ambient temperature and then cooled again to -78 °C. Trimethylsilyl chloride (0.86 g, 7.94 mmol) was added and the reaction mixture was magnetically stirred for 10 minutes at -78 °C. The reaction was warmed to ambient temperature and magnetically stirred for 30 minutes at ambient temperature under a N_2 atmosphere. The product was extracted with hexanes, washed with a sodium bicarbonate solution, washed with brine, dried over magnesium

sulfate, and purified by column chromatography with hexanes to give a colorless viscous liquid **4-15** (2.42 g, 4.98 mmol) in 68 % yield.

Compound **4-15** (10.00 g, 20.59 mmol) and anhydrous THF (200 cm^3) were added to a roundbottom flask and magnetically stirred under a N_2 atmosphere. The reaction mixture was cooled to -78 °C and t-BuLi (30.40 cm^3, 51.58 mmol) was added dropwise and magnetically stirred for 1 h at -78 °C. 2-isopropoxy-4,4,5,5,tetramethyl-1,3,2-dioxaboralane (5.6 cm^3, 26.74 mmol) was added dropwise and the reaction was magnetically stirred for 5 minutes at -78 °C. The reaction was warmed to ambient temperature and magnetically stirred for 12 h at ambient temperature under a N_2 atmosphere. The product was extracted with methylene chloride, washed with water, dried over magnesium sulfate and purified by column chromatography in ethyl acetate-hexanes mixed solvent to give a colorless solid **4-16** (4.61 g, 8.65 mmol) in 42 % yield.

Compound **4-16** (1.07 g, 2.2 mmol), compound **4-17** (0.39 g, 1.33 mmol) (prepared according to the literature procedure[20]), aqueous 2 M potassium carbonate solution (10 cm^3), Aliquat 336 (0.50 cm^3), toluene (19.5 cm^3), water (5 cm^3), and tetrakis(triphenylphosphine) palladium (0.05 g, 0.05 mmol) were added to a Schlenk tube and magnetically stirred at 80 °C for 2 h under a N_2 atmosphere. The product was extracted with methylene chloride, washed with brine, dried over magnesium sulfate, and purified by column chromatography with methylene chloride-hexanes mixed solvent to give a bright yellow solid **4-18** (0.24 g, 0.25 mmol) in 23 % yield.

Compound **4-18** (0.24 g, 0.23 mmol) and anhydrous methylene chloride (10 cm^3) were added to a roundbottom flask and magnetically stirred under a N_2 atmosphere. The reaction mixture was cooled to 0 °C and iodochloride (0.58 cm^3, 0.58 mmol) was added to the reaction. The solution was magnetically stirred at 0 °C for 90 minutes. The solution was warmed to ambient temperature and stirred for 3 h at

ambient temperature under a N_2 atmosphere. The product was extracted with methylene chloride, washed with an aqueous sodium bicarbonate solution, dried over magnesium sulfate and passed through a plug of silica gel with methylene chloride. The product was further purified by column chromatography with methylene chloride to give a yellow solid **4-19** (0.23 g, 22 mmol) in 94 % yield.

Compound **4-14** (0.30 g, 0.45 mmol), compound **4-19** (0.21 g, 0.18 mmol), aqueous 2 M potassium carbonate solution (2.50 cm^3), Aliquat 336 (0.20 cm^3), toluene (5 cm^3), water (1 cm^3), and tetrakis(triphenylphosphine) palladium (0.01 g, 0.01 mmol) were added to a Schlenk tube and magnetically stirred at 80 °C for 2 d under a N_2 atmosphere. The product was extracted with methylene chloride, washed with brine, dried over magnesium sulfate, and purified by column chromatography with hexanes to give a bright yellow solid **4-20** (0.06 g, 0.03 mmol) in 18 % yield.

Electroluminescent compound **4-25**

2,7-Dibromofluorene (3.00 g, 9.26 mmol) (**4-1**), 1,1,1,2,2,3,3,4,4,5,5,6,6,7,7,8,8-heptadecafluoro-12-iododododecane (13.94 g, 23.15 mmol) (prepared according to the literature procedure[21]), tetrabutylammonium bromide (0.30 g, 0.93 mmol), sodium hydroxide pellets (16.00 g), water (16 cm^3), and toluene (16 cm^3) were added to a roundbottom flask and magnetically stirred for 12 h at 80 °C under a N_2 atmosphere. The product was extracted with hexanes, washed with water and dried over magnesium sulfate. The solution was purified by column chromatography in hexanes. The product was recrystallized from methylene chloride to give a colorless solid **4-21** (3.83 g) in 56 % yield.

Compound **4-21** (3.50 g, 2.75 mmol) and anhydrous diethyl ether (35 cm^3) were added to a roundbottom flask and magnetically stirred under a N_2 atmosphere. The solution was cooled to -78 °C and n-BuLi (3.74 cm^3, 3.03 mmol) was added

dropwise. The solution was warmed to ambient temperature and again cooled to -78 °C and propionaldehyde (0.32 g, 5.50 mmol) was added to the reaction mixture. The reaction was warmed to ambient temperature and magnetically stirred for 15 minutes at ambient temperature under a N_2 atmosphere. The product was extracted with diethyl ether, washed with water and brine, dried over magnesium sulfate and purified by column chromatography with methylene chloride-hexanes mixed solvent to give a colorless viscous liquid **4-22** (1.81 g, 1.48 mmol) in 54 % yield.

Compound **4-22** (1.20 g, 0.96 mmol), tert-butyl malonate (0.23 g, 1.44 mmol), dicyclocarbodiimide (0.30 g, 1.44 mmol), dimethylaminopyridine (0.01 g, 0.10 mmol) and methylene chloride (10 cm^3) were added to a roundbottom flask and magnetically stirred for 2 h at ambient temperature under a N_2 atmosphere. The product was filtered through a short plug of silica gel with methylene chloride, then further purified by column chromatography with methylene chloride-hexanes mixed solvent to give a colorless viscous liquid **4-23** (1.09 g, 0.80 mmol) in 81 % yield.

Compound **4-23** (1.09 g, 0.78 mmol), bis(pinacolato)diboron (0.25 g, 0.98 mmol), Pd(dppf)Cl_2 DCM (0.03 g, 0.04 mmol), potassium acetate (0.23 g, 2.34 mmol) and dimethylformamide (10 cm^3) were added to a Schlenk tube and magnetically stirred for 2 h at 80 °C under a N_2 atmosphere. The product was extracted with ether, washed with water and brine, dried over magnesium sulfate and purified by column chromatography with methylene chloride-hexanes mixed solvent to give a colorless viscous liquid **4-24** (0.50 g, 0.35 mmol) in 45 % yield.

Compound **4-24** (0.13 g, 0.09 mmol), compound **4-19** (0.03 g, 0.04 mmol), aqueous 2 M potassium carbonate solution (1.00 cm^3), Aliquat 336 (0.10 cm^3), toluene (3 cm^3), water (0.05 cm^3), and tetrakis(triphenylphosphine) palladium (0.01 g, 0.01 mmol) were added to a Schlenk tube and magnetically stirred at 80 °C for 2 d under a N_2 atmosphere. The product was extracted with methylene chloride, washed with

water and brine, dried over magnesium sulfate, and purified by column chromatography with –methylene chloride-hexanes mixed solvent to give a bright yellow solid **4-25** (0.04 g, 0.01 mmol) in 30 % yield.

4.2.3 Characterization

4-2

^{1}H NMR (400 MHz, $CDCl_3$), δ: = 7.54-7.38 (m, 6H, Ar-*H*), 1.90 (m, 4H, C*H*$_2$CH$_2$CH$_3$), 0.67 ppm (m, 10H, CH$_2$C*H*$_2$C*H*$_3$).

4-3

^{1}H NMR (400 MHz, $CDCl_3$), δ: = 7.68-7.20 (m, 6H, Ar-*H*), 4.65 (m, 1H, O*H*), 3.50 (m, 1H, C*H*OH), 1.98-1.71 (m, 5H, CHC*H*$_2$C*H*$_3$), 1.40 ppm (m, 14H, C*H*$_2$C*H*$_2$C*H*$_3$).

4-4

^{1}H NMR (400 MHz, $CDCl_3$), δ: = 7.72-7.20 (m, 6H, Ar-*H*), 5.79 (m, 1H, C*H*O), 3.32 (s, 2H, OCC*H*$_2$CO), 1.91 (m, 6H, CHC*H*$_2$, C*H*$_2$C*H*$_2$), 1.43 (s, 9H, C(C*H*$_3$)$_3$, 0.89 (m, 3H, CHCH$_2$C*H*$_3$), 0.63 ppm (m, 10H, CH$_2$C*H*$_2$C*H*$_3$).

4-5

^{1}H NMR (400 MHz, $CDCl_3$), δ: = 7.81-7.60 (m, 6H, Ar-*H*), 5.78 (m, 1H, C*H*O), 3.30 (s, 2H, OCC *H*$_2$CO), 1.97 (m, 6H, CHC*H*$_2$, C*H*$_2$C*H*$_2$), 1.42 (s, 9H, C(C *H*$_3$)$_3$), 1.36 (s, 12H, C(C*H*$_3$)$_2$), 0.88 (m, 3H, CHCH$_2$C*H*$_3$), 0.61 ppm (m, 10H, CH$_2$C*H*$_2$C*H*$_3$).

4-6

^{1}H NMR (400 MHz, $CDCl_3$), δ: = 7.73 (m, 6H, Ar-*H*), 1.99 (m, 4H, C*H*$_2$CH$_2$CH$_3$), 1.36 (s, 12H, C(C*H*$_3$)$_2$), 0.61 ppm (m, 10H, CH$_2$C*H*$_2$C*H*$_3$).

4-7

^{1}H NMR (400 MHz, $CDCl_3$), δ: = 7.74-7.40 (m, 6H, Ar-*H*), 1.94 (m, 4H, CH_2CH$_2$CH$_3$), 0.68 (m, 10H, CH$_2$CH_2CH_3), 0.32 ppm (s, 9H, Si(CH_3)$_3$).

4-8

^{1}H NMR (400 MHz, $CDCl_3$), δ: = 7.86-7.44 (m, 18H, Ar-*H*), 2.04 (m, 12H, CH_2CH$_2$CH$_3$), 0.71 (m, 30H, CH$_2$CH_2CH_3), 0.32 ppm (s, 18H, Si(CH_3)$_3$).

4-9

^{1}H NMR (400 MHz, $CDCl_3$), δ: = 7.87-7.40 (m, 18H, Ar-*H*), 1.97 (m, 12H, CH_2CH$_2$CH$_3$), 0.70 ppm (m, 30H, CH$_2$CH_2CH_3).

4-10

^{1}H NMR (400 MHz, $CDCl_3$), δ: = 7.82-7.52 (m, 30H, Ar-*H*), 5.76 (m, 2H, C*H*O), 3.28 (s, 4H, OCC H_2CO), 2.13-1.79 (m, 24H, CHCH_2, CH_2CH$_2$), 1.40 (s, 19H, C(CH_3)$_3$), 0.96-0.53 ppm (m, 56H, CH$_2$CH_2CH_3, CHCH$_2$CH_3).

4-11

IR (neat): ν = 2920, 2852, 1445, 1255, 1058, 1002, 875, 802, 745, 723, 663 cm^{-1}; ^{1}H NMR (400 MHz, $CDCl_3$, δ): = 7.42 (m, 6H, Ar-*H*), 1.87 (m, 4H, CH_2CH$_2$), 1.04 (m, 12H, CH_2CH_2CH_2), 0.76 (m, 6H, CH$_2$CH_3), 0.55 ppm (m, 4H, CH_2CH$_2$); elemental analysis: C (61.10 %), H (6.51 %), N: (<0.05 %).

4-12

^{1}H NMR (400 MHz, $CDCl_3$, δ): = 7.70-7.21 (m, 6H, Ar-*H*), 4.64 (m, 1H, CHO*H*), 3.64 (s, 1H, C*H*OH), 1.81 (m, 8H, CH_2CH_2), 0.96 (m, 12H, CH_2CH_2CH_2), 0.84 (m, 2H, CHCH_2CH$_3$), 0.68 (m, 6H, CH$_2$CH$_2$CH_3), 0.53 ppm (m, 3H, CHCH$_2$CH_3).

4-13

^{1}H NMR (400 MHz, $CDCl_3$, δ): = 7.74-7.19 (m, 6H, Ar-*H*), 5.81 (m, 1H, C*H*O), 3.30 (s, 2H, OCC H_2CO), 1.91 (m, 6H, CHCH_2, C H_2CH_2), 1.44 (s, 9H, C(C

$H_3)_3$), 1.01 (m, 12H, CH_2CH_2CH_2), 0.89 (m, 3H, CHCH$_2$CH_3), 0.73 (m, 6H, CH$_2$CH_3), 0.59 ppm (m, 4H, CH_2CH$_2$).

4-14

^{1}H NMR (400 MHz, CDCl$_3$, δ): = 7.83-7.01 (m, 6H, Ar-*H*), 5.80 (m, 1H, C*H*O), 3.30 (s, 2H, OCC H_2CO), 1.96 (m, 6H, CHCH_2, C H_2CH_2), 1.44 (s, 9H, C(C $H_3)_3$), 1.37 (s, 12H, C(C $H_3)_2$), 1.00 (m, 12H, CH_2CH_2CH_2), 0.87 (m, 3H, CHCH$_2$CH_3), 0.72 (m, 6H, CH$_2$CH_3), 0.56 ppm (m, 4H, CH_2CH$_2$).

4-15

IR (film on NaCl): ν = 3739, 3640, 2904, 1879, 1603, 1562, 1463, 1392, 1254, 1092, 1002, 865, 754, 626 cm^{-1}; ^{1}H NMR (400 MHz, CDCl$_3$, δ): = 7.66-7.38 (m, 6H, Ar-*H*), 1.92 (m, 4H, CH_2CH$_2$), 1.33 (m, 12H, CH_2CH_2CH_2), 0.76 (m, 6H, CH$_2$CH$_2$CH_3), 0.61 (m, 4H, CH_2), 0.29 ppm (m, 9H, Si(C$H_3)_3$); elemental analysis: C (69.25 %), H (7.88 %), N: (0.09 %).

4-16

IR (neat): ν = 2928, 2858, 1610, 1349, 1247, 1139, 1080, 860, 827, 754, 690, 663, 528 cm^{-1}; ^{1}H NMR (400 MHz, CDCl$_3$, δ): = 7.82-7.43 (m, 6H, Ar-*H*), 1.99 (m, 4H, CH_2CH$_2$), 1.39 (s, 12H, C(C$H_3)_2$), 1.03 (m, 12H, CH_2CH_2CH_2), 0.75 (m, 6H, CH$_2$CH$_2$CH_3), 0.59 (br s, 4H, CH_2), 0.30 ppm (s, 9H, Si(C$H_3)_3$); elemental analysis: C (76.40 %), H (9.10 %), N: (0.09 %).

4-18

IR (neat): ν = 2929, 2859, 1462, 1247, 1092, 814, 691, 693, 621 cm^{-1}; ^{1}H NMR (400 MHz, CDCl$_3$, δ): = 8.07-7.48 (m, 14H, Ar-*H*), 2.06 (m, 8H, CH_2CH$_2$), 1.10 (m, 24H, CH_2CH_2CH_2), 0.78 (m, 20H, CH$_2$CH_2CH_3), 0.34 ppm (s, 9H, Si(C$H_3)_3$); elemental analysis: C (78.55 %), H (8.69 %), N: (2.84 %).

4-19

IR (neat): ν = 2921, 2851, 1454, 1399, 1338, 1245, 1053, 1003, 890, 814, 749 cm^{-1}; ^1H NMR (400 MHz, $CDCl_3$, δ): = 8.07-7.51 (m, 14H, Ar-*H*), 2.05 (m, 8H, CH_2CH_2), 1.11 (m, 24H, $CH_2CH_2CH_2$), 0.80 ppm (m, 20H, $CH_2CH_2CH_3$); elemental analysis: C (65.72 %), H (5.88 %), N: (2.50 %).

4-20

^1H NMR (400 MHz, $CDCl_3$), δ: = 8.10-7.31 (m, 26H, Ar-*H*), 5.84 (m, 2H, O*H*), 3.35 (m, 2H, C*H*OH), 2.12 (m, 18H, $C(CH_3)_3$), 1.90 (m, 4H, $OCCH_2CO$), 1.27-0.58 ppm (m, 104H).

4-21

IR (neat): ν = 1449, 1197, 1145, 811, 706, 656, 560, 522 cm^{-1}; ^1H NMR (400 MHz, $CDCl_3$ (1 part by volume) + $CFCl_3$ (1 part by volume), δ): = 7.50 (m, 6H, Ar-*H*), 2.03 (m, 4H, CH_2CH_2), 1.82 (m, 4H, CH_2CF_2), 1.45 (m, 4H, CH_2CH_2), 0.70 ppm (m, 4H, CH_2CH_2); elemental analysis: C (35.14 %), H (1.70 %), N: (<0.05 %).

4-22

IR (film on NaCl): ν = 3362, 2949, 2867, 2364, 1455, 1210, 1144, 1032, 819, 704, 656, 534 cm^{-1}; ^1H NMR (400 MHz, $CDCl_3$, δ): = 7.68-7.22 (m, 6H, Ar-*H*), 4.64 (m, 1H, O*H*), 2.01-1.19 (m, 16H), 0.86 (m, 2H, $CHCH_2CH_3$), 0.59 ppm (br s, 3H, $CHCH_2CH_3$); elemental analysis: C (38.77 %), H (2.38 %), N: (<0.05 %).

4-23

IR (film on NaCl): ν = 3362, 2949, 2867, 2364, 1455, 1210, 1144, 1032, 819, 704, 656, 534 cm^{-1}; ^1H NMR (400 MHz, $CDCl_3$, δ): = 7.83-7.12 (m, 6H, Ar-*H*), 5.68 (m, 1H, C*H*OH), 3.20 (m, 2H, $COCH_2CO$), 2.06-1.80 (m, 10H), 1.39 (s, 9H, $C(CH_3)_3$), 1.27 (m, 3H, $CHCH_2CH_3$), 0.91-0.50 ppm (m, 8H).

4-24

IR (film on NaCl): ν = 3002, 2868, 2372, 1737, 1610, 1215, 963, 830, 704 cm^{-1}; ^1H NMR (400 MHz, $CDCl_3$, δ): = 7.80-7.29 (m, 6H, Ar-*H*), 5.80 (m, 1H,

C*H*OH), 3.29 (m, 2H, COCH_2CO), 2.19-1.84 (m, 10H), 1.46 (s, 9H, C(CH_3)$_3$), 1.38 (s, 12H, C(CH_3)$_2$), 1.34 (m, 3H, CHCH_2CH_3), 0.90-0.55 ppm (m, 8H).

4-25

^{1}H NMR (400 MHz, $CDCl_3$), δ: = 7.98-7.27 (m, 26H, Ar-*H*), 5.83 (m, 2H, O*H*), 3.30 (m, 2H, C*H*OH), 2.15 (m, 18H, C(CH_3)$_3$), 1.86 (m, 4H, OCCH_2CO), 1.25-0.52 ppm (m, 64H).

4.2.4 Lithographic Evaluation

The lithographic properties of the oligomer **4-20** were investigated using an ABM contact aligner fitted with a 248 nm mirror. A resist mixture was prepared with 5 wt. % bis(4-*tert*-butylphenyl)iodonium perfluoro-1-butanesulfonate photoacid generator (PAG). Resist films were spin-coated from a 5 wt. % resist solution in o-xylene at 750 rpm onto silicon followed by post-apply bake (PAB) at 90 °C. The resulting film had a thickness of *ca*. 100 nm. After UV exposure, the film was post-exposure baked (PEB) at 65 °C for 5 minutes. The film was developed in ethanol for one minute and then baked again at 160 °C for one minute.

4.3 Results

Synthesis of compound **4-10** began with alkylation of 2,7-dibromofluorene (**4-1)** with iodopropane under phase transfer catalysis conditions to give compound **4-2.** Compound **4-2** was treated with n-BuLi to generate a metal-halogen exchange; compound **4-3** was obtained by a 1,2-addition to the carbonyl group of propionaldehyde. Compound **4-4** was obtained through a standard esterification reaction using dicyclocarbodiimide to couple compound **4-3** and tert-butyl malonate. A Miyaura borylation[22] of compound **4-4** resulted in compound **4-5**.

Compound **4-2** was treated with n-BuLi to generate a metal-halogen exchange; compound **4-7** was obtained through a substitution with trimethylsilyl chloride. Compound **4-2** was also transformed into the diboronate **4-6** through lithiation and substitution with 2-isopropoxy-4,4,5,5,tetramethyl-1,3,2-dioxaboralane. Compound **4-8** was obtained by a Suzuki coupling of compounds **4-6** and **4-7**. Iodination of **4-8** with iodochloride gave compound **4-9**. Another Suzuki coupling of **4-5** and **4-9** gave electroluminescent fluorene pentamer **4-10**.

The synthetic scheme for compound **4-10** is shown in Figure 4.1. This compound proved to be crystalline by x-ray diffraction (XRD) analysis. The XRD spectrum, shown in Figure 4.2, exhibits several sharp peaks, rather than a smooth curve, thereby denoting crystallinity in the compound. Being crystalline, a uniform film could not be formed by spin-casting, which requires an amorphous material. Therefore a slightly modified fluorene oligomer **4-20**, which might prove amorphous, was designed and synthesized.

Synthesis of compound **4-20** began with alkylation of 2,7-dibromofluorene (**4-1)** with iodohexane under phase transfer catalysis conditions to give compound **4-11.** Compound **4-11** was treated with n-BuLi to generate a metal-halogen exchange; compound **4-12** was obtained by a 1,2-addition to the carbonyl group of propionaldehyde. Compound **4-13** was obtained through a standard esterification reaction using dicyclocarbodiimide to couple compound **4-12** and tert-butyl malonate. A Miyaura borylation of compound **4-13** resulted in compound **4-14**.
Compound **4-11** was treated with n-BuLi to generate a metal-halogen exchange; compound **4-15** was obtained through a substitution with trimethylsilyl chloride. A Miyaura borylation of compound **4-15** resulted in compound **4-16**. Benzothiadizole **4-17** was prepared according to the literature procedure and attached to two equivalents of compound **4-16** through a Suzuki coupling reaction to give **4-18**. Iodination of **4-18**

Figure 4.1: Synthetic scheme for compound **4-10.** Reagents and conditions: (i) iodopropane, TBAB, NaOH, water, toluene, 12 h, 80°C; (ii) ether, n-BuLi, propionaldehyde; (iii) tert-butyl malonate, DCC, DMAP, DCM; (iv) bis(pinacolato)diboron, Pd(dppf)Cl_2, KOAc, DMF, 80°C, 2h; (v) 2-isopropoxy-4,4,5,5,tetramethyl-1,3,2-dioxaboralane, t-BuLi, THF; (vi) n-BuLi, TMS-Cl, ether; (vii) $Pd(PPh_3)_4$, Et_4NOH, toluene; (viii) ICl, DCM; (ix) $Pd(PPh_3)_4$, Et_4NOH, toluene.

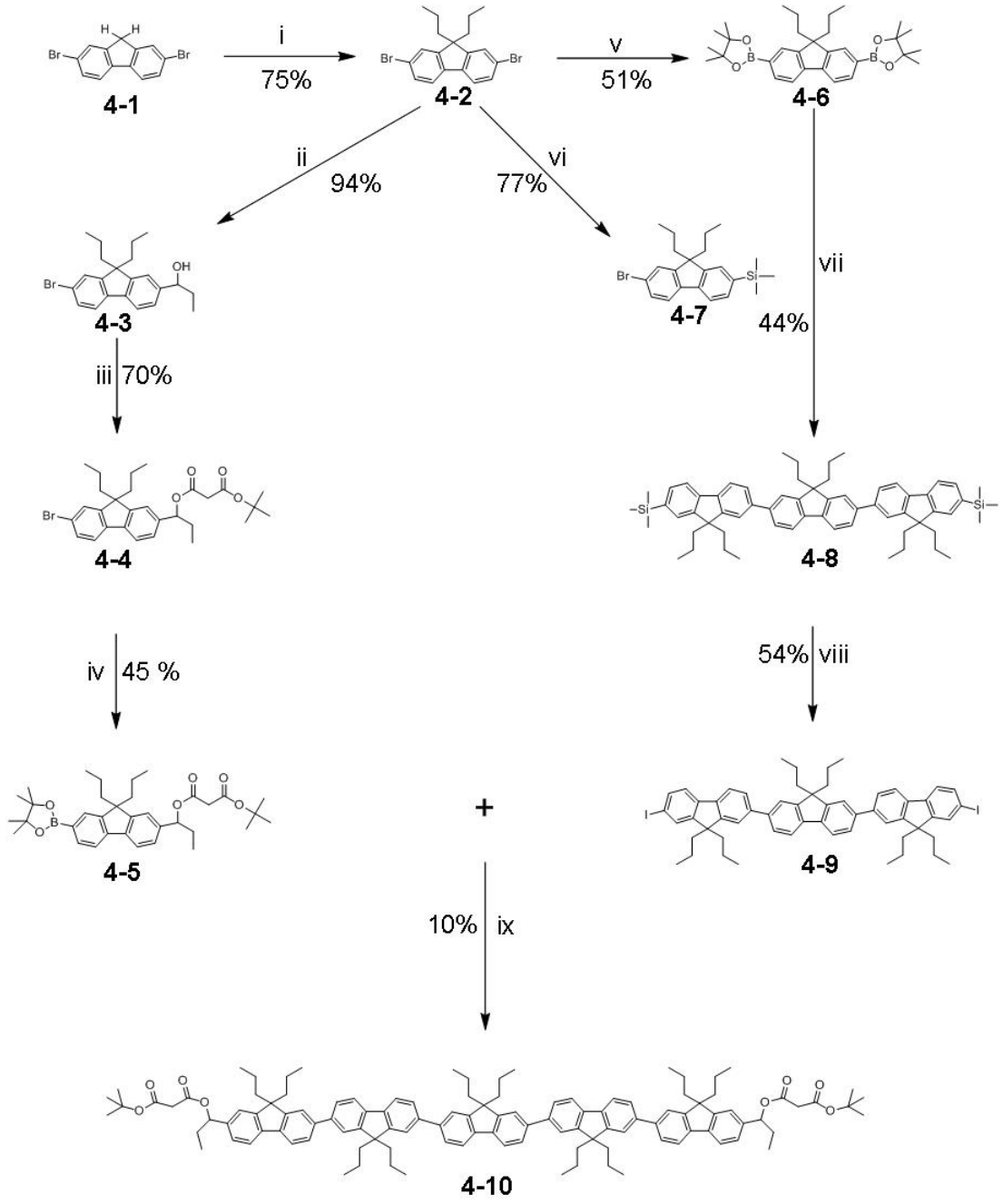
4-1
i
75%
4-2
v
51%
4-6
ii
94%
vi
77%
4-3
4-7
vii
44%
iii 70%
4-4
4-8
iv 45 %
54% viii
4-5
+
4-9
10% ix
4-10

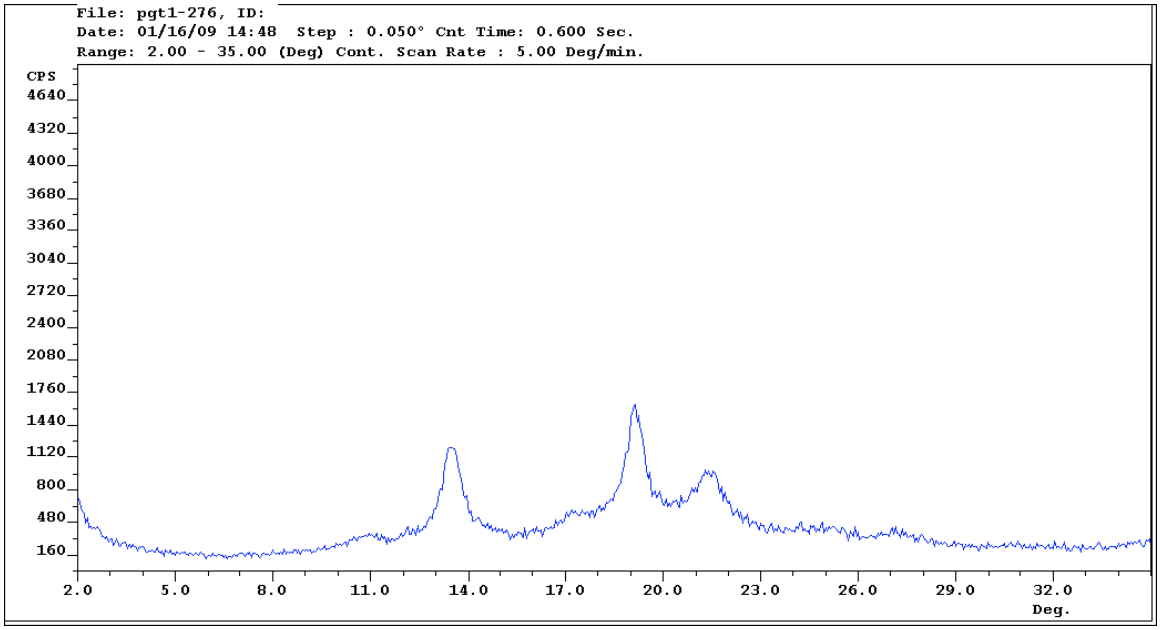

Figure 4.2: X-ray diffraction spectrum of compound **4-10.**

with iodochloride gave compound **4-19**. Another Suzuki coupling of **4-14** and **4-19** gave electroluminescent fluorene pentamer **4-20**.

The synthetic scheme for hexyl-substituted fluorene pentamer **4-20** is shown in Figure 4.3. A well-known chromophore for green emission, benzothiadizole[23], was incorporated into the oligomer structure to give a green electroluminescent material. Furthermore, this oligomer proved amorphous and exhibited good film-forming properties. To test photolithographic properties, the oligomer was mixed with 5 wt. % bis(4-*tert*-butylphenyl)iodonium perfluoro-1-butanesulfonate photoacid generator (PAG) and spun-cast onto silicon. The film was exposed at 248 nm on a contact aligner, post-exposure baked and developed. Submicron resolution was obtained; optical images are shown in Figure 4.4. Based on these results, a third analog of this oligomer was designed to incorporate perfluoroalkyl moieties in order to render the final material soluble and processable in hydrofluoroether solvents.

Synthesis of compound **4-25** began with perfluoroalkylation of 2,7-dibromofluorene (**4-1)** with 1,1,1,2,2,3,3,4,4,5,5,6,6,7,7,8,8-heptadecafluoro-12-iododododecane (prepared according to the literature procedure[21]) under phase transfer catalysis conditions to give compound **4-21.** Compound **4-21** was treated with n-BuLi to generate a metal-halogen exchange; compound **4-22** was obtained by a 1,2-addition to the carbonyl group of propionaldehyde. Compound **4-23** was obtained through a standard esterification reaction using dicyclocarbodiimide to couple compound **4-22** and tert-butyl malonate. A Miyaura borylation of compound **4-23** resulted in compound **4-24**. Suzuki coupling of **4-19** and **4-24** gave electroluminescent fluorene pentamer **4-25**.

Figure 4.3: Synthetic scheme for compound **4-20.** Reagents and conditions: (i) iodohexane, TBAB, NaOH, water, toluene, 12 h, 80°C; (ii) ether, n-BuLi, propionaldehyde; (iii) tert-butyl malonate, DCC, DMAP, DCM; (iv) bis(pinacolato)diboron, Pd(dppf)Cl_2, KOAc, DMSO, 80°C, 2h; (v) n-BuLi, TMS-Cl, ether; (vi) 2-isopropoxy-4,4,5,5,tetramethyl-1,3,2-dioxaboralane, t-BuLi, THF; (vii) potassium carbonate, Aliquat 336, toluene, water, Pd(PPh_3)$_4$, 80°C, 2h; (viii) ICl, DCM; (ix) potassium carbonate, Aliquat 336, toluene, water, Pd(PPh_3)$_4$, 80°C, 2d.

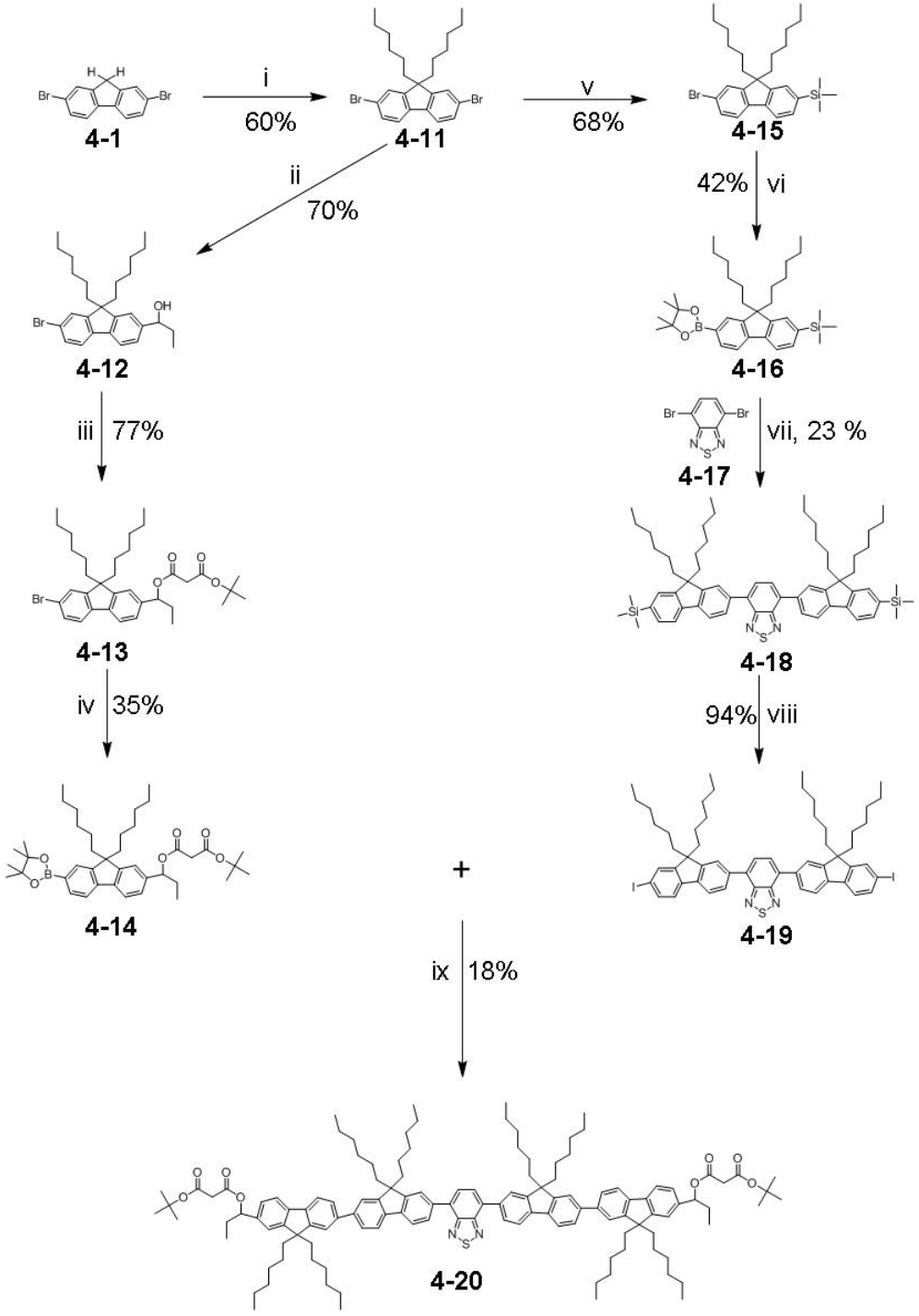
4-1
i
60%
4-11
v
68%
4-15
ii
70%
42%
vi
4-12
4-16
iii
77%
4-17
vii, 23 %
4-13
4-18
iv
35%
94%
viii
4-14
+
4-19
ix
18%
4-20

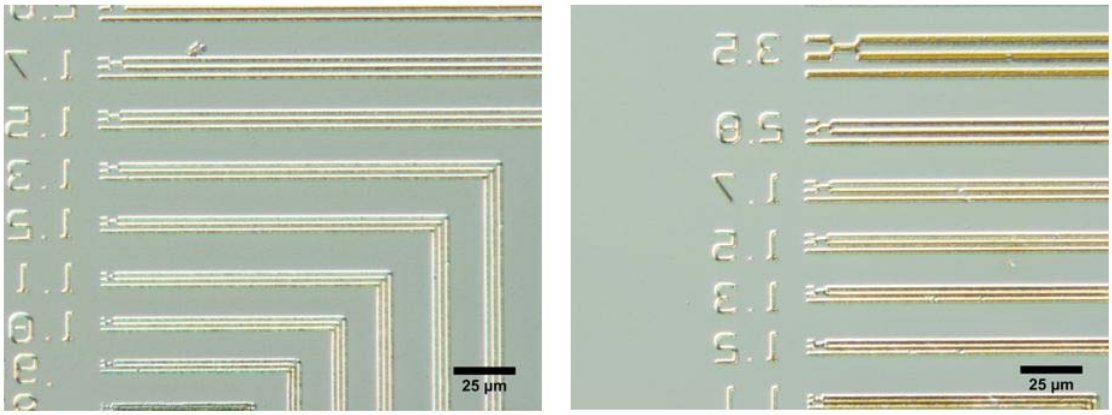

Figure 4.4: Optical microscope images of patterned oligomer **4-20**.

The structure of compound **4-25** was designed to include perfluoroalkyl units in place of four of the hexyl groups present in oligomer **4-20**. Based on this design, the final compound would have 37.7 % fluorination, which may be enough for the compound to show sufficient solubility in hydrofluoroether solvents. The synthetic scheme for oligomer **4-25** is shown in Figure 4.5. Although this final compound proved to be electroluminescent and amorphous, solubility in hydrofluoroether solvents alone was limited.

4.4 Discussion

The issue of organic materials incompatibility with lithographic processing solvents and resists has inhibited the implementation of this well-established, high-resolution and high-throughput patterning process in organic electronics fabrication. Ober *et al*. have recently reported an elegant solution to this problem: substitution of compatible photoresists and processing solvents in order to directly apply photolithographic patterning to organic electronic materials. Although the idea of orthogonal processing was originally developed to address this patterning problem, the concept of orthogonality is much more widely applicable. This idea enables a new concept in materials handling. For the current application, fluorination of the material allows more diverse options in processing and device architecture than would be available with a purely organic material.

This fluorene pentamer with patternable end groups was designed to serve as an example of the concept of an orthogonal self-patternable functional material. It was likely that significant modifications would later need to be implemented to tune the electroluminescent properties of the material.

Figure 4.5: Synthetic scheme for compound **4-25.** Reagents and conditions: (i) 1,1,1,2,2,3,3,4,4,5,5,6,6,7,7,8,8-heptadecafluoro-12-iododododecane, TBAB, NaOH, water, toluene, 12 h, 80°C; (ii) ether, n-BuLi, propionaldehyde; (iii) tert-butyl malonate, DCC, DMAP, DCM; (iv) bis(pinacolato)diboron, Pd(dppf)Cl_2, KOAc, DMF, 80°C, 2h; (v) potassium carbonate, Aliquat 336, toluene, water, Pd(PPh_3)$_4$, 80°C, 2d.

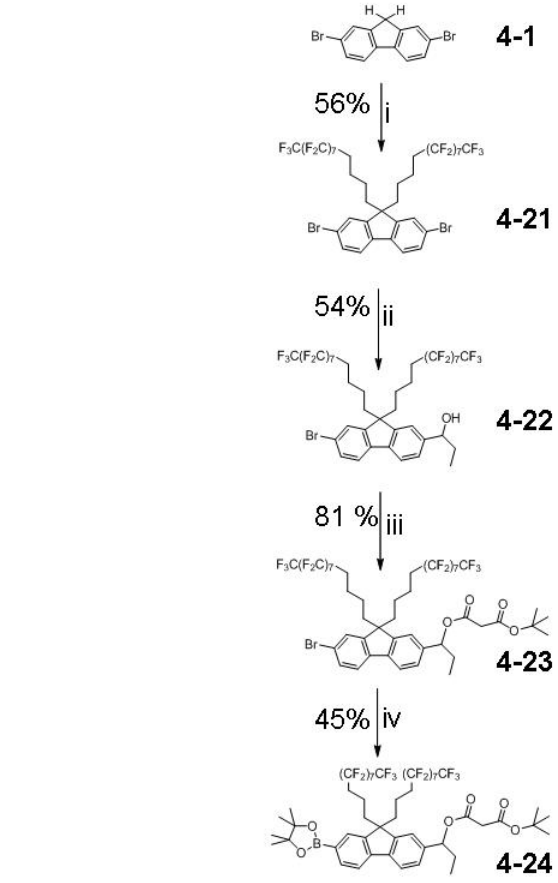
4-1
56% i
4-21
54% ii
4-22
81 % iii
4-23
45% iv
4-24

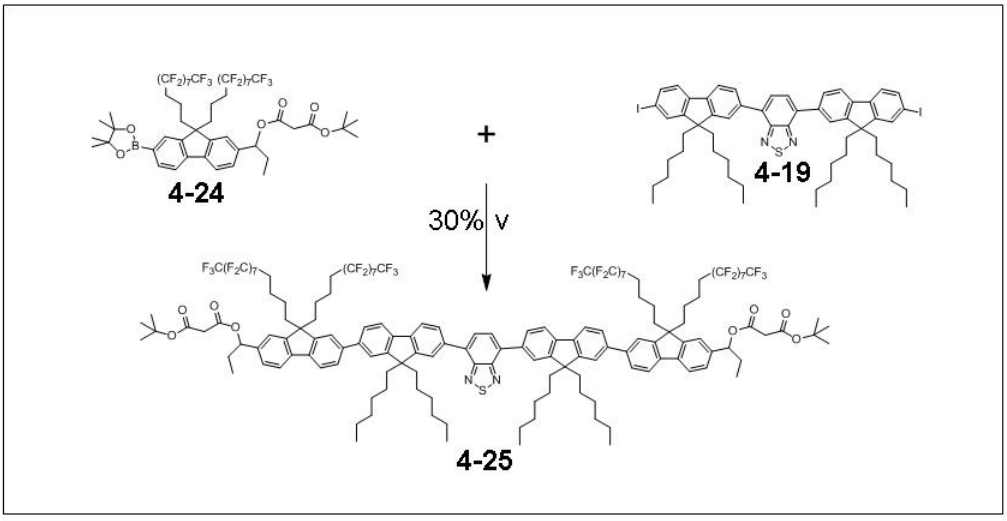
4-24
+
4-19
30% v
4-25

The oligomer backbone was chosen to be polyfluorene-based with the addition of a well-known chromophore for green emission, to create a green-emitting material. As expected, the polyfluorene oligomers **4-10**, **4-20**, and **4-25** all exhibited electroluminescence. **4-20** and **4-25** in particular showed green emission. Although rudimentary electroluminescence was easily observed in these compounds, extensive optimization of the structure would likely be necessary to develop a competitive electroluminescent material.

The patternable end groups were specifically designed to decompose during patterning and subsequent heating to leave only carbon and hydrogen behind in the final patterned material. The presence of oxygen in the end groups would likely decrease the lifetime of the material by premature degradation, as oxygen is able to oxidize the oligomer. The end group structure is based on malonic acid with a tertiary butyl moiety. The tertiary butyl group is widely used in chemically-amplified photoresists as it is acid-labile and cleaves easily in the presence of acid. It was expected that upon UV exposure with a photoacid generator and subsequent heating, the end groups in the exposed regions would cleave to a malonic acid structure **4-26**. This malonic acid structure should subsequently decompose to an acetic acid group in the presence of any acid and heat, according to basic malonic acid chemistry. The resulting acetic acid end groups are then known to decarboxylate under high temperatures to yield unsaturated alkyl groups, shown in structure **4-27**[24]. Development of the film in hydrofluoroether solvents should remove the original compound and leave behind only the active material in a negative-tone pattern. The active form should contain no oxygen and should provide a stable electroluminescent structure.

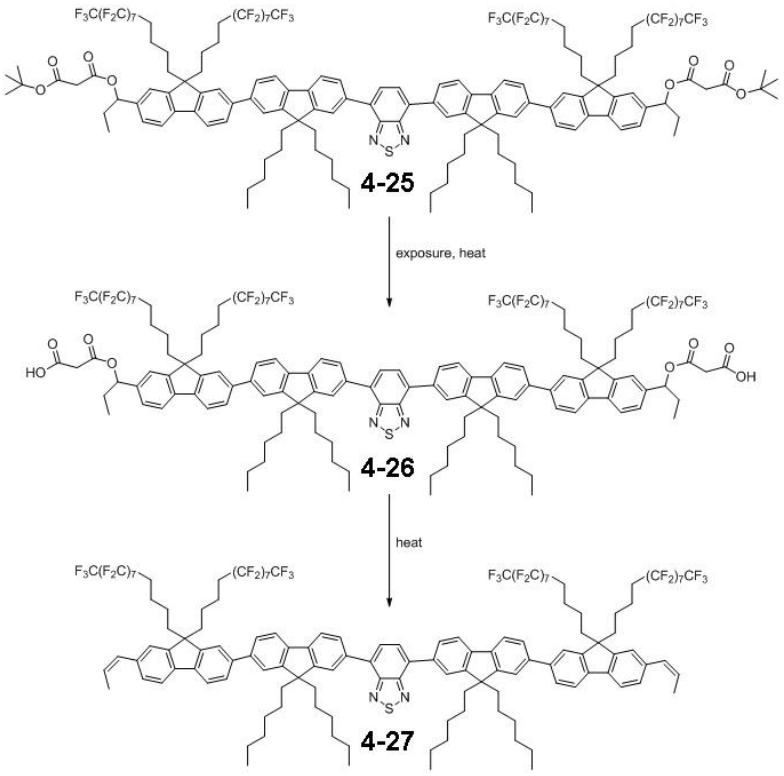

Figure 4.6: Method of decomposition for compound **4-25** during patterning

The fluorination of this self-patternable oligomer was also not trivial. It is well-known that perfluoroalkyl groups can be strongly electron-withdrawing[25], and therefore may perturb the electronic characteristics of the polyfluorenes[26]. Two methylene groups were therefore inserted as alkyl spacers between the fluorinated chain and the polyfluorene. Furthermore, by introducing alkyl spacers, perfluoroalkylation of the fluorenes was easily achieved by S_N2 reaction at the reactive 9-position of the polyfluorene with a semiperfluoroalkyl halide.

4.5 Conclusion

An orthogonal, self-patternable electroluminescent material was designed and synthesized as a model study. A polyfluorene structure was chosen for the oligomer backbone, with the addition of benzothiadizole as a chromophore for green-emission. The patternable end groups were based on the cleaving ability of the acid-labile tertiary butyl moiety upon UV exposure with a photoacid generator. Malonic acid chemistry was relied upon to generate an acetic acid structure in the presence of acid and heat. Finally, the acetic acid structure is known to decarboxylate under high temperatures to leave a simple unsaturated alkyl group. Fluorination of the compound allows for orthogonal processing.

This material is presented as an example of the potential of orthogonal self-patternable functional materials to expand the processing options and device architecture possibilities in organic electronics by introducing a new concept in materials handling.

Acknowledgements

I gratefully acknowledge support from the National Science Foundation (Materials World Network DMR-0908994) and the IGERT Fellowship. The work was performed in part at the Cornell NanoScale Facility, a member of the National Nanotechnology Infrastructure Network, which is supported by the National Science Foundation (Grant ECS-0335765). Also, special thanks to Martin Scherer (University of Mainz, Germany) and Colin Calabrese for their help with synthesis of materials and to Dr. Jin-Kyun Lee (Cornell University) for his advice and continued guidance.

REFERENCES

(1) Tang, C. W.; Vanslyke, S. A. *Appl. Phys. Lett.* 1987, *51*, 913-915.

(2) Burroughes, J. H.; Bradley, D. D. C.; Brown, A. R.; Marks, R. N.; Mackay, K.; Friend, R. H.; Burns, P. L.; Holmes, A. B. *Nature* 1990, *347*, 539-541.

(3) Forrest, S. R. *Nature* 2004, *428*, 911-918.

(4) Malliaras, G.; Friend, R. *Phys. Today* 2005, *58*, 53-58.

(5) Geffroy, B.; Le Roy, P.; Prat, C. *Polym. Int.* 2006, *55*, 572-582.

(6) Kraft, A.; Grimsdale, A. C.; Holmes, A. B. *Angew. Chem.-Int. Edit.* 1998, *37*, 402-428.

(7) Menard, E.; Meitl, M. A.; Sun, Y. G.; Park, J. U.; Shir, D. J. L.; Nam, Y. S.; Jeon, S.; Rogers, J. A. *Chem. Rev.* 2007, *107*, 1117-1160.

(8) Loo, Y. L. *Aiche J.* 2007, *53*, 1066-1074.

(9) Bernius, M. T.; Inbasekaran, M.; O'Brien, J.; Wu, W. S. *Adv. Mater.* 2000, *12*, 1737-1750.

(10) Neher, D. *Macromol. Rapid Commun.* 2001, *22*, 1366-1385.

(11) Scherf, U.; List, E. J. W. *Adv. Mater.* 2002, *14*, 477-+.

(12) Chen, S. A.; Lu, H. H.; Huang, C. W. In *Polyfluorenes*; Springer-Verlag Berlin: Berlin, 2008; Vol. 212, p 49-84.

(13) Ariu, M.; Lidzey, D. G.; Lavrentiev, M.; Bradley, D. D. C.; Jandke, M.; Strohriegl, P. *Synth. Met.* 2001, *116*, 217-221.

(14) Huang, J.; Xia, R.; Kim, Y.; Wang, X.; Dane, J.; Hofmann, O.; Mosley, A.; de Mello, A. J.; de Mello, J. C.; Bradley, D. D. C. *J. Mater. Chem.* 2007, *17*, 1043-1049.

(15) Lee, J. K.; Taylor, P. G.; Zakhidov, A. A.; Fong, H. H.; Hwang, H. S.; Chatzichristidi, M.; Malliaras, G. G.; Ober, C. K. *J. Photopolym Sci. Technol.* 2009, *22*, 565-569.

(16) Zakhidov, A. A.; Lee, J. K.; Fong, H. H.; DeFranco, J. A.; Chatzichristidi, M.; Taylor, P. G.; Ober, C. K.; Malliaras, G. G. *Adv. Mater.* 2008, *20*, 3481-+.

(17) Hwang, H. S.; Zakhidov, A. A.; Lee, J. K.; Andre, X.; DeFranco, J. A.; Fong, H. H.; Holmes, A. B.; Malliaras, G. G.; Ober, C. K. *J. Mater. Chem.* 2008, *18*, 3087-3090.

(18) Lee, J. K.; Chatzichristidi, M.; Zakhidov, A. A.; Taylor, P. G.; DeFranco, J. A.; Hwang, H. S.; Fong, H. H.; Holmes, A. B.; Malliaras, G. G.; Ober, C. K. *J. Am. Chem. Soc.* 2008, *130*, 11564-+.

(19) Taylor, P. C.; Lee, J. K.; Zakhidov, A. A.; Chatzichristidi, M.; Fong, H. H.; DeFranco, J. A.; Malliaras, G. C.; Ober, C. K. *Adv. Mater.* 2009, *21*, 2314-+.

(20) Pilgram, K.; Zupan, M. *J. Org. Chem.* 1971, *36*, 207-&.

(21) Lee, J. K.; Fong, H. H.; Zakhidov, A. A.; McCluskey, G. E.; Taylor, P. G.; Santiago-Berrios, M.; Abruna, H. D.; Holmes, A. B.; Malliaras, G. G.; Ober, C. K. *Macromolecules*, *43*, 1195-1198.

(22) Miyaura, N.; Suzuki, A. *Chem. Rev.* 1995, *95*, 2457-2483.

(23) Luo, J.; Li, X. Z.; Hou, Q.; Peng, J. B.; Yang, W.; Cao, Y. *Adv. Mater.* 2007, *19*, 1113-1117.

(24) Murphy, A. R.; Frechet, J. M. J.; Chang, P.; Lee, J.; Subramanian, V. *J. Am. Chem. Soc.* 2004, *126*, 1596-1597.

(25) Alvey, L. J.; Meier, R.; Soos, T.; Bernatis, P.; Gladysz, J. A. *Eur. J. Inorg. Chem.* 2000, 1975-1983.

(26) Amara, J. P.; Swager, T. M. *Macromolecules* 2006, *39*, 5753-5759.

CHAPTER 5

BENIGN PROCESSING METHODS FOR PATTERNING MULTIPLE BIOMOLECULES

Abstract

The ability to pattern multiple biomolecules on a single substrate is crucial to the realization of state-of-the-art bio-devices. However due to the delicate nature of biomolecules, patterning has proved challenging. Despite the many methods that have been developed for biomolecule patterning, a method, which allows for high-resolution multicomponent patterning without non-specific binding or damage to the biomolecules has yet to be developed. To address this issue, a new paradigm in biomolecule patterning is presented: resists and processing solvents, which are benign to biomolecules are applied to the lithographic patterning of proteins and cells. A fluorinated resist, processable in hydrofluoroether solvents, was synthesized and patterned by imprint lithography with feature sizes of 100 μm down to 1 μm. Both the imprint resist and the hydrofluoroether solvents are shown to be benign to biomolcules. Through repeated patterning steps by imprint lithography, a 3-protein array was fabricated with features sizes from 100 μm down to 1 μm.

5.1 Introduction: Multicomponent Patterning Methods for Biomolecules

Significant advances have recently been made in the field of bioelectronics. Biosensors, bio-MEMs and microfluidic devices are revolutionizing biological and medical research[1-5]. Similarly, the development of biomolecular arrays and regenerative therapies are enabling unprecedented studies in fundamental biology and applications in tissue engineering, respectively[6-9]. The ability to specifically and discretely place multiple biomolecules on a single surface is integral to the

development of bio-devices such as biomolecule microarrays and in tissue engineering[10,11].

Consequently, multicomponent patterning of biomolecules has become an active area of research. Patterning techniques for single component patterning have been extensively developed[10,12]. However, multicomponent patterning introduces unique challenges, which have yet to be satisfactorily addressed. Multicomponent protein patterning requires the ability to define multiple zones of biomolecules on a single substrate while avoiding non-specific binding and retaining functionality. All of these issues must be addressed in evaluating a patterning method.

Techniques using photolithography, soft-lithography, dip-pen lithography and spot-arraying have all been explored and represent the principal advances in the field of multicomponent protein patterning[13-17]. They are briefly discussed below.

5.1.1 Photolithography

Photolithography is a mature patterning technique that is promising for biomolecule applications as it allows for high-resolution and precise alignment, and is a high-throughput process. The greatest disadvantage of photolithography is that it traditionally requires harsh chemicals such as photoresists and developers as well as requiring thermal steps which often lead to denaturation of delicate biomolecules. Many clever strategies have been developed to circumvent these requirements.

In 1995, Pritchard *et al*. were among the first to demonstrate multi-component protein patterning using photolithography[13,18]. Biotin with a photoactive aryl-azide group was bound to the substrate by adsorbed avidin. A protein solution was incubated on top of this surface and selective UV irradiation through a photomask created reactive aryl nitrene groups in the exposed regions. These groups were able to

bind the protein to the surface in the exposed regions. Successive protein immobilizations on the same substrate were achieved with this method.

In a similar example, a nitroveratryloxycarbonyl protected biotin was bound to a substrate followed by selective UV irradiation to deprotect the biotin in the exposed regions. The deprotected biotin was allowed to bind streptavidin which would subsequently bind the target biotinylated protein. In this example, the irradiation and protein binding steps are separated, thus biomolecules are not directly exposed to damaging UV irradiation[14].

Sorribas *et al*. described a photolithography based patterning technique that employed a protective sucrose layer on top of a protein layer immobilized onto a substrate[19]. Traditional lithographic patterning was carried out on top of this protective layer. Oxygen plasma etching transferred the patterns through the sucrose and protein layers to expose patterned regions where a second protein was deposited to give two patterned biomolecules on a single substrate.

Holden *et al*. were able to immobilize two different biomolecules onto a substrate through selectively photobleaching fluorescent dye molecules linked to target proteins to create photogenerated radicals which are able to bind to a bovine serum albumin (BSA) coated substrate[20]. This method is advantageous in that it operates in an aqueous environment and with longer wavelengths of light, which can be less damaging.

Douvas *et al*. were able achieve two-protein patterns through a chemically-amplified resist (CAR) system[21-24]. This system had relatively low post-exposure bake (PEB) temperature requirements (50°C) and required a relatively weak aqueous base developer. Traditional photolithography was carried out to obtain a patterned photoresist film on a substrate. Protein was bound to the open regions on the substrate

followed by lift-off of the resist film. A second protein was then bound to the regions left open by the resist lift-off to give two proteins patterned on a single substrate.

An aqueous-processable non-CAR system was later reported by Doh *et al*. Here, a photoresist system was designed to have pH-dependant solubility behavior. In this way, the photoresist was processable solely in aqueous solutions, thus avoiding the need for the typically harsh photolithographic processing solvents. Using this method, the resist was lithographically patterned and developed. Target proteins were immobilized on the patterned substrate followed by resist lift-off. The second target protein was then subsequently bound to the open, patterned regions[25].

Patterning by parylene lift-off is another method which has been applied to multicomponent biomolecule patterning. An inert, protective layer of parylene is deposited and photolithographically patterned. Following biomolecule deposition, the parylene may be peeled off to leave behind the patterned biomolecules. Craighead *et al*. have recently demonstrated multicomponent protein patterning based on this method.[26]

Most photolithographic methods for multi-component biomolecule patterning are restrictive in that they are based on a "backfilling" strategy; one layer is patterned and the second is deposited in the background. Most of these methods are highly susceptible to cross-contamination and also may not be compatible with less robust biomolecules.

In addition to photolithography, multi-component protein patterning based on ion-beam sputtering[27] and electron beam (e-beam) lithography[28] have also been demonstrated.

5.1.2 Soft Lithography

Soft-lithography is an inexpensive and parallel patterning process, which also has the ability to produce three-dimensional structures and pattern non-planar surfaces.

Microcontact printing (μCP) is a patterning technique that utilizes an elastomeric stamp, usually composed of polydimethylsiloxane (PDMS), to transfer patterns to a surface. Extensive work has been done on μCP of proteins. Multi-component protein patterning has been achieved with μCP through both sequential printing of patterns and through a single printing step of multiple biomolecules from a single stamp[29].

Delamarche *et al*. have demonstrated immunoglobulin patterning through microfluidic networks (μFN)[15, 30]. In μFN, an elastomeric stamp usually made of PDMS, is conformed to a substrate to form microchannels through which solutions of biomolecules can be passed by capillary force. Two different immunoglobulins, chicken immunoglobulin G (IgG) and mouse IgG were patterned through adjacent microchannels.

Kaji *et al*. took this method a step further to show specifically-placed multi-component protein patterns, using μFN[31]. The microchannels were coated with polyethyleneimine/heparin which resisted protein adsorption. Select areas inside the microchannel were activated with a microelectrode which electrochemically generated hypobromous acid (HBrO) to remove the blocking layer. Proteins were able to selectively bind to these areas, and by repeating this process with multiple protein solutions, multi-component protein patterns were achieved.

A technique similar to μCP, called affinity contact printing (αCP) has also been developed for multi-component protein patterning[32, 33]. In this approach, an elastomeric stamp is loaded with multiple capture biomolecules, which are able to specifically bind target biomolecules from solution. This stamp is then applied to a

surface with functional groups, which are able to bind to the target biomolecules and transfer them from the stamp. This method has been used to pattern multiple immunoglobulins on a single substrate.

Whitesides *et al*. describe a membrane-based patterning method[34]. Here, a patterned PDMS membrane was sealed against a substrate and the open areas were coated with a first protein. The membrane was then peeled off and a second protein was bound to the newly opened areas. This method was used to pattern cells.

Tian *et al*. report an elastomeric stamp with surface relief structures at various depths[35]. The magnitude of pressure applied to the stamp determined which levels could contact the substrate. Each level of the stamp was loaded with a different protein to enable multi-component protein patterning. Multi-component cell patterning was also achieved with this multilevel stamp method.

Despite the advances that have been reported for multi-component protein patterning by soft lithography, these techniques are limited by lack of registration capabilities. Furthermore, due to the elastomeric nature of the stamps, mechanical deformation necessarily occurs and results in pattern deformation.

5.1.3 Dip-pen Lithography

Mirkin *et al*. first introduced dip-pen lithography in 1999[16]. Their technique utilized an atomic force microscopy (AFM) probe to transfer molecules onto a substrate. Dip-pen lithography (DPN) offers the ability to precisely place nanoscale arrays of proteins. Patterns below 100 nm are easily achieved with this method.

Lee *et al*. have shown multi-component protein arrays by using DPN[36]. They have reported a two-protein nanodot array consisting of rabbit IgG and human IgG, fabricated by this method[37].

A technique very similar to DPN, called nanografting, utilizes an AFM tip to selectively remove areas of a pre-deposited layer from a surface (nanoshaving), and then fill in the empty space with another material via AFM tip[12]. This technique has also been applied to multi-component protein patterning. Acetylcholinesterase (AChE) and insulin were both patterned onto an ethylene oxide functionalized surface[38]. Zhao *et al*. showed nanografted arrays of mouse IgG and human IgG antigens onto which they immobilized anti-mouse IgG and anti-human IgG antibody-coated nanotubes[39].

Tinazli *et al*. reported an AFM-based method capable of writing, reading and erasing protein patterns[40]. An AFM contact oscillation mode (COM) in combination with a tapping mode was used to achieve this. They demonstrate multi-component protein features by "writing" a protein, erasing it, and then replacing it with another protein. This method is also able to control the orientation of immobilized molecules.

Impressive patterning control has been demonstrated with dip pen lithography and related techniques. However, despite the incomparable resolution this technique enables, it is also by nature prohibitively time-consuming for all but academic research applications.

5.1.4 Spot-arraying

Spot-arraying techniques, including ink-jet printing, are able to generate multi-component protein arrays with spot sizes close to 100 μm[17, 41]. Spot-arraying is accomplished through a robotic spotter delivering protein solutions to a substrate. Both thermal and piezoelectric inkjet printing have also been reported for protein patterning applications[42, 43].

Bruckbauer *et al*. developed a nanopipet system to deliver proteins to a substrate[44]. With this method, they were able to achieve submicron multi-component protein

patterns through spotting rabbit IgG onto an amine-functionalized substrate and then backfilling with human IgG. They also were able to form discreet patterns of both rabbit IgG and anti-rabbit IgG on an amine-functionalized substrate.

Xu *et al*. described the design of a cantilever-based microfluidic system, which was able to deliver multiple protein solutions to multiple cantilever tips for deposition onto a substrate[45]. They were able to fabricate a two-protein array of Donkey anti-rabbit IgG and Donkey anti-goat IgG with no detectable cross-contamination.

Although spot-arraying and inkjet printing can be very cost-effective methods for multi-component protein patterning, resolution is still too low to be practical for many applications.

5.1.5 Outlook

Despite the great advances that have recently been made in multi-component protein patterning research, the goal of a universal, efficient patterning method able to achieve nanoscale biomolecule patterns without cross-contamination or diminished functionality, has remained elusive. All of the patterning methods presented thus far offer some advantages as well as disadvantages.

This chapter presents a universally-applicable approach to developing a high-resolution, high-throughput and fully repeatable patterning method for multi-component biomolecule patterning. This method avoids problems with cross-contamination and is benign such that it does not deteriorate biomolecule functionality.

Through the use of biocompatible resists and processing solvents, the ubiquitous obstacle of biomolecules and imaging materials incompatibility is circumvented. Deterioration of biomolecule functionality due to their interaction with resist and solvents does not occur in this processing system. The patterning system presented

herein relies on high-throughput and high-resolution imprint lithography to generate multi-component protein patterns through the use of a novel and biocompatible fluorinated resist and biocompatible fluorinated processing solvents.

The biocompatibility of this resist and these solvents with biomolecules is demonstrated. The fabrication of a three-protein array is described to establish the potential for repeatability of this method for multi-component biomolecule patterning without danger of cross-contamination.

5.2 Experimental Section

5.2.1 Materials

Chemicals, Solvents, Proteins and Fluorophores

Benzotrifluoride (TFT) and 3,3,4,4,5,5,6,6,7,7,8,8,9,9,10,10,10-heptadecafluorodecyl methacrylate were purchased from Sigma-Aldrich and used as received. 2,2,3,3,4,4,5,5,6,6,7,7,8,8,9,9,9-Heptadecafluorononyl methacrylate was purchased from Synquest and used as received. Azobisisobutyronitrile (AIBN) was purchased from Sigma-Aldrich and recrystallized from $CHCl_3$. 3M™ Novec™ Engineered Fluid HFE-7200 and 7500 were purchased from 3M USA. Biotin-Bovine Serum Albumin (Biotin-BSA) and Rabbit γ Globulin IgG were purchased from Sigma-Aldrich and used as received. Dinitrophenyl-Bovine Serum Albumin (DNP-BSA) was prepared from BSA, purchased from Sigma-Aldrich, conjugated to 2,4-dinitrophenyl (DNP), purchased from Invitrogen, with a yield of *ca*. 20 DNP per BSA. Mouse monoclonal anti-DNP Immunoglobulin E (IgE) was purified according to the procedure given by Subramanian *et al*.[46] and then modified with Alexa Fluor 488 (Anti-DNP A488) according to the labeling kit instructions, all purchased from Invitrogen. Streptavidin-Alexa Fluor 568 (Streptavidin-A568) was purchased from Invitrogen and used as received. Goat anti-Rabbit IgG Alexa Fluor 647 (Goat Anti-

Rabbit A647) was prepared from Goat anti-Rabbit IgG, purchased from Jackson ImmunoResearch Laboratories, Inc. and conjugated to Alexa Fluor 647, purchased from Invitrogen, with a yield of about 9 A647 per anti-Rabbit IgG.

Cells

Rat basophilic leukemia 2H3 (RBL-2H3) cells[47] were maintained in a monolayer culture in Minimum Essential Medium (MEM) supplemented with 20% fetal bovine sera (FBS), purchased from Atlanta Biologicals, and 10 μg/mL gentamicin sulfate. Cells were harvested with trypsin-ethylenediaminetetraacetic acid (trypsin-EDTA), purchased from Invitrogen, three to five days after passage[48].

Buffer Solutions

A 0.05 M pH 9.2 carbonate buffer solution was prepared with 3.61 g sodium bicarbonate ($NaHCO_3$), 0.74 g sodium carbonate (Na_2CO_2), 0.5 g sodium azide (NaN_3) and 1 L of deionized water (dH_2O).

A 0.05 M pH 6.5-7.0 phosphate buffer was prepared with 2.79 g disodium hydrogen phosphate (Na_2HPO_4-$2H_2O$), 4.68 g potassium dihydrogen phosphate (KH_2PO_4) and 1 L deionized water.

A pH 8.25 washing buffer was prepared from 96 mL deionized water with 0.9 g sodium chloride (NaCl) and 4 mL of 10 mM tris(hydroxymethyl)aminomethane-hydrochloric acid (Tris-HCl). To prepare the 10 mM Tris-HCl solution: 3.03 g of tris(hydroxymethyl)aminomethane (Tris) was dissolved in 90 mL deionized water, and the pH was adjusted to 8.25 by addition of 5 N HCl solution and then the total volume adjusted to 100 mL by addition of deionized water.

A pH 8.25 no-salt washing buffer was prepared with 4 mL of 10 mM Tris-HCl and 96 mL deionized water. The no-salt buffer solution is a buffer solution made without salt.

The TWEEN washing buffer was prepared from 4 mL of 10 mM Tris-HCl, 96 mL deionized water, 0.9 g NaCl and 50 μL TWEEN20 (commercially available). This solution was stirred for at least 20 minutes.

A pH 8.5 BSA blocking solution was prepared from 1 g BSA in 100 mL 0.1 M $NaHCO_3$ (8.4 g $NaHCO_3$ dissolved in 100 mL deionized water).

A pH 7.8 buffer solution was prepared by dissolving 0.61 g Tris and 0.9 g NaCl in 90 mL deionized water. The pH was adjusted to about 8.5 with the addition of 5 N HCl. 0.5 g BSA was added and the solution was stirred until fully dissolved. The pH was again adjusted to about 8.25 with the addition of 1 N HCl. The final volume was adjusted to 100 mL with the addition of deionized water.

Biotinylated BSA solution: 0.9 g of NaCl and 1 g BSA are added to 100 mL 0.05 M pH 6.5 phosphate buffer solution. 5 μg/mL biotinylated BSA was dissolved in the solution.

Alexafluor-streptavidin solution: 0.9 g of NaCl and 1 g BSA are added to 100 mL 0.05 M pH 6.5 phosphate buffer solution (recipe above). 5 μg/mL streptavidin was dissolved in the solution.

Protein stock solutions: stock solutions of proteins are prepared by dissolving 1 mg/mL of protein in the 0.05 M pH 9.2 carbonate buffer (recipe above).

Protein solutions for deposition: 25 μL of each protein stock solution are added to each 1 mL of 0.05 M pH 6.5-7.0 phosphate buffer solution (recipe above) to prepare the final solution of proteins that are deposited on the substrates for adsorption and patterning.

5.2.2 Synthesis

Imprint resist **5-1**

3,3,4,4,5,5,6,6,7,7,8,8,9,9,10,10,10-heptadecafluorodecyl methacrylate (7.00 g, 13.15 mmol) was added to a 25 cm^3 schlenk tube. Benzotrifluoride (7 cm^3) and AIBN (0.07 g, 0.43 mmol) were then added to the mixture. The tube was sealed then degassed by three freeze-thaw cycles in liquid N_2 under reduced pressure. The solution was magnetically stirred at 72 °C for 12 h under a N_2 atmosphere. The solution was precipitated in hexanes then dried under reduced pressure to give a colorless solid (6.5 g) in approximately 93 % yield.

Imprint resist **5-2**

2,2,3,3,4,4,5,5,6,6,7,7,8,8,9,9,9-heptadecafluorononyl methacrylate (7.00 g, mmol) was added to a 25 cm^3 schlenk tube. Benzotrifluoride (7 cm^3) and AIBN (0.07 g, 0.43 mmol) were then added to the mixture. The tube was sealed then degassed by three freeze-thaw cycles in liquid N_2 under reduced pressure. The solution was magnetically stirred at 75 °C for 12 h under a N_2 atmosphere. The solution was precipitated in hexanes then dried under reduced pressure to give a colorless solid (5.91 g) in approximately 84 % yield.

5.2.3 Characterization

Imprint resist **5-1**

IR: ν = 1732, 1194, 1144, 704, 655, 559 cm^{-1}; ^1H NMR (400 MHz, $CDCl_3$ (1 part by volume) + $CFCl_3$ (1 part by volume), δ): = 4.25 (br s, 2H, CH_2CF_2), 2.49 (m, 2H, $CH_2CH_2CF_2$), 1.67-0.80 ppm (m, 5H); T_d (TGA) = 168.92 °C; M_n = 611,000, M_w/M_n = 1.2.

Imprint resist **5-2**

IR: ν = 1734, 1199, 1142, 704, 655, 555 cm^{-1}; ^1H NMR (400 MHz, $CDCl_3$ (1 part by volume) + $CFCl_3$ (1 part by volume), δ): = 4.23 (br s, 2H, CH_2CF_2), 2.47-0.78 ppm (m, 5H); T_d (TGA) = 165.55 °C.

5.2.4 Lithographic Evaluation

The lithographic properties of the imprint resists **5-1** and **5-2**, using two different substrates (silicon and optical glass wafers), were investigated using a Nanonex NX-2500 nanoimprint lithography tool. The resist films were spin-coated from the polymer (0.15 g) solution in HFE-7500 (1.5 g) at 1000 rpm followed by post-apply bake (PAB) at 40 °C. The resulting films had a thickness of *ca.* 600 nm. Films were imprinted at 300 psi, at 50 °C for 5 minutes with a fused silica stencil with *ca.* 600 nm feature relief. The imprint stencil was prepared through standard photolithographic technique on a fused silica mask with feature sizes 1 μm to 100 μm. After imprint, the film was Ar/O_2 plasma etched on an Oxford PlasmaLab 80+ RIE System.

5.2.5 BSA Assay

The effect of imprint resist **5-1** and hydrofluoroether solvents on streptavidin was investigated. 100 μL of each 1 μg/mL, 2 μg/mL and 5 μg/mL concentration solutions of streptavidin in pH 9.2 carbonate buffer were deposited into microtitration wells and left 1 h at ambient temperature to adsorb. Wells were then decanted of the streptavidin solution and washed twice with pH 8.25 buffer. As a blocking step, all wells were filled with a concentrated BSA solution and left 1 h at ambient temperature to adsorb. This solution was then decanted. To a control set of wells (Set 1), including each of the 1 μg/mL, 2 μg/mL and 5 μg/mL streptavidin concentrations, was added an aqueous buffer solution. To a second set of wells (Set 2), including each of

the1 μg/mL, 2 μg/mL and 5 μg/mL streptavidin concentrations, was added 300 μL hydrofluoroether solvent. To a third set of wells (Set 3), including each of the 1 μg/mL, 2 μg/mL and 5 μg/mL streptavidin concentrations, were added a 10 wt. % solution of imprint resist **5-1** dissolved in hydrofluoroether solvent. This resist solution was left in the wells for 2 minutes at ambient temperature, and then decanted. The residual resist and solvent solution was baked for 5 minutes in a 50 °C oven and then the wells were washed in hydrofluoroether solvents four times, for three minutes each time to remove the residual resist. This step mimics the processing conditions required for lithographic patterning. All wells in Sets 1, 2 and 3 were decanted and washed with a no-salt buffer solution (described in section 5.2.1 of this chapter), followed by washing with an aqueous buffer solution. 100 μL of biotinylated BSA in buffer solution was deposited in all wells in Sets 1, 2 and 3 and left for 30 minutes at ambient temperature to bind to the previous streptavidin layer. All wells were then washed with a TWEEN buffer solution four times. 100 μL of streptavidin - horseradish peroxidase (strep-HRP) in aqueous buffer solution was deposited in all wells and left for 15 minutes at ambient temperature. All wells were then decanted and washed with a TWEEN buffer solution four times each. All wells were then filled with a 2,2'-azino-bis(3-ethylbenzthiazoline-6-sulphonic acid) (ABTS) solution and left for 30 minutes at ambient temperature for 30 minutes. Absorption signals were measured at 15 minutes and 30 minutes on a Labsystems Multiskan RC microplate reader.

5.2.6 Monoclonal Antibodies Assay

The effect of imprint resist **5-1** and hydrofluoroether solvents on monoclonal antibodies was investigated. 100 μL of a 5 μg/mL concentration solution of monoclonal antibody – prostate-specific antigen (Mab-PSA) in pH 9.2 buffer solution

was deposited into a set of microtitration wells. Following adsorption, all wells were decanted and washed with a pH 8.25 buffer solution twice each. As a blocking step, all wells were filled with a concentrated BSA solution and left 1 h at ambient temperature to adsorb. This solution was then decanted. To a control set of wells (Set 1), was added a no-salt buffer solution (described in section 5.2.1 of this chapter). To a second set of wells (Set 2), was added 300 μL hydrofluoroether solvent. To a third set of wells (Set 3), was added 50 μL of a 10 wt. % solution of polymer resist **5-1** dissolved in hydrofluoroether solvent. This resist solution was left in the wells for 3 minutes at ambient temperature, and then decanted. The residual resist and solvent solution was baked for 5 minutes in a 50 °C oven and then the wells were washed in hydrofluoroether solvents four times, for three minutes each time to remove the residual resist. This step mimics the processing conditions required for lithographic patterning. All wells in Sets 1, 2 and 3 were decanted and washed with a no-salt buffer solution (described in section 5.2.1 of this chapter), followed by washing with an aqueous buffer solution. For each of these Sets 1, 2 and 3 of microtitration wells, a PSA assay was performed. 25 μL of each PSA standard of 0%, 1%, 3% and 10% in aqueous buffer solution was added to individual wells in each of the Sets 1, 2 and 3. 75 μL of detection antibody in aqueous buffer solution was added to all wells and left for 2 hours at ambient temperature to bind. All wells were then decanted and washed with a TWEEN buffer solution four times each. 100 μL of strep-HRP was added to all wells and left for 14 minutes at ambient temperature. All wells were then decanted and washed again with a TWEEN buffer solution four times each. All wells were then filled with an ABTS solution and left for 30 minutes at ambient temperature for 30 minutes. Absorption signals were measured at 15 minutes and 30 minutes on a Labsystems Multiskan RC microplate reader.

5.2.7 Multiple-Cycles Tests

The repeatability of this patterning method was investigated by testing the effect of multiple applications and removals of the imprint resist **5-1** in hydrofluoroether solvents on biotin-BSA. An assay, similar to the BSA assay described in Section 2.5.1 of this chapter, was performed on an aminosilanized silicon substrate coated with biotinylated BSA. Imprint resist **5-1,** 10 wt. % solution in hydrofluoroether solvent, was deposited onto the surface and left for 2 minutes at ambient temperature. The sample was baked for 5 minutes at 50 °C and then the resist was removed by washing with hydrofluoroether solvents. This resist deposition and removal step was repeated ten times to mimic the lithographic processing steps required to create a ten-protein array. Biomolecule functionality was measured by fluorescence intensity for 0, 2, 4, 6, 8, and 10 resist deposition and removal cycles.

5.2.8 Fabrication of Protein Arrays

Three-protein arrays were fabricated as follows: imprint resist **5-**1 was spun-cast from solution in HFE-7500 onto a silicon substrate to give a *ca.* 600 nm polymer film. The film was then imprinted and etched. (3-Aminopropyl)trimethoxysilane (APTMS) was vapor deposited with an Applied MicroStructures MVD100 molecular vapor deposition tool. Dinitrophenyl-bovine serum albumin (DNP-BSA), 25 μg/mL in phosphate buffer solution, was incubated for one hour at room temperature on the wafer surface. The resist was then lifted-off in HFE-7200. Onto this patterned DNP-BSA layer was spin-coated another layer of polymer resist, which was then imprinted and etched. APTMS was vapor deposited on the surface of the resist. Biotin-BSA, 25 μg/mL in phosphate buffer solution, was incubated for one hour at room temperature on the wafer surface. The resist was then lifted-off in HFE-7200. Onto these patterned DNP-BSA and biotin-BSA layers was spin-coated a third layer of polymer

resist, which was then imprinted and etched. APTMS was vapor deposited on the surface of the resist. Rabbit γ Globulin IgG, 25 μg/mL in phosphate buffer solution, was incubated for one hour at room temperature on the wafer surface. The resist was then lifted-off in HFE-7200 to leave a three-protein patterned array.

5.2.9 Protein-Assisted Cell Patterning

A silicon substrate was lithographically patterned with imprint resist **5-1**. Onto this surface, DNP-BSA, conjugated to a cyanine fluorescent dye (Cy3-Cy5), was deposited and left for 1 h at ambient temperature to adsorb. The resist was then lifted-off in HFE-7200 to give patterned DNP-BSA. RBL-2H3 cells were sensitized by incubating for 40 to 60 minutes at 37 °C with 2-3 μg/mL Alexa Fluor 488-labeled IgE, specific for DNP. Cells were suspended at a concentration of 1-2 x 10^6 cells per mL and plated on the patterned-protein silicon substrate[49]. The sample was incubated at 37 °C for 30-60 minutes in a petri dish. The cells were then fixed with 4% paraformaldehyde in phosphate buffered solution (PBS) for 20 minutes followed by quenching with 10 mg/mL BSA in PBS. The cells and patterned proteins were imaged by fluorescence microscopy.

5.3 Results

Imprint resist **5-1** (shown in Figure 5.1) was synthesized by radical polymerization with AIBN as the radical initiator. The resulting polymer demonstrated sufficient solubility to be processable in hydrofluoroether solvents HFE-7200 and 7500. The resist structure was designed to be fluorinated enough to be processable in hydrofluoroether solvents and also free of unnecessary functional groups that would be able to interact with biomolecules.

To demonstrate patterning properties, polymer resist **5-1** was imaged by imprint lithography. Imprint lithography generally operates by "stamping" a pattern through pressure and heat, rather than relying on UV-exposure to pattern, as with typical photolithography. This absence of UV-exposure is a significant advantage of this patterning method, as biomolecules are very susceptible to damage through UV exposure. Polymer films were spin-coated from solution in HFE-7200. Imprinting was carried out at 50 °C and 300 psi. 50 °C was empirically found to be a temperature high enough to form patterns, yet low enough to avoid any observable protein degradation. Features from 1 μm to 100 μm were obtained by imprint with a fused silica template with 1 μm to 100 μm features and *ca*. 600 nm relief, and subsequent oxygen plasma etching. The patterned imprint resist **5-1** is shown in Figure 5.2.

Once patternability of imprint resist **5-1** was established, the biocompatibility of the resist was investigated. BSA and monoclonal antibody assays were performed to determine the effect of the polymer resist and hydrofluoroether solvents on both streptavidin and monoclonal antibodies. For each assay, the resist and hydrofluoroether solutions were deposited onto the biomolecules in such a way as to mimic the lithographic processing steps required for patterning. For the BSA assay (described in section 2.5.1 of this chapter), streptavidin functionality following resist exposure, was tested by its ability to bind to biotin-BSA via a biotin-avidin linkage. Strep-HRP was subsequently bound to the BSA via another biotin-avidin linkage. The extent of strep-HRP binding by the biomolecules was measured by interaction with ABTS, which produces a measureable fluorescent signal. The extent of strep-HRP binding was similarly measured for the monoclonal antibody assay (described in section 2.5.2 of this chapter). Absorption signals were measured and compared to a control sample with no resist or hydrofluoroether solvent exposure. The BSA assay demonstrates essentially no deterioration of biomolecule functionality, as the

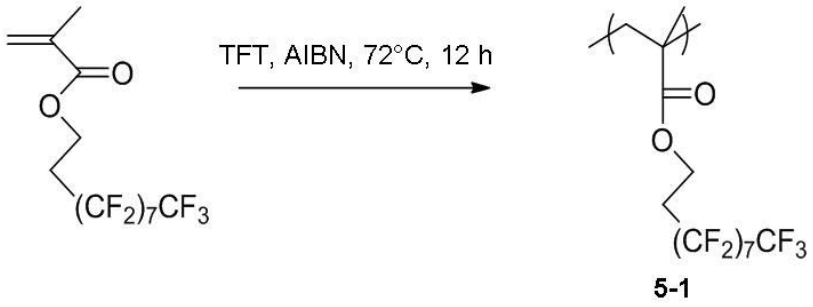

Figure 5.1: Synthetic scheme for polymer resist **5-1.**

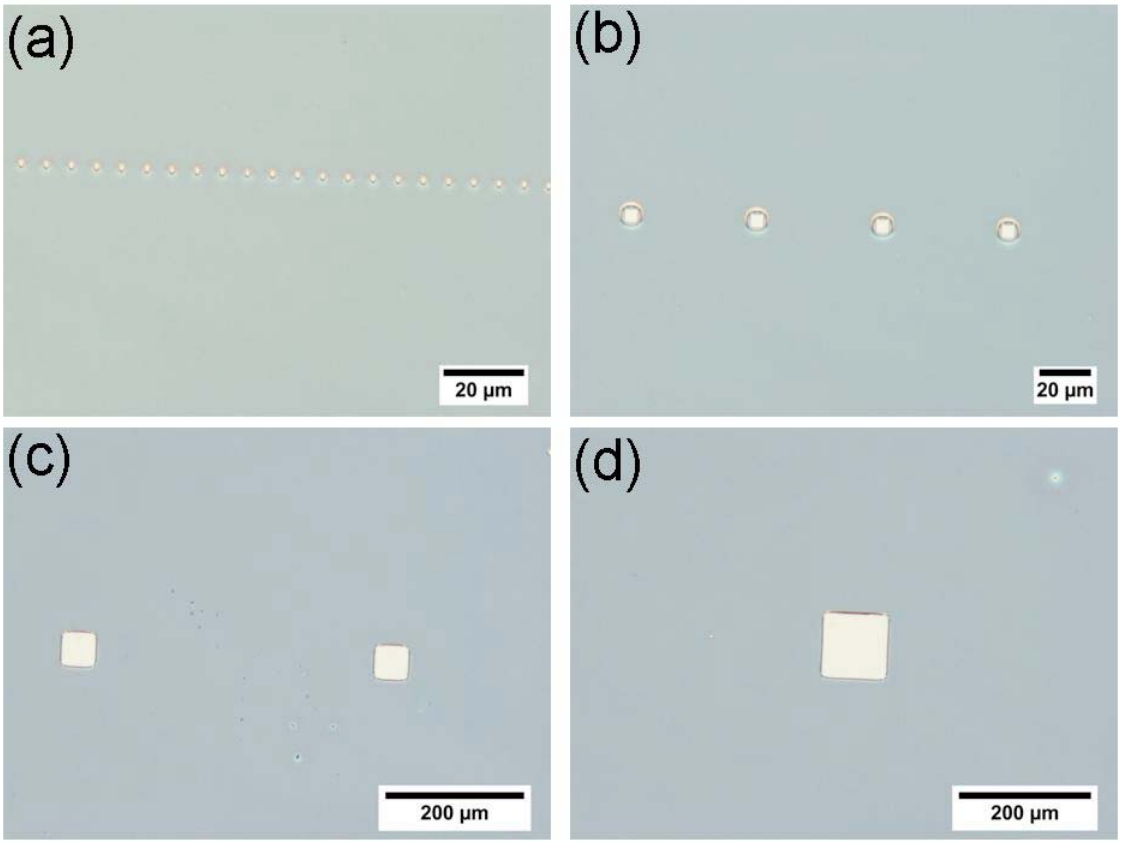

Figure 5.2: Polymer resist **5-1** patterned by imprint lithography. (a) 1 μm features, (b) 5 μm features, (c) 50 μm features, (d) 100 μm features.

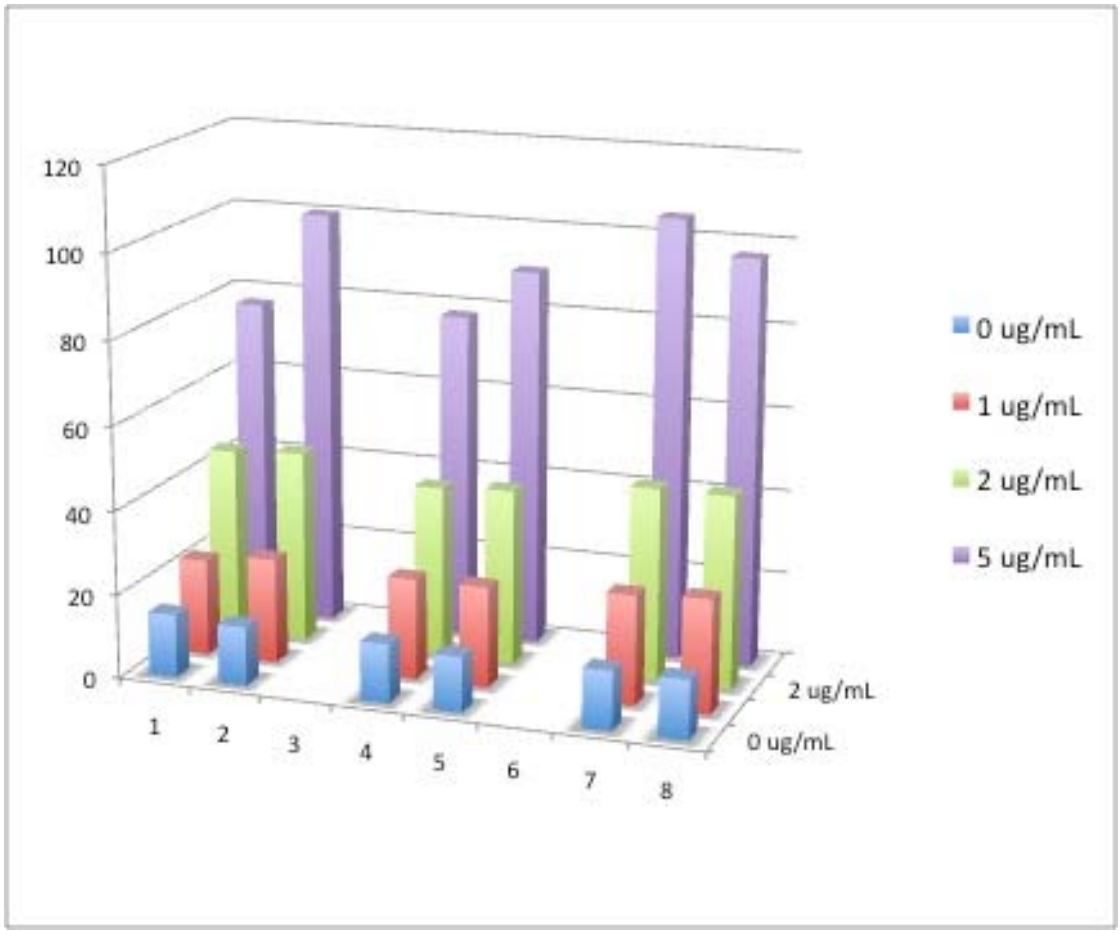

Figure 5.3: Results of BSA/resist biocompatibility assay. Two sets of data were taken for each condition. The graph shows the increasing concentrations of streptavidin used in the assay, from 0 μg/mL to 1 μg/mL, 2 μg/mL, and 5 μg/mL along the Y-axis. The Z-axis gives normalized percentages of the absorption signals, using the highest experimental control-set absorption signal as 100%. Along the X-axis, from the left is the control set (1 and 2 on the X-axis). The middle set (4 and 5) shows the effect of hydrofluoroether exposure, and the rightmost data set (7 and 8) shows the effects of resist and hydrofluoroether solvent exposure.

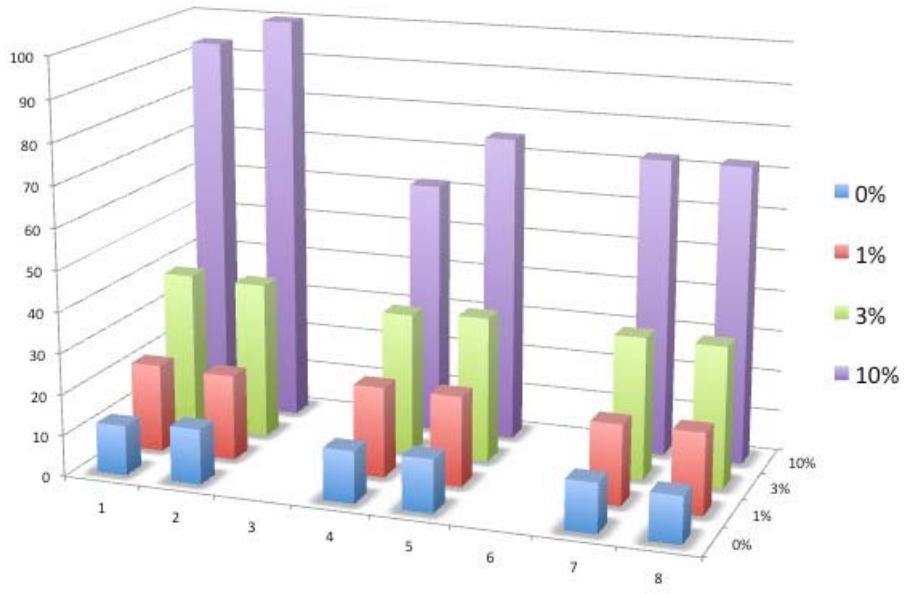

Figure 5.4: Results of monoclonal antibody/resist biocompatibility assay. Two sets of data were taken for each condition. The graph shows the increasing percentages of PSA standard used in the assay, from 0 % to 1 %, 3 %, and 10 % along the Y-axis. The Z-axis gives normalized percentages of the absorption signals, using the highest experimental control-set absorption signal as 100%. Along the X-axis, from the left is the control set (1 and 2 on the X-axis). The middle set (4 and 5) shows the effect of hydrofluoroether exposure, and the rightmost data set (7 and 8) shows the effects of resist and hydrofluoroether solvent exposure

fluorescence intensity measurements are very similar to those of the control sets, which had no resist or hydrofluoroether exposure. In fact, the signals obtained for the control set are slightly lower than those obtained for the hydrofluoroether/resist exposure experimental set. These results suggest that both hydrofluoroether solvents and the imprint resist do not significantly affect the ability of streptavidin to bind to biotin. In the monoclonal antibody assay, the fluorescence signals for 1% and 3% are extremely similar. The signals at the higher concentration, 10%, show more variability; the experimental sets show lower absorption. This could be due to either partial denaturation of the antibodies or else experimental error of the assay itself. The absorption signals obtained for the BSA and monoclonal antibody assays are shown in Figures 5.3 and 5.4, respectively.

Further tests were performed to show the potential of this method for multi-layer patterning by imprint lithography. A similar assay to the aforementioned BSA test was performed, where a biotinylated BSA-coated silicon surface was covered with resist in such a way as to mimic the required lithographic processing steps for patterning. The resist was removed in hydrofluoroether solvents and reapplied and then removed again for a total of ten deposition cycles. These ten cycles effectively imitate the processing effects, from imprint patterning ten subsequent layers, on the first layer of biomolecules. Biomolecule functionality was tested by the ability of the biotin-BSA to bind to strep-HRP. Subsequent interaction of HRP with ABTS produces a fluorescent signal proportional to the magnitude of bound streptavidin. Absorption signals were measured for 0, 2, 4, 6, 8 and 10 resist deposition cycles, with 0 being the control set, having no exposure to resist or hydrofluoroether solvents. Biomolecule functionality seems unaffected throughout the ten cycles, as measured by the assay absorption signals; the signals are extremely similar. A graph of the absorption signals are shown in Figure 5.5.

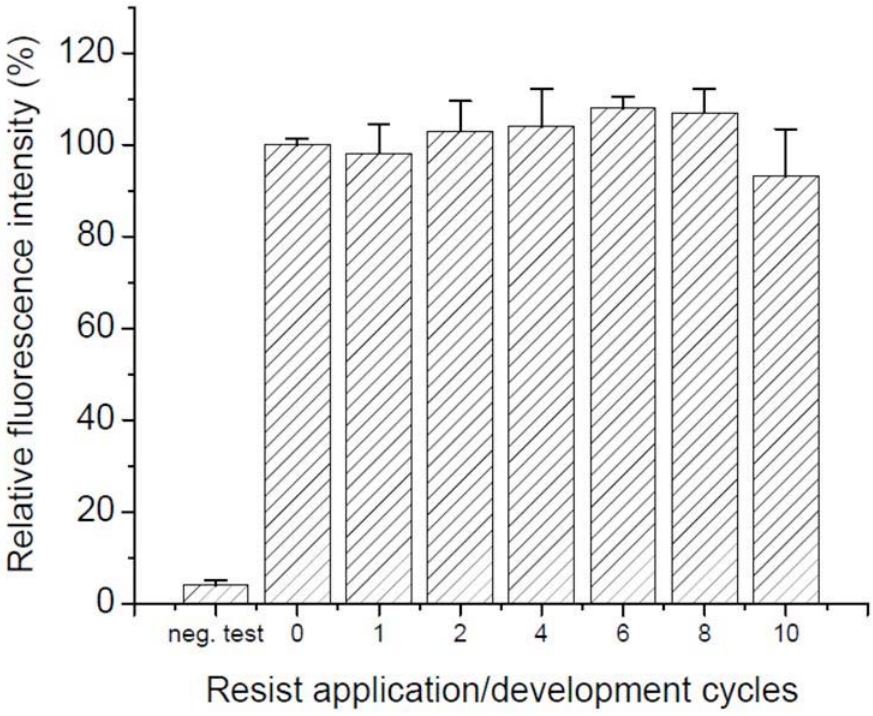

Figure 5.5. Results from multiple-cycle tests, showing effects of repeated exposure of BSA to the fluorinated resist and hydrofluoroether solvents, up to 10 cycles of deposition and removal. The X-axis shows the number of cycles, measured at 0 (control set), 2, 4, 6, 8 and 10. The Y-axis shows the relative fluorescence intensity, with the control absorption signal set at 100%. The leftmost bar shows the negative control set.

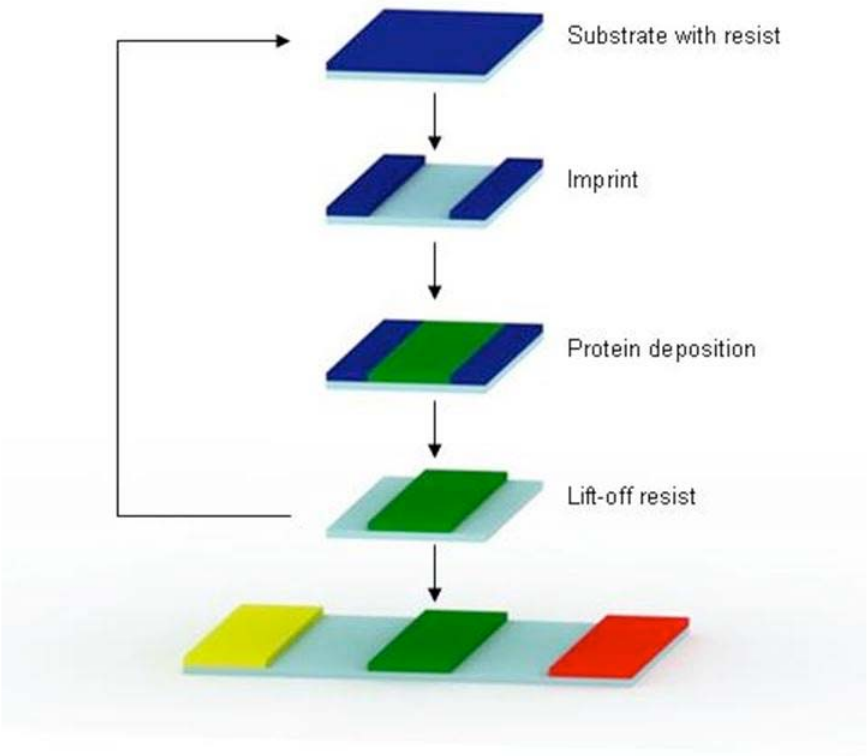

Figure 5.6: Patterning process scheme for patterning a three-protein array by imprint lithography with imprint resists **5-1 and 5-2** and hydrofluoroether solvents.

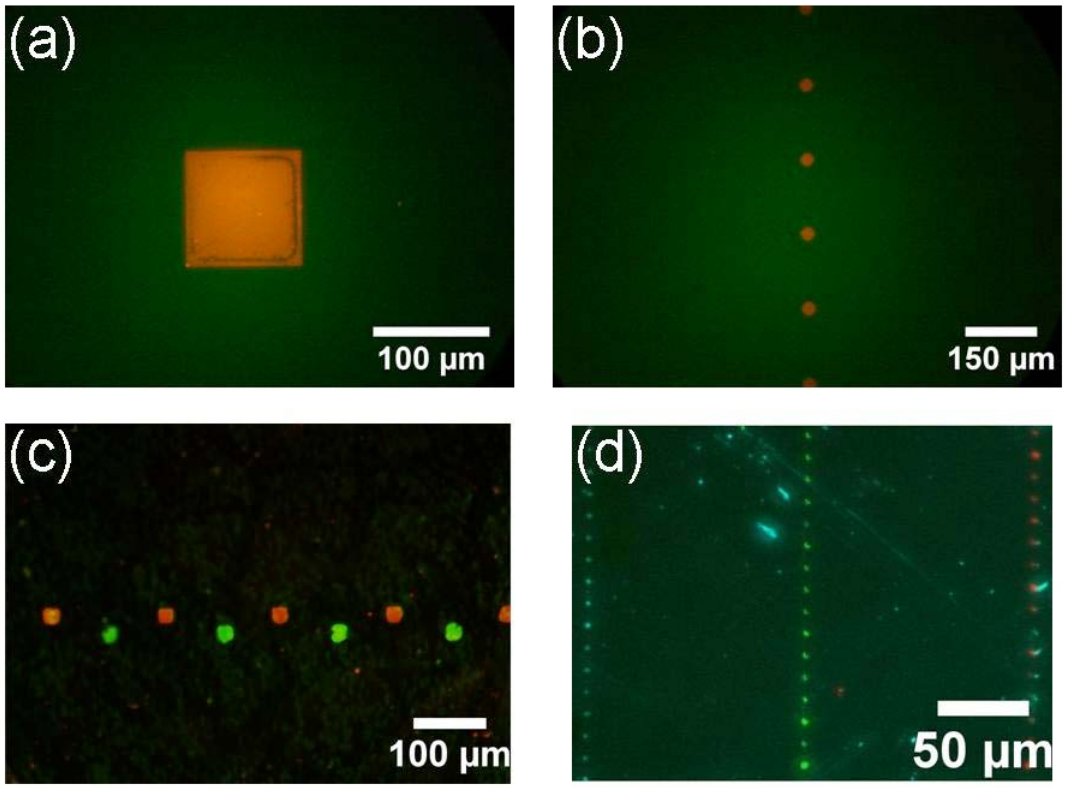

Figure 5.7: Fluoresence microscope images of patterned proteins. (a) 100 μm square of patterned DNP-BSA on silicon, (b) 20 μm squares of patterned DNP-BSA on silicon, (c) 20 μm squares of patterned DNP-BSA and Biotin-BSA, (d) 1 μm squares of patterned DNP-BSA, biotin-BSA and rabbit γ globulins.

A three-protein array was fabricated to demonstrate the potential of this method for multi-component biomolecule patterning. DNP-BSA, biotin-BSA and rabbit γ globulin IgG were patterned in three subsequent layers with feature sizes ranging from 1 μm to 100 μm by imprint lithography with imprint resist **5-1** and hydrofluoroether solvents HFE-7200 and 7500. A schematic of the patterning procedure is shown in Figure 5.6. The proteins were fluorescently labeled and imaged by fluorescence microscopy. Images of single protein patterns, a two-protein array and a three-protein array are shown in Figure 5.7.

Further tests were performed to demonstrate the compatibility of this method for protein-assisted cell patterning. A single protein array of DNP-BSA, patterned by this method was incubated with cells. The cells were allowed to acclimate to the surface for several hours before being fixed and imaged (described in section 2.7 of this chapter). The imaged cells show intra-cell clustering in a puncta formation, which is characteristic of the cell-protein interaction. No apoptosis is observed. Cell images are shown in Figure 5.8. These results suggest that this patterning method is also compatible with cell patterning.

5.4 Discussion

Recently, our research group along with our collaborators, have published work involving fluorinated resists and active materials, which are processable in fluorinated hydrofluoroether solvents, in application to organic electronic device patterning[50-52]. Similar to biomolecule patterning, organic electronic materials also can be damaged by the harsh photoresists and solvents required by photolithography. We have shown that these highly-fluorinated solvents and resist materials are completely benign to delicate organic electronic materials and are capable of serving as photoresists and processing solvents for photolithographic patterning of organic electronic materials[53].

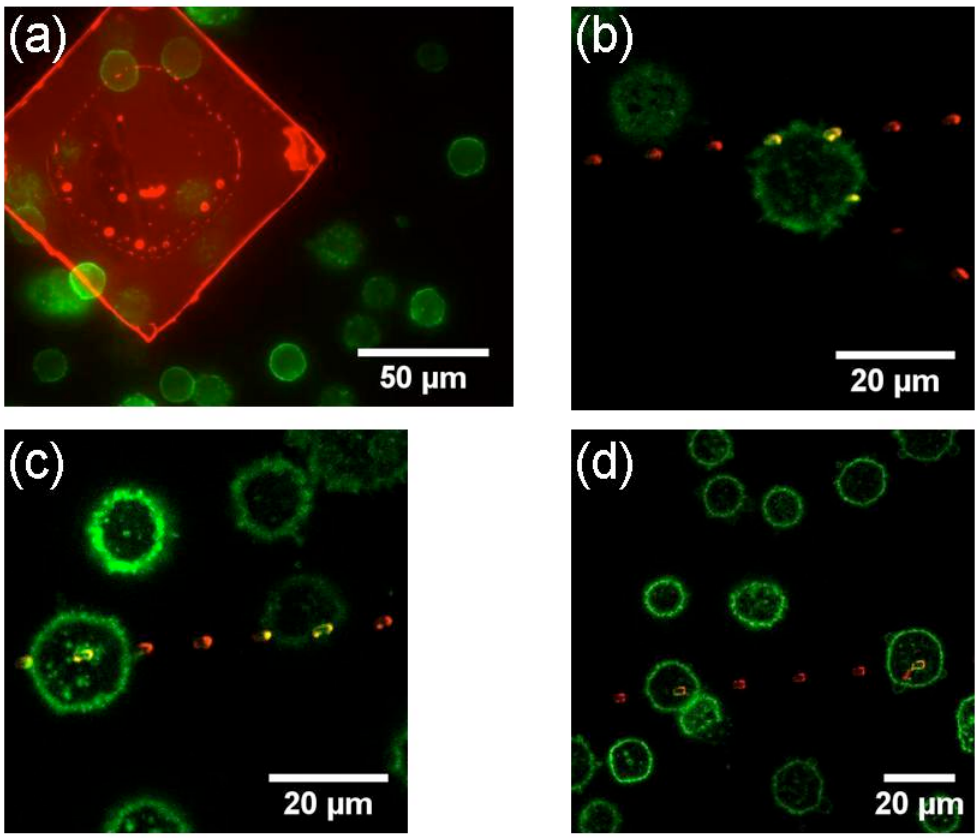

Figure 5.8: Fluoresence microscope images of patterned BSA-DNP protein and RBL-2H3 cells. (a) 100 μm protein pattern, (b) 1 μm protein patterns, (c) and (d) 2 μm protein patterns.

Hydrofluoroethers have been shown to be environmentally-friendly, non-flammable and non-toxic. Hydrofluoroethers have also found previous use in protein research[54]. Furthermore, as process solvents, hydrofluoroethers are recyclable to enable a sustainable processing system.

Based on the favorable results obtained in these previous studies, the idea of benign lithographic processing was extended to biomolecule patterning. A fluorinated resist structure was chosen which would be fluorinated enough to be processable in hydrofluoroether solvents and which was also free of unnecessary functional groups that would be able to interact with biomolecules. Imprint resist **5-1** was synthesized as a potential resist for this application and proved to be soluble in hydrofluoroether solvents.

Imprint lithography was selected to demonstrate the lithographic patterning properties of this processing system. Imprint lithography has recently received significant attention as a patterning technique with the potential to assume a key role in the manufacture of nanoscale structures for electronic, optical, biological and energy applications[55, 56]. Because of its ability to produce patterns as small as 10 nm over large areas, high-reproducibility and high-throughput, imprint lithography has also found applications in protein patterning[57]. One particular advantage of protein patterning by imprint lithography is that biomolecules are not exposed to the denaturing effects of UV radiation as with photolithography. However, as with photolithography, imprint lithography also typically requires harsh resists and developers. Here, the harsh processing conditions are replaced with a benign fluorinated polymer resist and unreactive hydrofluroethers as processing solvents.

Imprint lithography requires a resist, which can be molded; the resist should be able to "flow" into the recesses of the stamp as well as be able to release from the stamp after imprinting. Several parameters, including pressure values and temperature

values can be varied to achieve this effect. Imprinting occurs through applied pressure of the stamp and heating of the resist. Typically, samples are significantly heated, to temperatures above the glass transition temperatures (T_g) of the resist material. However, for biomolecule patterning applications, significant heating would damage proteins and DNA. Therefore, imprinting temperatures were kept at or below 50 ºC. This temperature was empirically identified as high enough to form imprint patterns, yet low enough to cause no obersavable adverse effects to the proteins. In order to identify the optimal set of processing conditions, several parameters were varied and tested, including temperature values, pressure values, length of imprint, resist thickness and surface treatments of both the stamp and substrate. Temperature values of 30 ºC, 40 ºC and 50 ºC and pressures of 100 psi, 200 psi and 300 psi were investigated, as well as imprint times of 1 minute, 2 minutes, 3 minutes and 5 minutes. Imprinting at 50 ºC and 300 psi for 5 minutes gave the highest feature relief (*ca*. 200 nm). The effect of varying the resist thickness from 400 nm to 600 nm and 900 nm was also examined. The relief magnitude did not noticeably change with differing resist thicknesses. 600 nm was arbitrarily selected for the processing condition set.

Finally, different surface treatments for both the stamp and substrate were investigated, including (1H,1H,2H,2H-Perfluorooctyl)Trichlorosilane (FOTS), oxygen plasma treatment and untreated silicon, with a native oxide. For both the stamp and substrate, it was determined that untreated surfaces often exhibited a "peeling" effect during imprint; most features were "peeled" out from the resist layer to give patterns which were clean to the substrate, without the residue that is common in imprint lithography. In these cases, the feature relief is *ca*. 600 nm for a *ca*. 600 nm thick resist film. Typically with imprint lithography, patterns are stamped into the resist layer to give a degree of feature relief. The resist is then anisotropically etched to remove the remaining resist residue in the thinner regions to give patterns, which are

clean to the substrate. Following imprint at 50 ºC, at 300 psi for 5 minutes, samples were anisotropically etched with Ar/O_2 plasma (Ar: 85%, O_2: 15%) for 5 minutes at an etch rate of approximately 100 nm/minute, to give a final resist thickness of *ca*. 100 nm. Ar/O_2 etching exhibits a lower etch rate than with O_2 alone, therefore Ar/O_2 etching was selected to enable a greater degree of control in determining the final resist thickness post-etching.

Both the imprint resist **5-1** and the hydrofluoroethers were demonstrated to be benign to biomolecules in that they did not detectably deteriorate functionality. Streptavidin, a robust and well-known protein was liberally exposed to both the resist and hydrofluoroether solvents under such conditions as to imitate lithographic processing. Functionality of the streptavidin, post-exposure, was experimentally measured to be very similar to functionality of streptavidin without exposure to any fluorinated resist or hydrofluoroethers. The hydrofluoroether solvents and imprint resist do not seem to affect the functionality of the streptavidin. As a more sensitive test for functionality, a similar assay was performed with a monoclonal antibody. Similar results were obtained; functionality of the protein after exposure to the resist and solvents was very similar to functionality of the protein without any exposure for 1% and 3% concentrations of the monoclonal antibody. The 10% concentration experimental set shows more variability between the control and experimental sets. This difference in fluorescence signal could be due to either partial antibody denaturation or else experimental error of the assay.

There is a fair degree of experimental error that can be observed in these assays. For example, two identical control experiments were performed for the BSA assay with a 5 μg/mL concentration. The measurable intensity of the final absorption signals differed by nearly 25%, despite the identical materials and procedures of the assay (absorption signals shown in Figure 5.3). Arguably, all of the final absorption

signals in both the BSA and monoclonal antibody assays, for all concentrations tested, and for both the control and experimental tests, differed by approximately 25% or less. This observation suggests that for both the BSA and monoclonal antibody assays, the absorption signals for the control and experimental tests were essentially equivalent within the empirically oberserved experimental error.

For both of the assays, control sets were tested for each set of conditions. The control sets had no exposure to either the imprint resist or hydrofluoroethers. Negative controls were also set up to ensure that the fluorescent signals obtained, correlated with actual biomolecule binding and were not simply due to non-specific adsorption of the protein or fluorescent compound. All negative controls exhibited a signal approximately 10 % or less as compared to the experimental set. This indicates that the fluorescent signals obtained from the experimental set are indeed due to biomolecule binding and not nonspecific adsorption.

One of the greatest advantages of this patterning method is the design for multi-component patterning. As many patterned layers as desired in an array are possible with this method. Because the processing conditions are benign to biomolecules, proteins may be lithographically patterned as with any other typical lithographically patterned material. Layer upon layer may be patterned without concern for additional protection steps for the biomolecules. To validate this claim, an additional assay was performed to determine the effect of repeated lithographic processing steps on biomolecules. An assay very similar to the BSA assay (described in section 2.5.1) was performed where resist was deposited onto a biotin-BSA coated surface and then removed again in hydrofluoroethers 10 times. Biomolecule functionality was tested by the ability of the biotin-BSA to bind with streptavidin at 0, 2, 4, 6, 8, and 10 cycles, with 0 being the control set, having no resist or hydrofluoroether exposure. The results suggest that the ability of the biotin to bind to streptavidin is not affected by

exposure to hydrofluoroether solvents or the imprint resist. Negative controls were also tested for this assay to ensure the viability of the experimental set.

The ability to pattern cells is of enormous importance, in particular for tissue engineering applications[8] as well as fundamental cell studies. Cell patterning was explored to determine the biocompatibility of this patterning method with living cells. RBL-2H3 cells were plated atop silicon surfaces with DNP-BSA protein, patterned with polymer resist **5-1** and hydrofluoroether solvents. After several hours of incubation on the surface, the cells show no signs of apoptosis. There is even visible evidence of cell-protein interaction. These results suggest that any residual polymeric resist or hydrofluoroether solvents left behind on the patterned silicon surface do not have adverse effects on cells and furthermore that the processing conditions for this patterning method are biocompatible for protein-assisted cell-patterning.

Despite the success seen with this patterning method, one significant drawback is that the imprint resist **5-1** seemed to be partially degraded by the Ar/O_2 plasma etching such that lift-off of the resist in HFE-7200 was not always complete. For example, in Fig. 5.8, it can be seen that there are small patches of resist that are left behind. The proteins and fluorophores show a particular affinity for the resist, hence the fluorescent labeling of the resist in Fig. 5.8. Furthermore, the edges of the protein patterns generally appear brighter due to better fluorescent labeling of the leftover imprint resist than the actual proteins. This problem was addressed with the synthesis and application of imprint resist **5-2**. The synthesis details for polymer resist **5-2** are given in the Experimental section of this chapter. It is structurally a very similar polymer, but perhaps not so susceptible to the chemical degradation by oxygen plasma that was exhibited by resist **5-1.** Unfortunately, after lithographic evaluation, it was seen that this resist also exhibits the lift-off problems seen with resist **5-1** although to a lesser extent. Perhaps by exploring other fluorinated polymers with similar structures,

a resist material may be identified which does not exhibit these lift-off problems and which is still patternable and biocompatible.

Although imprint patterning has distinct advantages for biomolecule patterning, including high-resolution, relatively low-cost and absence of UV radiation, this patterning method is still largely in the developmental stage. The adaptation of a more established patterning method, for example photolithography, to biomolecule patterning would be very useful. By using a positive-tone biocompatible photoresist and hydrofluoroether solvents, biomolecules could still be patterned without direct UV exposure. Furthermore, because an etching step would not be necessary with photolithography, a single APTMS layer could be deposited at the beginning of the fabrication process, instead of after each imprinting step, thereby simplifying the patterning process.

Additional biocompatibility testing of this imprint resist **5-1**, as well as other resists developed for this purpose would also be useful. The tests performed thus far suggest that the hydrofluoroether solvents and imprint resist are mostly benign to biomolecules, however they do not conclusively prove that. Additional testing with different proteins or antigens would provide useful results.

5.5 Conclusion

A new concept in biomolecule patterning has been described. By applying biocompatible resists and processing solvents to lithography, biomolecules may be straightforwardly patterned by high-resolution, high-throughput and well-established lithographic methods. A fluorinated polymer, processable in hydrofluoroether solvents, was designed and synthesized. This polymer was shown to be patternable by imprint lithography, giving feature sizes down to 1 μm. Both this resist and the hydrofluoroethers were then demonstrated to be benign to biomolecules, including

monoclonal antibodies and cells. This imprint resist system was used to pattern a three-protein array of DNP-BSA, biotin-BSA and rabbit γ globulins with feature sizes from 100 μm down to 1 μm. This array demonstrates only the potential of this resist for multicomponent patterning. As many layers as desired, may be patterned by this method. It has been shown that the effects of lithographic processing, up to ten cycles, are negligible to biomolecules. More importantly, the success of this patterning method demonstrates a new paradigm in multicomponent biomolecule patterning. Through the design and use of similar fluorinated resist materials and solvents, other patterning methods, for example photolithography, may also be similarly adapted to multicomponent protein patterning. By using benign resists and processing solvents, the common obstacles in multicomponent biomolecule patterning, including loss of biomolecule functionality and non-specific binding, are removed. Furthermore, multicomponent biomolecule arrays may be patterned in a straightforward manner through the high-resolution, high-throughput and well-established lithographic patterning method.

Acknowledgements

I gratefully acknowledge support from the National Science Foundation (Materials World Network DMR-0908994) and the IGERT Fellowship. The work was performed in part at the Cornell NanoScale Facility, a member of the National Nanotechnology Infrastructure Network, which is supported by the National Science Foundation (Grant ECS-0335765). Special thanks to Dr. Margarita Chatzichristidi (University of Athens, Greece) for her advice and guidance throughout this project, to Dr. Sotiris Kakabakos and Yiota Petrou (Demokritos, Greece) for their assistance with the biocompatibility assays, to Dr. Alexander Zakhidov (Technische Universitat Dresden, Germany) for his help with lithographic patterning, to Kari Midthun for her

help with protein deposition and cell tests, to Prof. Barbara Baird for her input and suggestions, to Yosuke Hoshi for his help with fluorescence microscopy imaging and to Dr. Jin-Kyun Lee (Cornell University, U.S.A.) for his advice and continued guidance.

REFERENCES

(1) Katz, E. *Electroanalysis* **2006**, *18*, 1855-1857.

(2) Berggren, M.; Richter-Dahlfors, A. *Adv. Mater.* **2007**, *19*, 3201-3213.

(3) James, T.; Mannoor, M. S.; Ivanov, D. V. *Sensors* **2008**, *8*, 6077-6107.

(4) Bashir, R. *Adv. Drug Deliv. Rev.* **2004**, *56*, 1565-1586.

(5) Domachuk, P.; Tsioris, K.; Omenetto, F. G.; Kaplan, D. L. *Adv. Mater.*, *22*, 249-260.

(6) Joos, T.; Bachmann, J. *Front. Biosci.* **2009**, *14*, 4376-4385.

(7) Wolf-Yadlin, A.; Sevecka, M.; MacBeath, G. *Curr. Opin. Chem. Biol.* **2009**, *13*, 398-405.

(8) Atala, A. *Curr. Opin. Biotechnol.* **2009**, *20*, 575-592.

(9) Bettinger, C. J. *Pure Appl. Chem.* **2009**, *81*, 2183-2201.

(10) Blawas, A. S.; Reichert, W. M. *Biomaterials* **1998**, *19*, 595-609.

(11) Kane, R. S.; Takayama, S.; Ostuni, E.; Ingber, D. E.; Whitesides, G. M. *Biomaterials* **1999**, *20*, 2363-2376.

(12) Christman, K. L.; Enriquez-Rios, V. D.; Maynard, H. D. *Soft Matter* **2006**, *2*, 928-939.

(13) Pritchard, D. J.; Morgan, H.; Cooper, J. M. *Angew. Chem.-Int. Edit. Engl.* **1995**, *34*, 91-93.

(14) Sundberg, S. A.; Barrett, R. W.; Pirrung, M.; Lu, A. L.; Kiangsoontra, B.; Holmes, C. P. *J. Am. Chem. Soc.* **1995**, *117*, 12050-12057.

(15) Delamarche, E.; Bernard, A.; Schmid, H.; Michel, B.; Biebuyck, H. *Science* **1997**, *276*, 779-781.

(16) Piner, R. D.; Zhu, J.; Xu, F.; Hong, S. H.; Mirkin, C. A. *Science* **1999**, *283*, 661-663.

(17) Mosbach, M.; Zimmermann, H.; Laurell, T.; Nilsson, J.; Csoregi, E.; Schuhmann, W. *Biosens. Bioelectron.* **2001**, *16*, 827-837.

(18) Pritchard, D. J.; Morgan, H.; Cooper, J. M. *Anal. Chem.* **1995**, *67*, 3605-3607.

(19) Sorribas, H.; Padeste, C.; Tiefenauer, L. *Biomaterials* **2002**, *23*, 893-900.

(20) Holden, M. A.; Cremer, P. S. *J. Am. Chem. Soc.* **2003**, *125*, 8074-8075.

(21) Petrou, P. S.; Chatzichristidi, M.; Douvas, A. A.; Argitis, P.; Misiakos, K.; Kakabakos, S. E. *Biosens. Bioelectron.* **2007**, *22*, 1994-2002.

(22) Douvas, A.; Argitis, P.; Misiakos, K.; Dimotikali, D.; Petrou, P. S.; Kakabakos, S. E. *Biosens. Bioelectron.* **2002**, *17*, 269-278.

(23) Douvas, A.; Argitis, P.; Diakoumakos, C. D.; Misiakos, K.; Dimotikali, D.; Kakabakos, S. E. *J. Vac. Sci. Technol. B* **2001**, *19*, 2820-2824.

(24) Diakoumakos, C. D.; Douvas, A.; Raptis, I.; Kakabakos, S.; Dimotikalli, D.; Terzoudi, G.; Argitis, P. *Microelectron. Eng.* **2002**, *61-2*, 819-827.

(25) Doh, J.; Irvine, D. J. *J. Am. Chem. Soc.* **2004**, *126*, 9170-9171.

(26) Tan, C. P.; Cipriany, B. R.; Lin, D. M.; Craighead, H. G. *Nano Lett.,* **2010,** *10,* 719-725.

(27) Brizzolara, R. A. *Biosens. Bioelectron.* **2000**, *15*, 63-68.

(28) Christman, K. L.; Schopf, E.; Broyer, R. M.; Li, R. C.; Chen, Y.; Maynard, H. D. *J. Am. Chem. Soc.* **2009**, *131*, 521-527.

(29) Bernard, A.; Renault, J. P.; Michel, B.; Bosshard, H. R.; Delamarche, E. *Adv. Mater.* **2000**, *12*, 1067-1070.

(30) Delamarche, E.; Bernard, A.; Schmid, H.; Bietsch, A.; Michel, B.; Biebuyck, H. *J. Am. Chem. Soc.* **1998**, *120*, 500-508.

(31) Kaji, H.; Hashimoto, M.; Nishizawa, M. *Anal. Chem.* **2006**, *78*, 5469-5473.

(32) Bernard, A.; Fitzli, D.; Sonderegger, P.; Delamarche, E.; Michel, B.; Bosshard, H. R.; Biebuyck, H. *Nat. Biotechnol.* **2001**, *19*, 866-869.

(33) Renault, J. P.; Bernard, A.; Juncker, D.; Michel, B.; Bosshard, H. R.; Delamarche, E. *Angew. Chem.-Int. Edit.* **2002**, *41*, 2320-2323.

(34) Ostuni, E.; Kane, R.; Chen, C. S.; Ingber, D. E.; Whitesides, G. M. *Langmuir* **2000**, *16*, 7811-7819.

(35) Tien, J.; Nelson, C. M.; Chen, C. S. *Proc. Natl. Acad. Sci. U. S. A.* **2002**, *99*, 1758-1762.

(36) Lee, K. B.; Lim, J. H.; Mirkin, C. A. *J. Am. Chem. Soc.* **2003**, *125*, 5588-5589.

(37) Lim, J. H.; Ginger, D. S.; Lee, K. B.; Heo, J.; Nam, J. M.; Mirkin, C. A. *Angew. Chem.-Int. Edit.* **2003**, *42*, 2309-2312.

(38) Jang, C. H.; Stevens, B. D.; Phillips, R.; Calter, M. A.; Ducker, W. A. *Nano Lett.* **2003**, *3*, 691-694.

(39) Zhao, Z. Y.; Banerjee, P. A.; Matsui, H. *J. Am. Chem. Soc.* **2005**, *127*, 8930-8931.

(40) Tinazli, A.; Piehler, J.; Beuttler, M.; Guckenberger, R.; Tampe, R. *Nat. Nanotechnol.* **2007**, *2*, 220-225.

(41) Pardo, L.; Wilson, W. C.; Boland, T. J. *Langmuir* **2003**, *19*, 1462-1466.

(42) Allain, L. R.; Stratis-Cullum, D. N.; Vo-Dinh, T. *Anal. Chim. Acta* **2004**, *518*, 77-85.

(43) Hasenbank, M. S.; Edwards, T.; Fu, E.; Garzon, R.; Kosar, T. F.; Look, M.; Mashadi-Hossein, A.; Yager, P. *Anal. Chim. Acta* **2008**, *611*, 80-88.

(44) Bruckbauer, A.; Zhou, D. J.; Ying, L. M.; Korchev, Y. E.; Abell, C.; Klenerman, D. *J. Am. Chem. Soc.* **2003**, *125*, 9834-9839.

(45) Xu, J. T.; Lynch, M.; Nettikadan, S.; Mosher, C.; Vegasandra, S.; Henderson, E. *Sens. Actuator B-Chem.* **2006**, *113*, 1034-1041.

(46) Subramanian, K.; Holowka, D.; Baird, B.; Goldstein, B. *Biochemistry* **1996**, *35*, 5518-5527.

(47) Barsumian, E. L.; Isersky, C.; Petrino, M. G.; Siraganian, R. P. *Eur. J. Immunol.* **1981**, *11*, 317-323.

(48) Pierini, L.; Holowka, D.; Baird, B. *J. Cell Biol.* **1996**, *134*, 1427-1439.

(49) Torres, A. J.; Vasudevan, L.; Holowka, D.; Baird, B. A. *Proc. Natl. Acad. Sci. U. S. A.* **2008**, *105*, 17238-17244.

(50) Lee, J. K.; Chatzichristidi, M.; Zakhidov, A. A.; Taylor, P. G.; DeFranco, J. A.; Hwang, H. S.; Fong, H. H.; Holmes, A. B.; Malliaras, G. G.; Ober, C. K. *J. Am. Chem. Soc.* **2008**, *130*, 11564-+.

(51) Taylor, P. C.; Lee, J. K.; Zakhidov, A. A.; Chatzichristidi, M.; Fong, H. H.; DeFranco, J. A.; Malliaras, G. C.; Ober, C. K. *Adv. Mater.* **2009**, *21*, 2314-+.

(52) Lee, J. K.; Fong, H. H.; Zakhidov, A. A.; McCluskey, G. E.; Taylor, P. G.; Santiago-Berrios, M.; Abruna, H. D.; Holmes, A. B.; Malliaras, G. G.; Ober, C. K. *Macromolecules*, *43*, 1195-1198.

(53) Zakhidov, A. A.; Lee, J. K.; Fong, H. H.; DeFranco, J. A.; Chatzichristidi, M.; Taylor, P. G.; Ober, C. K.; Malliaras, G. G. *Adv. Mater.* **2008**, *20*, 3481-+.

(54) Sarkari, M.; Darrat, I.; Knutson, B. L. *Biotechnol. Prog.* **2003**, *19*, 448-454.

(55) Balla, T.; Spearing, S. M.; Monk, A. *J. Phys. D-Appl. Phys.* **2008**, *41*, 10.

(56) Stuart, C.; Chen, Y. *ACS Nano* **2009**, *3*, 2062-2064.

(57) Hoff, J. D.; Cheng, L. J.; Meyhofer, E.; Guo, L. J.; Hunt, A. J. *Nano Lett.* **2004**, *4*, 853-857.

OUTLOOK AND FUTURE DIRECTIONS

Organic electronics and bioelectronics are still emerging technologies, with the potential to revolutionize the fields of conventional electronics and biology, among many others. Significant work remains to be done before the full potential of this technology reaches fruition. Although the development of efficient, high-resolution patterning methods for these organic electronic and bio-materials is only one of the issues which must be addressed on the path to realizing this vision, it is a significant step in that direction.

Chapters 2 and 3 of this thesis presented non-chemically amplified negative-tone and positive-tone polymeric photoresists, which are fully processable in hydrofluoroether solvents due to their heavily fluorinated structures. Hydrofluoroethers have been shown to be benign and inert to both organic electronic materials and biomolecules. By employing these hydrofluoroethers as processing solvents and designing photoresist materials, which are processable in them, the well-established photolithographic method can be directly applied to patterning organic electronic devices. This concept has been named *orthogonal* lithography. Both polymeric and molecular glass-based chemically-amplified negative-tone photoresists, which are also similarly applicable to organic electronics patterning, have recently been developed.

The development of additional positive-tone photoresists would extend this orthogonal patterning potential even further. A chemically-amplified, polymeric photoresist may exhibit higher sensitivity and thus lower exposure dose and time requirements, creating a more efficient process. The higher sensitivity may also lead to ease in creating an undercut profile in the resist, which is an important property for lift-off patterning schemes. Photoresists, which are each tuned to be particularly

sensitive to the various standard exposure wavelengths, would also be very useful in creating a more efficient patterning process. A molecular glass-based orthogonal photoresist would have to potential to achieve very high-resolution patterns.

Chapter 4 of this thesis presents a model study of self-patternable electroluminescent compounds. Organic light-emitting materials have thus far been the most commercially successful of all the organic electronics. Besides the fact that these materials can be made into large-area and flexible devices, they can also be chemically tuned to exhibit very specific properties, particularly in emission wavelength. By appending patternable end-groups to fluorene oligomers, these light-emitting materials may be patterned directly, without the need for an additional resist layer. A green-emitting fluorene oligomer was reported; red and blue-emitting self-patternable materials may also be developed. Furthermore, being only a model compound, extensive optimization of the structure may be required in order to match or exceed the performance of current light-emitting materials.

An important aspect of developing orthogonal functional materials is that they can greatly expand processing options and device architecture possibilities. Fluorinated functional materials may be patterned easily by conventional organic photoresists and processing solvents, just as organic materials are straightforwardly patterned by fluorinated resists and processing solvents. Aside from patterning capabilities, functional fluorinated orthogonal materials can provide opportunities to fabricate devices with architectures that are otherwise unobtainable, by virtue of their unique interaction properties. The development of fluorinated conducting polymers as well as other fluorinated functional materials for light-emitting devices, organic transistors and photovoltaics may enable more intricate device structures than would otherwise be possible.

Chapter 5 presents a new concept in biomolecule patterning: direct lithographic patterning through the use of biocompatible hydrofluoroethers as processing solvents, and complementary biocompatible resists. This patterning system was shown to be benign to proteins and cells. Imprint lithography was used to fabricate a three-protein array. As many layers as desired may be patterned by this method to create multicomponent arrays or devices. The research described serves as an example to demonstrate the potential of this concept.

With the development of additional biocompatible resists, processable in biocompatible hydrofluoroethers, orthogonal multicomponent biomolecule patterning can easily be extended to other lithographic patterning methods as well, for example, photolithography. In particular, non-chemically amplified positive-tone resists may be the best candidates for biocompatible photolithographic resists. Using a subtractive patterning scheme, biomolecules would not be directly exposed to the UV needed for patterning. Furthermore, a non-chemically amplified system would not require a photoacid generator, which may prove damaging to biomolecules. The non-chemically amplified positive-tone resist described in Chapter 3 of this thesis may be a candidate for this application. Although, it is questionable whether the nitrobenzyl-moiety present in the photoresist is biocompatible. With a photolithographic patterning method, the lift-off problems observed with the imprint resist should not occur. Alternatively, additional imprint resists may be designed, which are able to achieve better imprint patterning and which do not exhibit the lift-off problems previously seen. Because the lift-off problems may be caused by chemical degradation of the polymer resist structure during oxygen plasma etching, a slightly modified structure, which is not so susceptible to degradation by oxygen plasma etching may be all that is required to avoid this problem. A resist material with a

lower glass transition temperature may prove to "flow" better into the imprint stencil to create higher relief features than previously observed in Chapter 5.

This biomolecule patterning method is directly applicable to the fabrication of multicomponent protein arrays for fundamental biological studies as well as patterning of biomolecules for the fabrication of bio-devices.

These orthogonal patterning methods have the potential to straightforwardly enable lithographic patterning of organic electronic and biomaterials. Previously, lithographic patterning of these materials has been very limited due to incompatibility between the organic electronic and bio-materials and the conventional processing solvents and resists. By replacing the conventional processing solvents and resists required by lithography, with a benign system, the well-established, high-resolution and high-throughput lithographic method can be directly applied to both organic electronic device fabrication and multicomponent biomolecule patterning. Furthermore, although these orthogonal materials were originally developed for patterning applications, their unique properties may enable a much wider scope of applicability